

# OSTEOIMMUNOLOGICAL INTERACTIONS AT THE SWITCH FROM ACUTE TO CHRONIC ARTHRITIS



---

seit 1558

## DISSERTATION

TO FULFILL THE  
REQUIREMENTS FOR THE DEGREE OF

**“DOCTOR RERUM NATURALIUM” (DR. RER. NAT.)**

**SUBMITTED TO THE COUNCIL OF THE FACULTY  
OF BIOLOGY AND PHARMACY  
OF THE FRIEDRICH SCHILLER UNIVERSITY JENA**

BY MARTIN BÖTTCHER  
BORN ON 16<sup>TH</sup> OF JUNE 1984 IN SCHLEMA

1<sup>ST</sup> REFEREE:

PROF. DR. MED. THOMAS KAMRADT – INSTITUTE OF IMMUNOLOGY, UNIVERSITY HOSPITAL JENA

2<sup>ND</sup> REFEREE:

PROF. DR. PETER F. ZIPFEL – LEIBNIZ INSTITUTE FOR NATURAL PRODUCT RESEARCH AND  
INFECTION BIOLOGY, HANS KNÖLL INSTITUTE, JENA

3<sup>RD</sup> REFEREE:

UNIV.-PROF. DR. MED. THOMAS PAP - INSTITUTE OF EXPERIMENTAL MUSCULOSKELETAL MEDICINE,  
UNIVERSITY HOSPITAL MÜNSTER

THESIS DEFENSE: MAY 29<sup>TH</sup>, 2015

# TABLE OF CONTENTS

<b>ABSTRACT</b>	<b>5</b>
<b>ZUSAMMENFASSUNG</b>	<b>6</b>
<b>1. INTRODUCTION</b>	<b>7</b>
<b>1.1 RHEUMATOID ARTHRITIS</b>	<b>7</b>
1.1.1 Epidemiology and clinical features of rheumatoid arthritis	7
1.1.2 Pathogenesis of the disease	8
1.1.3 Treatment of patients	12
<b>1.2 THE G6PI-INDUCED ARTHRITIS MOUSE MODEL</b>	<b>14</b>
<b>1.3 FIBROBLAST-LIKE SYNOVIOCYTES</b>	<b>19</b>
<b>1.4 AIM OF THIS STUDY</b>	<b>22</b>
<b>2. MATERIALS</b>	<b>23</b>
<b>2.1 Biological material</b>	<b>23</b>
2.1.1 Mice	23
2.1.2 Cells	23
<b>2.2 Kits and chemicals</b>	<b>23</b>
<b>2.3 Antibodies, standards and cytokines</b>	<b>24</b>
2.3.1 In vivo proteins, antibodies and treatments	24
2.3.2 ELISA antibodies and standards	24
2.3.3 Flow cytometry antibodies	25
2.3.4 Cell culture antibodies, cytokines and treatments	26
<b>2.4 Devices, equipment and software</b>	<b>26</b>
<b>2.6 Cell culture media, Buffers and solutions</b>	<b>27</b>
2.6.1 Cell culture media	27
2.6.2 Buffers and solution	27
<b>3. METHODS</b>	<b>30</b>
<b>3.1 Methods of cell biology</b>	<b>30</b>
3.1.1 Isolation of cells	30
3.1.1.1 spleen and lymph nodes	30
3.1.1.2 blood	30
3.1.1.3 joint cells	30

3.1.2 Cell culture	31
3.1.2.1 <i>In vitro</i> restimulation of G6PI-specific T cells	31
3.1.2.2 Culture of fibroblast-like synoviocytes	31
3.1.2.3 Culture of MDCK-C7 cells	31
3.1.3 Flow Cytometry	32
3.1.3.1 Determination of G6PI-specific T cells	32
3.1.3.2 Staining of fibroblast-like synoviocytes	32
3.1.4 Cartilage attachment assay	32
3.1.5 Matrix-assisted transepithelial resistance invasion (MATRIN) assay	33
<b>3.2 Methods of molecular biology</b>	<b>33</b>
3.2.1 Enzyme-linked immunosorbent assay (ELISA)	33
3.2.2 Luminex multiplex assay	34
3.2.3 Gelatin-zymography	34
<b>3.3 Animal experiments</b>	<b>35</b>
3.3.1 Bleeding of animals	35
3.3.2 Genotyping of DERE mice	35
3.3.3 Immunization of mice	35
3.3.4 Intraperitoneal treatment of mice	36
3.3.5 Clinical scoring of mice	36
3.3.6 Dissections	37
3.3.7 Transfer of fibroblast-like synoviocytes into knee joints of recipients	37
3.3.8 Histology of knee joints	37
<b>4. RESULTS</b>	<b>39</b>
<b>4.1 SWITCH FROM ACUTE, SELF-LIMITING TO CHRONIC, NON-REMITTING ARTHRITIS AFTER TREG-DEPLETION IN THE DERE MOUSE MODEL</b>	<b>39</b>
<b>4.2 CHARACTERIZATION OF MURINE FIBROBLAST-LIKE SYNOVIOCYTES</b>	<b>42</b>
4.2.1 CELLS IN THE JOINT DURING ARTHRITIS PROGRESSION	42
4.2.2 CULTURES OF FIBROBLAST-LIKE SYNOVIOCYTES	44
<b>4.3 PROPERTIES OF FIBROBLAST-LIKE SYNOVIOCYTES DETERMINED BY <i>IN VITRO</i> EXPERIMENTS</b>	<b>45</b>
4.3.1 PHENOTYPIC ANALYSIS	45
4.3.1.1 The secretion of cytokines	45
4.3.1.2 The secretion of chemokines	48
4.3.1.3 The secretion of Matrix-metalloproteinases	49
4.3.2 FUNCTIONAL ANALYSIS	51
4.3.2.1 Attachment of fibroblast-like synoviocytes	52
4.3.2.2 Destructive potential of fibroblast-like synoviocytes	53
<b>4.4 <i>IN VIVO</i> ANALYSES OF FIBROBLAST-LIKE SYNOVIOCYTES</b>	<b>54</b>
<b>4.5 INSTRUCTION OF FIBROBLAST-LIKE SYNOVIOCYTES TO OBTAIN AN AGGRESSIVE, DESTRUCTIVE PHENOTYPE</b>	<b>56</b>
<b>4.6 OUTLOOK: G6PI-INDUCED ARTHRITIS IN OTHER MOUSE STRAINS</b>	<b>58</b>

<b>5. DISCUSSION</b>	<b>60</b>
<b>5.1 Regulatory T cells control the switch from acute, self-limiting to chronic, non-remitting arthritis in the G6PI-induced arthritis mouse model</b>	<b>60</b>
<b>5.2 The role of fibroblast-like synoviocytes for the chronicity of arthritis</b>	<b>62</b>
5.2.1 Cellular composition of isolates and purity of FLS cultures	63
5.2.2 Impact of phenotypic properties of fibroblast-like synoviocytes	64
5.2.3 Impact of functional properties of fibroblast-like synoviocytes	66
5.2.4 Transfer of arthritis by in vivo FLS-transfer	68
<b>5.3 Instruction of fibroblast-like synoviocytes by IL-17</b>	<b>70</b>
<b>5.4 Conclusion and outlook</b>	<b>71</b>
<b>ABBREVIATIONS</b>	<b>73</b>
<b>ACKNOWLEDGEMENT</b>	<b>76</b>
<b>LIST OF TABLES</b>	<b>77</b>
<b>LIST OF FIGURES</b>	<b>77</b>
<b>REFERENCES</b>	<b>78</b>
<b>DECLARATION OF ACADEMIC INTEGRITY</b>	<b>91</b>
<b>CURRICULUM VITAE</b>	<b>92</b>

## ABSTRACT

Immunization with Glucose-6-phosphate isomerase (G6PI), a ubiquitously expressed glycolytic enzyme, induces arthritis in susceptible strains of mice. Depletion of regulatory T cells (Tregs) prior to immunization switches the usually acute, self-limiting course to a non-remitting, destructive arthritis. This provides a possibility to study molecular switches for the transition from acute, self-limiting to chronic, destructive arthritis within one mouse model.

To examine the role of fibroblast-like synoviocytes (FLS), which are known to modulate immune responses via the production of pro- and anti-inflammatory mediators, the phenotype and function of FLS from mice with either acute, self-limiting or non-remitting, destructive arthritis was studied.

FLS from DBA/1 mice that developed either the acute or the chronic form of arthritis were isolated from joints over a time course of 56 days. The cellular composition of isolates and cultures was determined by flow cytometry. To investigate the phenotype of the FLS ELISA studies as well as zymography were performed. For the functional examination of these cells the matrix-associated transepithelial resistance invasion (MATRIN) assay and a cartilage attachment assay were used. Furthermore, FLS were transferred *in vivo* into the knee joints of immunodeficient mice and the joints were scored histologically. Clinical studies aiming at the identification of the FLS' instruction were performed with an anti-IL-17 treatment.

The cellular composition of isolates and cultured cells was found to be stably comprised mainly of fibroblasts and fibrocytes. The secretion of cytokines and chemokines did not differ significantly between FLS from nondepleted and Treg-depleted mice after *in vitro* stimulation. Furthermore, the secretion and activity of matrix metalloproteases (MMPs) was enhanced in the FLS from mice with chronic arthritis compared to samples from the ones with the acute form. Additional functional differences include the collagen-destructive potential and the potential to attach and eventually invade wild type cartilage. Here, FLS from Treg-depleted chronic arthritic mice showed a higher invasive and destructive potential. This aggressive phenotype could be reversed by the preventive and therapeutic treatment of the animals with anti-IL-17A. Ultimately, FLS from Treg-depleted mice were able to destroy cartilage and bone *in vivo* upon transfer into immunodeficient mice.

The results are compatible with the hypothesis that uninhibited inflammation in the early phase of Treg-depleted mice causes the acquisition of an autonomously aggressive phenotype of synoviocytes mediated via IL-17 which contributes to the switch from acute to chronic arthritis even in the absence of late support from T and B lymphocytes.

## ZUSAMMENFASSUNG

Arthritis kann in suszeptiblen Mausstämmen durch die Immunisierung mit Glukose-6-Phosphatisomerase, einem ubiquitär exprimierten Enzym der Glykolyse, induziert werden. Die Depletion regulatorischer T-Zellen vor der Immunisierung verändert den sonst akuten, selbst-limitierenden Krankheitsverlauf in einen destruktiven, nicht remittierenden. Dadurch eröffnet sich die Möglichkeit molekulare Schalter beim Übergang von akuter, selbst-limitierender zu destruktiver, chronischer Arthritis in ein und demselben Mausmodell zu studieren.

Für die Untersuchung der Rolle fibroblastenartiger Synoviozyten (FLS, engl. *fibroblast-like synoviocytes*), die dafür bekannt sind Immunantworten durch die Produktion von pro- und anti-inflammatorischen Mediatoren zu modulieren, wurden Phänotyp und Funktionen solcher FLS aus entweder akut oder chronisch arthritischen Mäusen verglichen.

FLS von DBA/1-Mäusen, die entweder den akuten oder den chronischen Krankheitsverlauf zeigten, wurden aus den Gelenken über einen Zeitraum von 56 Tagen isoliert. Die zelluläre Zusammensetzung der Isolate sowie der Zellkulturen wurden durchflusszytometrisch analysiert. Um den Phänotyp dieser Zellen näher zu bestimmen, wurden diverse ELISA-Versuche sowie zymographische Untersuchungen durchgeführt. Im Rahmen funktioneller Analysen wurde der MATRIN (engl. *Matrix-associated transepithelial resistance invasion*) Assay sowie ein Knorpelanlagerungsversuch benutzt. Desweiteren wurden isolierte FLS *in vivo* in die Kniegelenke von immundefizienten Empfänger-mäusen transferiert und anschließend die Gelenke histologisch analysiert. Klinische Studien, die Aufschluss über die Instruktion der FLS geben sollten, wurden mit Hilfe von anti-IL-17 Behandlungen durchgeführt.

Die zelluläre Zusammensetzung der FLS-Isolate und FLS-Zellkulturen erwies sich als konstant. Hauptsächlich Fibroblasten und Fibrozyten wurden als Bestandteile identifiziert. Die Sekretion von Zytokinen und Chemokinen zeigte keine Unterschiede zwischen FLS von nicht depletierten und Treg-depletierten Mäusen nach *in vitro* Stimulation. Darüber hinaus war die Sekretion aktiver Matrixmetalloproteasen (MMPs) in den Proben von Treg-depletierten Mäusen deutlich erhöht gegenüber denen aus nicht depletierten Individuen. Zusätzliche funktionelle Untersuchungen umfassen das Potential Kollagen zu zerstören sowie an Knorpelgewebe anzuhaften und möglicherweise anschließend einzuwandern. Dabei erwiesen sich die FLS der Tiere mit chronischem Krankheitsverlauf als wesentlich invasiver und destruktiver. Dieses aggressive Verhalten konnte sowohl durch präventive als auch therapeutische anti-IL-17 Behandlungen in den Ursprungszustand zurück versetzt werden. Schlussendlich waren transferierte FLS von Treg-depletierten Tieren in der Lage Knorpel und Knochen in immundefizienten Empfänger-mäusen abzubauen.

Diese Resultate sind mit der Hypothese vereinbar, dass es durch ungehemmte Inflammation in der frühen Phase in Treg-depletierten, arthritischen Mäusen zum IL-17 vermittelten Erwerb eines autonom-aggressiven Phänotyps synovialer Fibroblasten kommt, was zum Umschalten von akuter zu chronischer Arthritis sogar in Abwesenheit von späterer Hilfe durch B- und T-lymphozyten führt.

# 1. INTRODUCTION

## 1.1 RHEUMATOID ARTHRITIS

### 1.1.1 EPIDEMIOLOGY AND CLINICAL FEATURES OF RHEUMATOID ARTHRITIS

Rheumatoid arthritis is an autoimmune disease which affects about 1% of the world's population. It is 2,5-times more common in female than in male and occurs in the 4<sup>th</sup> decade of age although several cases are reported amongst younger individuals.<sup>1</sup> It is geographically distributed in a worldwide manner. RA patients have a higher mortality rate than the general population with a decrease of expected survival of 3-10 years<sup>1</sup> and an increased comorbidity of coronary heart diseases and infections.<sup>2-4</sup>

Rheumatoid arthritis is a multifactorial disease, influenced both by genetic and environmental factors. There are factors increasing the risk of developing arthritis, known as risk factors, and those believed to be beneficial for the patients.<sup>5-7</sup>

Twin and family studies revealed a genetic predisposition as one risk factor.<sup>5,6,8</sup> There have been several studies showing an association of the *HLA-DRB1* alleles, coding for MHC class II molecules, with RA.<sup>9-12</sup> Those alleles encode a common stretch of amino acids in the peptide binding groove, known as the shared epitope<sup>8,10</sup>, which confers particular susceptibility to RA. The consequences of this allelic risk factor are discussed and include a predisposed T cell repertoire selection, antigen presentation, alterations in peptide affinity, the induction of T cell senescence by shared epitope-containing HLA molecules, and potentially a pro-inflammatory signaling function.<sup>8</sup> Other risk alleles include those important for T cell stimulation, activation and functional differentiation, such as *PTPN22*, *CTLA4*, *GZMB*, and *PRKCQ*.<sup>8,13</sup> Moreover, associations with immune regulation pathways, such as the NFκB or the TNF pathway have been implicated to the disease.<sup>8,13</sup> In general, approximately 60 % of a population's predisposition to RA can be accounted for by genetic risk factors.<sup>1</sup>

Since the concordance rate in monozygotic twins is described to be around 15-30% a strong contribution by environmental factors is suggested.<sup>6,14</sup> It is believed that at least one third of susceptibility to RA is due to environmental influences.<sup>6</sup> For example, the fact that RA incidence is higher in women<sup>15</sup> suggests a hormonal influence on the onset.<sup>6</sup> There are also certain aspects of lifestyle that contribute to the development and severity of RA. The most prominent one is smoking.<sup>16,17</sup> There has been evidence for a link between smoking and genetic risk factors. Carriers of the shared epitope that are smokers have an 8-fold higher risk to develop RA. This risk increases further to almost 16-fold if the smokers are homozygous carriers of the share epitope.<sup>18,19</sup> Additionally, a synergistic effect of smoking and *HLA-DRB1* alleles on the formation of anti-citrullinated protein antibodies (ACPAs) has been suggested.<sup>8</sup>

Rheumatoid arthritis onset is in most cases very insidious and diagnosis is often ascertained only after several months.<sup>1</sup> Patients often suffer from joint swelling, pain and stiffness, weakness, fatigue, weight loss and depression. Articular characteristics include tenderness on palpation and synovial thickening, effusion and erythema during the early stage, as well as decreased range of motion and ankylosis during the later phase. Symptoms are mostly symmetrical distributed and can affect distal (more commonly) as well as proximal joints.<sup>1</sup>

However, also other organs can be affected in a multisystem inflammation situation. This includes organ systems such as the respiratory, cardiac, neurological, hematological and vascular system often leading to profound morbidity and mortality.<sup>1</sup>

### 1.1.2 PATHOGENESIS OF THE DISEASE

The pathogenesis of rheumatoid arthritis is a very complex process and despite great research efforts still insufficiently understood. Characteristic events are the inflammation of the synovium, pronounced angiogenesis, cellular hyperplasia, the infiltration of the synovial compartment by leukocytes, the production of autoantibodies (such as rheumatoid factor or ACPAs) and subsequently the degradation of cartilage and the destruction of subchondral bone.<sup>1,8,20,21</sup> The early phase is mainly characterized by tissue edema and fibrin deposition resulting in joint swelling and pain. Later, the synovial sublining becomes hyperplastic and transforms from a single-cell layer to a lining of >10 cells depth. This layer is mainly comprised of macrophage-like (MLS) and fibroblast-like synoviocytes (FLS). The sublining gets infiltrated by mononuclear cells, including T cells, B cells, macrophages and plasma cells.<sup>1</sup> Synovial-vessel endothelial cells transform into high endothelial venules to facilitate the transit of leukocytes from the blood stream into the tissue.<sup>22</sup> The increased expression of adhesion molecules and chemokines in the synovial compartment supports the infiltration even more.<sup>8</sup> Further on, there is the formation of a histologically distinct locally invasive synovial tissue, called the pannus, which penetrates the cartilage.<sup>23</sup> This cellular pannus is later replaced by a fibrous pannus with a minimally vascularized layer of pannus cells and collagen overlying cartilage.<sup>24</sup> (see Figure 1)

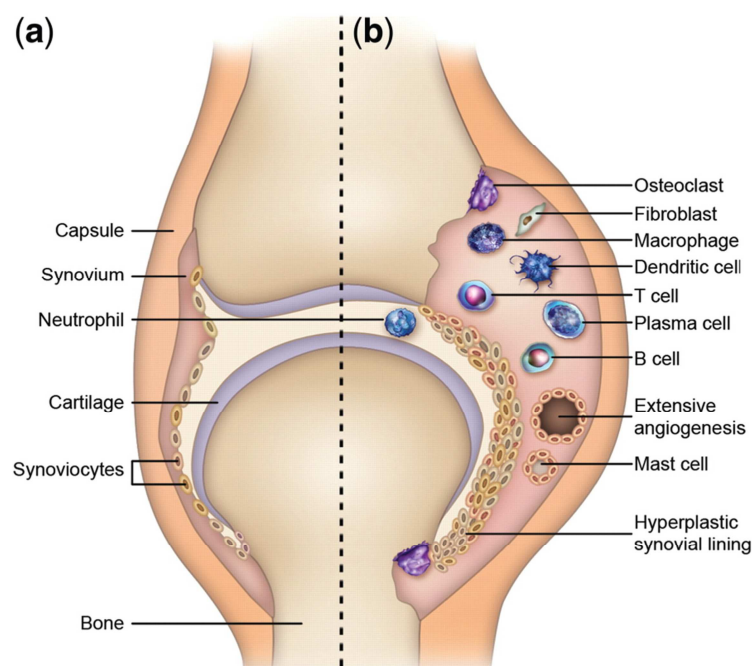


**Figure 1: Schematic view of a normal joint (a) and a joint affected by RA (b)**  
(from Choy E Rheumatology 2012;51:3-11.)

The adaptive immunity is believed to be important during the early pathogenesis although the functional role of T cells is incompletely understood.<sup>8,25</sup> Even though the efficacy of T cell-depleting therapy is as limited<sup>26</sup> as others (see 1.1.3 Treatment of patients) there is evidence for the role of T cells in RA pathogenesis. As described above, genes important for T cell activation and function such as the *HLA-DRB1* alleles or the *PTPN22* and *CTLA4* gene are amongst the most prominent genetic risk factors.<sup>20,25</sup> Furthermore, the inflamed synovium of RA patients shows a high number of T cells which were also shown to be necessary in various animal models of arthritis.<sup>26</sup> Moreover, the presence of autoreactive T cells against citrullinated self-proteins has been demonstrated.<sup>8</sup> Initially, RA was thought to be a Th1-driven disorder characterized by cytokines and chemokines such as IFN $\gamma$ , LT $\beta$  and TNF family members.<sup>27</sup> But, only low levels of IFN $\gamma$  were found in the synovium of RA patients.<sup>28</sup> Instead, Th17 cells came into focus because they were also found in the rheumatoid synovial membranes, though at low numbers.<sup>29</sup> The inhibition or overexpression of IL-17 in the joints of animals could reduce or worsen the joint inflammation and damage, respectively.<sup>30</sup> Their differentiation is supported by macrophage-, synovial fibroblast- and dendritic cell-derived TGF $\beta$ , IL-1, IL-6, IL-7, IL-12, IL-15, IL-21 and IL-23.<sup>8,20</sup> Those cell types are also found in the synovial compartment. At the same time, these cytokines can suppress the differentiation of regulatory T cells (Tregs). Although Tregs were detected in the RA synovium their regulatory function seems to be impaired.<sup>31-33</sup> Thus, RA patients show an imbalance of Th17 cells and Tregs towards the IL-17 producing cells. The site of effector cell differentiation is mainly unknown.<sup>20</sup> Yet, the great abundance of T cells in the inflamed synovium is widely believed to be due to migration and not proliferation in the joint.<sup>8</sup> Furthermore, there are indications both for antigen-specific as well as antigen-independent effects of T cells during synovitis. There is a decreased diversity of the T cell receptor (TCR) repertoire, changes in the receptor selection and clonal outgrowth of certain CD4 subsets in the synovial compartment observable.<sup>34</sup> These facts together with observations of germinal-center reactions and B cell somatic hypermutations support the ongoing antigen-specific T cell-mediated B cell help.<sup>35-37</sup> Synovial T cells and B cells form aggregates resulting in ectopic lymphoid follicles similar to lymph nodes or Peyer's patches.<sup>38,39</sup> However, also antigen-nonspecific T cell contact-mediated activation of MLS and FLS via CD40/CD40L, CD200/CD200L and ICAM-1/LFA-1 interactions takes place.<sup>40</sup>

The importance of B cells during pathogenesis is strengthened by findings after B cell depletion. It prevents germinal center formation and subsequently T cell activation.<sup>41</sup> The depletion of CD20<sup>+</sup> B cells (but not plasma cells) with Rituximab leads to a significant clinical benefit.<sup>42</sup> The survival of synovial B cells is supported by DC-derived APRIL and MLS/FLS-derived BAFF.<sup>39,43</sup> B cells cannot only contribute to arthritis pathogenesis by the production of autoantibodies and ACPAs but also by the secretion of cytokines and chemokines, e.g. IL-6, IL-10 and LT $\beta$ .<sup>20</sup> Those in turn are thought to contribute to regulatory feedback loops for the interaction between T cells and macrophages as well as T and B cells. Furthermore, the formerly mentioned formation of ectopic germinal centers is believed to lead to local affinity maturation and receptor editing of B cells resulting in self-reactive ones with high autoantibody production.<sup>20,44</sup> There is also increasing evidence that autoantibodies itself can directly activate osteoclasts and their precursors independent from inflammation to facilitate bone resorption.<sup>45</sup>

The role of Tregs in rheumatoid arthritis or other arthritic diseases is highly controversial. Different studies determining Treg populations and their functions in RA came up with

various and sometimes conflicting results. In many studies the frequency of circulating Tregs was reported to be decreased<sup>46-49</sup>, but some others show increased frequencies<sup>50-52</sup>. Surprisingly, all studies report elevated numbers of Tregs in the joints of RA patients<sup>46-48,52-56</sup>. This seems paradoxical in the first place. However, the expression of FoxP3 and CD25 and thereby the function of Tregs can be modulated by inflammation and T cell activation.<sup>57</sup> Results for the suppressive capacity of circulating Tregs are again heterogeneous. While some studies report impaired suppressive functions<sup>32,56,58</sup> others show the opposite<sup>50,52,53</sup>. Again, most studies agree on the fact that local Tregs in the inflamed joints are fully suppressive at least *in vitro*.<sup>46,52-54</sup> Yet, the highly inflammatory synovial milieu is suspected to alter the Treg activity *in vivo*.<sup>55</sup> Cytokines such as TNF $\alpha$  or IL-7 which are known to be important for arthritis pathogenesis, found in high concentrations in RA patients, and expressed by immune cells involved in the disease were shown to be partly responsible for the Treg activity suppression in *in vitro* experiments<sup>55</sup>. Also IL-6 was shown to repeal the Treg-mediated suppression.<sup>59</sup> Thus, it seems that either impaired suppressive capacity of Tregs or resistance of effector cells against Treg modulation is taking place in the inflamed joints of RA patients. Another controversial part is the fact that Tregs were found to prevent bone erosion by the inhibition of differentiation and activation of osteoclasts by unknown modes of action.<sup>60-64</sup> Still, the exact mechanisms by which Tregs contribute beneficial or harmful to the disease are mainly unknown but most likely depend on the local inflammatory milieu. Moreover, it is unclear if Tregs can also directly interact with and modulate other cells apart from immune cells, especially fibroblast-like synoviocytes.

The synovium is not only infiltrated by adaptive immune cells but also by innate effector cells. Macrophages, mast cells and NK cells can be found in the synovial membrane; neutrophils reside mainly in the synovial fluid.<sup>8</sup> Currently, macrophages are amongst them regarded as the central effectors of synovitis. Effective biologic agents can reduce the macrophage infiltration in the synovium.<sup>65</sup> Their effector functions include the production of cytokines, ROS, NO intermediates, matrix metalloproteases (MMPs), phagocytosis and antigen presentation.<sup>8</sup> Their activation occurs most likely via toll-like receptors (TLRs) and NOD-like receptors (NLRs) recognizing PAMPs and DAMPs.<sup>66</sup> Other activation mechanisms encompass cytokines, cognate T cell interactions (as described above), immune complexes and lipoprotein particles.<sup>67</sup> Differentiation, maturation and activation of neutrophils are driven by IL-17 leading in turn to additional cytokine release.<sup>68</sup> Moreover, activated neutrophils start to secrete prostaglandins, proteases and ROS.<sup>69</sup> Mast cells in the synovium produce vasoactive amines, cytokines, chemokines and proteases.<sup>70,71</sup> Some ACPAs present in the serum of RA patients are of the IgE isotype pointing towards a possible involvement of mast cells.<sup>72</sup> IL-17 drives not only the activation of neutrophils in the synovial compartment but also of FLS. This leads to cytokine, chemokine, prostaglandin and MMP release.<sup>68</sup> This activation also occurs at low concentrations of IL-17 in synergy with TNF $\alpha$  and IL-1.<sup>73</sup> The loss of normally protective effects of the synovium (e.g. due to reduced expression of lubricin) promotes the adhesion and invasion of FLS.<sup>74</sup> The MMP production by FLS together with the limited ability of cartilage to regenerate leads to biomechanical dysfunction of the joints.<sup>75</sup> An IL-1/IL-17 triggered apoptosis of chondrocytes results in the loss of physiologically regulated matrix formation and subsequently to surface cartilage destruction.<sup>8</sup>

The following bone erosion is often very rapid affecting 80% of the patients already in the first year after diagnosis<sup>76</sup>. This is accompanied by prolonged and increased inflammation.<sup>77</sup>

The bone erosion is primarily conducted by osteoclasts populating the synovial membrane of RA patients.<sup>78,79</sup> Osteoclast differentiation, maturation and invasion are mediated by M-CSF and RANKL mainly derived from macrophages, FLS and also activated T cells.<sup>78,80,81</sup> A possible involvement of B cells via the expression of RANKL has just recently been discussed.<sup>82</sup> These processes can be amplified by TNF $\alpha$ , IL-1, IL-6 and IL-17.<sup>78,83</sup> The central and unique role of RANKL for osteoclastogenesis is validated by findings that the blockade of RANKL is beneficial to stop bone erosion but unable to interfere with joint inflammation and cartilage degradation.<sup>84</sup> This is justified by the fact that osteoclasts have an acidic enzymatic machinery which enables the destruction of mineralized tissue (mineralized cartilage and subchondral bone) resulting in deep resorption pits which can be and are filled by inflammatory tissue.<sup>8</sup> However, there is also RANKL-independent osteoclastogenesis from PBMCs via M-CSF, IL-6 and IL-11.<sup>85</sup> In the end, the osteoclast-mediated bone resorption leads to breach of cortical bone permitting synovial access to the bone marrow.<sup>8</sup> Finally, medulla ossium flava (yellow marrow) is gradually replaced by aggregates of T and B cells causing inflammation of the bone marrow, called osteitis.<sup>86</sup> Under normal physiological conditions there is a balance between bone resorption and bone formation. This balance is shifted towards bone resorption in RA patients. However, it is not only due to enhanced osteoclastogenesis and activation but also caused by reduced, almost absent osteoblast function. The mechanisms are not well understood but evidence is available showing an involvement of cytokines.<sup>20</sup> A prominent example is TNF which was shown to inhibit osteoblast differentiation and function.<sup>87</sup> Furthermore, indirect pathways of TNF-mediated inhibition of bone and cartilage formation via inhibition of WNT signaling have been described.<sup>88</sup>

The interplay between adaptive and innate immune cells as well as resident cells of the joint seems to be a very complex process involving numerous different pathways and feedback mechanisms. So far, none of those interactions are fully understood. It is also hard to determine which of the measured mediators and functions are cause or consequence of alterations. The assignment of findings to certain cell types is also not always assured. Nevertheless, research efforts have focused more and more on those processes in the past years leading to new therapeutic strategies.

The inflammation of the joints and bone marrow of RA patients does also have systemic consequences. This is mainly caused by circulating inflammatory pathways mediated by cytokines (e.g. IL-6 and TNF $\alpha$ ), acute-phase reactants, immune complexes and altered lipid particles.<sup>8</sup> It causes for example an increased rate of cardiovascular diseases, i.e. myocardial infarction, cerebrovascular defects and heart failure.<sup>89-91</sup> Acute-phase reactants, as the C-reactive protein, have been described as important risk factors for cardiovascular disorders.<sup>92</sup> Increased endothelial activation, insulin-resistance of muscle and adipose tissue, and atheromatous lesions are also a consequence of the systemic inflammation.<sup>93,94</sup> Other affected organs are the brain (fatigue and depression), the liver (elevated acute-phase response), lungs (inflammatory and fibrotic diseases), muscles (sarcopenia), and bones (osteoporosis).<sup>8</sup> Cytokines like IL-1, IL-6 and TNF $\alpha$  which are highly abundant in RA patients can dysregulate the hypothalamic-pituitary-adrenal axis<sup>95</sup> causing fatigue and high rates of depression. RA-related osteoporosis is mainly driven by IL-6.<sup>96</sup> RA patients show also an increased risk of lymphomas most likely resulting from clonal selection of B cells, impaired regulatory function of Tregs, and dysfunctional NK cells.<sup>97,98</sup>

### 1.1.3 TREATMENT OF PATIENTS

Rheumatoid arthritis patients are treated with so called disease modifying anti-rheumatic drugs (DMARDs) which impede both inflammatory and destructive processes. Their mode of action mostly starts after several weeks or month after the first medication and reduces both pain and swelling, and halts the progression of destruction.<sup>99</sup> However, only 20-25 % of the patients show complete remission. A continuous administration of DMARDs is indispensable since stopping DMARDs results in a significant risk of flares.<sup>100</sup> DMARDs are divided into two groups; small-molecule DMARDs and biological DMARDs (see Table 1).

Small-molecule DMARDs have been used since the 1920s. The most commonly one is methotrexate (MTX) which was first used in the 1950s and is considered to be the gold standard for DMARD therapy.<sup>99</sup> All small-molecule DMARDs have in common that they act in an anti-inflammatory manner. However, strong side effects are always accompanying the beneficial effects. Those include liver toxicity, cytopenia, mucositis, teratogenicity and nodulosis.<sup>99</sup>

Biological DMARDs were and are developed as highly specific agents to target pro-inflammatory cytokines and different cell types that play important roles in RA pathogenesis (see 1.1.2 Pathogenesis of the disease). Three different strategies are pursued: 1) the inhibition of pro-inflammatory cytokines and their receptors by monoclonal antibodies, soluble receptors, binding proteins or receptor antagonists; 2) the use of anti-inflammatory cytokines such as IL-4, IL-10 or IL-13; 3) the target of cell surface antigens by monoclonal antibodies.<sup>99</sup>

**Table 1: Biological DMARDs in clinical use**

(modified from Smolen JS et al Nature Reviews Drug Discovery 2003;2:473-488 and Vivar N et al F1000 Prime Reports 2014;6:31).

Agent	Format	Mechanism
<b>anti-TNF therapies</b>		
Etanercept	recombinant human fusion protein of TNF receptor and the Fc part of IgG1	decoy receptor capturing soluble TNF preventing it from binding to TNF receptor
Adalimumab	human IgG1 monoclonal antibody	binding of TNF
Infliximab	chimeric murine/human IgG1 monoclonal antibody	binding of soluble and membrane-bound TNF
Golimumab	human IgG1 monoclonal antibody	binding of soluble and membrane-bound TNF
Certolizumab-pegol	humanized pegylated anti-TNF Fab' fragment	binding of TNF
<b>IL-1 blocking agent</b>		
Anakinra	recombinant human IL-1ra	binding of IL-1 type I receptor
<b>IL-6 blocking agent</b>		
Tocilizumab	humanized recombinant IgG1 monoclonal antibody	binding of soluble and membrane-bound IL-6 receptor
<b>Cell-targeting agents</b>		
Rituximab (B cells)	chimeric murine/human IgG1 monoclonal antibody	binding of CD20, depletion of CD20 <sup>+</sup> B cells
Abatacept (T cells)	recombinant human fusion protein of extracellular domain of CTLA-4 and Fc part of IgG1	high affinity binding of CD80/86, inhibition of T cell costimulation

Since TNF is one key cytokine in the pathogenesis of RA anti-TNF therapy is widely used. There are antibodies directed against TNF and TNF signaling available. All of them have one thing in common, patients observe a clinical improvement. Their function-related quality of life is also significantly enhanced. Moreover, radiographic progression is significantly reduced. Nevertheless, there is still a prominent proportion of patients not responding to this treatment. Remissions are very rare and the treatments do have side effects.<sup>101-105</sup>

Another approach is targeting IL-1 as another key cytokine. Under physiological conditions IL-1 binds to the IL-1 receptor (IL-1R) allowing the engagement of the IL-1R accessory protein (IL-1RacP) which is necessary for the signaling cascade. A natural inhibitor called IL-1 receptor agonist (IL-1ra) competes with IL-1 for the receptor. Upon binding of IL-1ra the engagement of IL-1RacP and thereby signaling is inhibited.<sup>106</sup> The so far only IL-1 blocking drug is a recombinant form of IL-1ra called anakinra. However, the effects of anakinra seen in clinical trials seem to be more modest than those of other drugs.

There are currently two biological DMARDs directed against pathogenesis-involved lymphocytes. Rituximab is a chimeric murine/human monoclonal antibody against CD20. The surface antigen CD20 is expressed by several B cell differentiation stages ranging from pre-B cell to mature B cells. Hematopoietic stem cells and plasma cells lack CD20. Thus, rituximab depletes B cells and thereby inhibits the production of autoantibodies, B cell – T cell help and subsequently the production of pro-inflammatory cytokines.<sup>107</sup> It is commonly used as a second-line defense if anti-TNF therapy failed. Studies showed a relative benefit of rituximab over anti-TNF agents but the radiographic erosion progression was similar.<sup>108</sup> Seropositive RA patients (which have autoantibodies in the serum) show a better response to rituximab than seronegative RA patients (which have no autoantibodies in the serum).<sup>109</sup> The second biological DMARD against lymphocytes is called abatacept, a fusion protein consisting of the extracellular domain of CTLA-4 and the Fc portion of human IgG.<sup>110</sup> T cell activation is usually a two-step process; first the recognition of presented antigen on the MHC of an APC via the TCR complex and second the costimulation of the T cell via CD80/86 on the APC and CD28 on the T cell surface. This fully activates the T cells but also triggers a feedback loop leading to the expression and surface presentation of CTLA-4. The CTLA-4 also interacts with CD80/86 but with a higher affinity than CD28 inhibiting the costimulation. Thus, T cell activation is shut off and an overshooting immune reaction is prohibited. Abatacept acts similarly through binding with its CTLA-4 part to CD80/86 hampering the T cell activation by outcompeting the costimulatory CD28.<sup>110</sup>

In summary, most treatments so far are focusing on the containment of the inflammation in the joint by interfering with the inflammatory processes and signaling cascades. However, this is just partially beneficial and often accompanied by heavy side effects.

DMARDs targeting other cell types and processes involved in the RA pathogenesis are under development or subject of current research. For example, several small-molecule DMARDs for the inhibition of MMPs have been tested both in animal models and also in clinical trials. However, their efficacy so far was not very promising and safety issues lead to a discontinuation in several cases.<sup>99</sup> The interference with intracellular signaling leading to the induction of MMP or cytokine production is also discussed and investigated. But again, there are numerous side effects due to toxicities of the compounds. Possible further targets are chemokines secreted by resident cells of the joint, cell surface antigens on several involved cells, adhesion molecules for example on FLS as well as the direct inhibition of cartilage and

bone erosion by the interference with osteoclast differentiation and activation. However, most strategies still focus on anti-inflammatory instead of anti-destructive mechanisms and so far, none of the last mentioned possibilities has been successfully addressed.

## 1.2 THE G6PI-INDUCED ARTHRITIS MOUSE MODEL

In 1996 researchers of Diane Mathis lab coincidentally found a new mouse model for rheumatoid arthritis. Initially, they were aiming to study the selection of a certain T cell receptor (TCR) specificity which recognizes a peptide of bovine pancreas ribonuclease, R28. Therefore, they generated a R28 TCR transgenic mouse line. This KRN mouse line turned out to be useless for their purpose because transgene-encoded TCRs were ineffective at promoting allele-specific positive selection.<sup>111</sup> Fortuitously, they crossed this KRN strain to the already existing NOD mouse line. Surprisingly, this mouse strain, referred to as K/BxN, developed an interesting phenotype with pronounced joint inflammation. They observed several deformations such as hyperextension of the ankle, valgus deviation of the knee, hyperpronation of the toes as well as compromised animals' mobility. Histology of the joints showed neovascularization, extensive synovitis, hyperplastic synovium, a massive immune cell infiltration, fibrosis, exudation of neutrophils from the synovium into the articular cavity, formation of a pannus-like structure which was able to invade the cartilage and subchondral bone, and remodeling of the joint architecture all of which are reminiscing of symptoms seen in RA patients. The underlying mechanism was postulated as an alloreactive recognition of antigen-presenting cells (APCs) derived from the NOD mice via the MHC class II molecule I-A<sup>g7</sup> by R28 transgenic T cells leading to systemic autoimmunity.<sup>111</sup> Thereby, they showed for the first time, that a systemic autoreactivity can provoke an organ-specific immune response breaking with the former dogma of joint-specific antigens for arthritis development. Further studies revealed an imbalance in cytokines (especially TNF $\alpha$  and IL-6) as well as B cell hyperactivity accompanied by hypergammaglobulinemia and autoantibody production as hallmarks of the K/BxN arthritis model.<sup>112</sup> Tolerance against the initial R28 specificity was evoked by clonal deletion of thymocytes, diminished levels of TCR clonotypes and a clonal anergy of peripheral T cells.<sup>112</sup> The self-peptide recognized by the KRN T cells was identified as glucose-6-phosphate isomerase (G6PI)<sup>113</sup>, a ubiquitously expressed enzyme of glycolysis. This led to the interaction of T and B cells via TCR:I-A<sup>g7</sup> and CD40:CD40L which further stimulated the T cells, activated the B cells and resulted in autoantibody production.<sup>112</sup> Those immunoglobulins could then bind together with complement components and other unknown factors in the joint to form immune complexes and elicit a local inflammation. Further experiments showed that even the transfer of serum from K/BxN mice or a pool of several anti-G6PI antibodies was able to induce arthritis when transferred into healthy recipients.<sup>112,114</sup> However, the transfer with the pooled antibody mix against G6PI could never be reproduced. Still, the serum-transfer even worked in *rag2*<sup>-/-</sup> recipients indicating that T and B cells only play an important role in the induction phase of the K/BxN arthritis model and that they are dispensable once autoantibodies are produced.<sup>115</sup>

After the discovery of G6PI as the antigen in this model the question arose whether this could also be a relevant antigen in human RA patients. There was an initial study reporting that 64% of RA patients had increased concentrations of anti-G6PI IgG in serum and the synovial fluid.<sup>116</sup> However, this could not be reproduced by other studies. Sera of patients with RA,

collagen tissue disease, or other chronic arthritides did not contain elevated levels of anti-G6PI antibodies.<sup>115</sup> Later it could be proven that this discrepancy was due to a contamination of the commercial detection kit in that first survey.<sup>117</sup> Nevertheless, the concept of systemic autoimmunity with local inflammatory responses as seen in RA patients is very good mirrored by that mouse model. Other mouse models for arthritis such as the antigen-induced arthritis where an inflammation is triggered by a local injection of an antigen fail to reproduce this hallmark of RA. Further models having local effects of systemic autoimmunity include fibrinogen-induced<sup>118</sup> arthritis, TNF $\alpha$ <sup>119</sup> or IL-1 $\alpha$ <sup>120</sup> transgenic mice, IL-1ra<sup>-/-</sup> mice<sup>121</sup> and the recently published A20 mice with a TNFAIP3-deficiency in myeloid cells<sup>122</sup>. Thus, the murine system showing a local inflammation in the joints evoked by the systemic antigen G6PI is a very good tool to study mechanisms of the human autoimmune disease where a local inflammation in the joints is also evoked by systemic autoimmunity as seen by the presence of ACPAs and the rheumatoid factor.

Several years later Schubert *et al* published another mouse model where they used recombinant human G6PI (rhG6PI) emulsified in complete Freund's adjuvant (CFA) to immunize several mouse strains.<sup>123</sup> They found one strain to be susceptible to G6PI-immunization bearing the MHC haplotype H-2<sup>q</sup>, named DBA/1. The incidence of arthritis was almost 100% and characterized by redness and severe swelling of hind and front paws. The first clinical symptoms started to appear 9 days after the immunization, reached a maximum at around day 15 and then slowly resolved until day 40. The histopathology of G6PI-immunized DBA/1 mice showed severe symmetric arthritis of distal joints which affected wrist, metacarpal joints, and proximal and distal interphalangeal joints at the front limbs as well as tarsal, ankle and knee joints at the hind limbs. The spine and other joints including elbow, shoulder or hip joints were not compromised.<sup>123</sup> Resembling symptoms found in RA patients the G6PI-immunized animals showed severe synovitis, tenosynovitis, sometimes even rupture of the tendons, destruction of bone and cartilage as well as fibrin extravasation during their peak of the disease. At later time points inflammation was almost absent and regeneration and fibrosis occurred (see Figure 2). The same results could be obtained using recombinant murine G6PI and denatured rhG6PI suggesting that the biologic functions of the enzyme are irrelevant for the disease.<sup>123</sup> Immunization with other components of the same expression system as G6PI such as creatine kinase or fructose-1,6-bisphosphatase in CFA did not induce any signs of arthritis. The analysis of T cells from immunized DBA/1 mice showed that they proliferated strongest after *in vitro* G6PI restimulation at day 9 and day 12 post immunization. Furthermore, CD4<sup>+</sup> cells from draining lymph nodes and spleens produced TNF $\alpha$ , IL-6 and IL-17. Almost no secretion of IFN $\gamma$ , IL-2, IL-4 or IL-10 was detectable.<sup>123</sup> To check the importance of Th cells during the different disease stages the investigators depleted CD4<sup>+</sup> cells with a monoclonal antibody at different time points and analyzed the clinical outcome. Arthritis development could be completely prevented when anti-CD4 antibodies were applied either before the immunization (day -3, day 0 and day 5 relative to immunization) or in the induction phase (day 6 and day 9 relative to immunization). The CD4 depletion at later time points, i.e. right after disease onset (day 8 and day 11 relative to immunization) as well as around the disease peak (day 11 and day 14 relative to immunization), was able to ameliorate the arthritis and lead to a rapid and stable resolution.<sup>123</sup> Thus, it was concluded that Th cells are both required for induction and during the effector phase in G6PI-induced arthritis. Antibodies against G6PI were found from day 6 on with a peak at day 9. Thereafter, the antibody titers were almost constant up until day 30 when clinical symptoms already declined. The first immunoglobulin isotypes detectable were

IgM and IgG1 at day 6. From day 9 on additional IgG2a, IgG2b and IgG3 were measured. The isotypes IgG1 (which is the pathogenic one in K/BxN arthritis) and IgG2 (which is the pathogenic one in collagen-induced arthritis) were found to have the highest concentration of all.<sup>123</sup> The early CD4 depletion also diminished the production of G6PI-specific antibodies. However, although late CD4 depletion ameliorated and cured the disease, antibody titers against G6PI were not reduced. Furthermore, a serum transfer from G6PI-immunized animals to naïve recipients did not induce arthritis. On the other hand, DBA/1 mice deficient for the Fc $\gamma$ R common  $\gamma$ -chain immunized with rhG6PI had a much lower incidence of arthritis with a much less severe clinical outcome. In contrast, DBA/1 mice deficient for the inhibitory Fc $\gamma$ RIIB showed an exacerbated arthritis pathogenesis. Thus, it was concluded that antibodies against G6PI are necessary but alone not sufficient for arthritis development in this mouse model.<sup>123</sup>

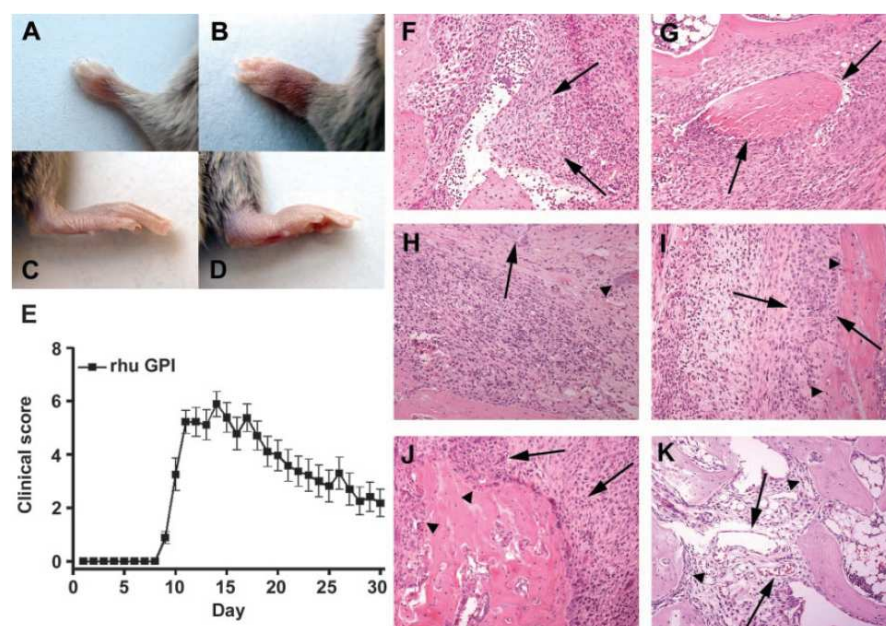


**Figure 2: Clinical course and histopathology of G6PI-induced arthritis.**

A-D shows picture of non-immunized (A,C) or G6PI-immunized (B,D) DBA/1 mice. E shows the clinical evaluation of G6PI-immunized mice for 30 days. F-K show histological analyzes of G6PI-immunized DBA/1 mice. F: Severe synovitis. Dense inflammatory infiltrates consisting of lymphocytes, plasma cells, and granulocytes within the synovial membrane (arrows) accompanied by strong activation of resident cells (fibroblasts, macrophages). G: Tenosynovitis. A dense inflammatory infiltrate around a tendon (arrows). H: Periarthritis with strong inflammatory reaction in s.c. tissue adjacent to the talocalcaneal joint. Arrow, sebaceous gland; arrowhead, hair follicle. I: Periostitis with strong stroma activation and moderate inflammatory infiltrate inside the periost (between arrows) adjacent to the shank (arrowheads). J: Bone destruction (arrowheads) mediated by pannus (arrows), consisting of strongly activated fibrous tissue. K: Regenerative process with fibroblastic synovial tissue containing small blood vessels (arrows) and osteoblasts repairing bone destruction (arrowheads). (from Schubert *et al*<sup>123</sup>)

Another important finding resulted from the treatment with Etanercept. Administration of the TNF $\alpha$ -blocking agent to G6PI-immunized mice resulted in a dose-dependent block of arthritis development showing a TNF $\alpha$ -dependency of G6PI-induced arthritis pathogenesis. Further studies revealed that the effector T cells were mainly of the Th1 and Th17 phenotype.<sup>124,125</sup> The most abundant cytokines produced during the early phase were IFN $\gamma$  and IL-17. A treatment of G6PI-immunized mice with anti-IL-17 mAb early on resulted in a

reduction of disease severity.<sup>124</sup> However, no effect on antibody titers was measurable. In addition, a supportive role of IL-6 to IL-17 production was shown. Anti-IL-6R treatment before the peak of the disease lead to a block or at least significant reduction of severity depending on the time point of administration which was accompanied by a reduction of IL-17 producing CD4<sup>+</sup> T cells. Additionally, also anti-G6PI antibodies were reduced after the blockade of the IL-6R<sup>124</sup> suggesting a supportive role of Th17 cells for antibody production by B cells in this context. Yet, a blockade of the IL-6R after the maximum of arthritis severity did not have any effect, indicating that the IL-6/IL-17 axis is mainly important during the induction phase of G6PI-induced arthritis.

To determine the role of B cells during arthritis pathogenesis in this mouse model researchers conducted two different approaches. In the first scenario Tanaka-Watanabe *et al* performed a transfer of splenocytes from G6PI-immunized DBA/1 mice into SCID mice together with 100 µg of rhG6PI. Thereby, they could show that arthritis was transferable.<sup>126</sup> More importantly, they depleted the splenocytes either of CD19<sup>+</sup> or CD4<sup>+</sup> cells and repeated the experiment. Then, arthritis induction by splenocyte transfer in conjunction with G6PI administration did not work anymore. Neither CD4 depleted nor CD19 depleted splenocytes were able to evoke any sign of arthritis. But, when CD19 depleted splenocytes were inoculated into SCID mice together with immunoglobulins purified from G6PI-immunized DBA/1 mice arthritis was efficiently induced.<sup>126</sup> Those findings were confirming the arguments that T and B cells are important for the induction of G6PI-induced arthritis and that autoantibody production is crucial. Furthermore, they could shed some light on the previously hypothesized mechanism for the induction of an organ-specific immune response by a systemic autoreactivity. Kamradt *et al* already described in a review from 2005 that anti-G6PI antibodies were localized to peripheral joints.<sup>115,127,128</sup> This was already suggested in the initial description of G6PI-induced arthritis since it was known that cationic agents can bind to negatively charged structures of joints<sup>129,130</sup> and thereby could probably provoke a locally higher concentration of the autoantigen. Matsumoto *et al* could then show a deposition of G6PI together with immunoglobulins and C3 of the complement system in arthritic joints.<sup>131</sup> Those immune complexes could be a possible explanation for the organ-specificity of the systemic autoimmunity. The same was shown in the splenocyte inoculation experiments into SCID mice. They nicely depicted the colocalization of IgG and C3 on the cartilage surface after splenocyte transfer and G6PI administration.<sup>126</sup> Thus, complement activation by immune complexes in the joint seems to be a likely scenario for local inflammation. The second approach for investigating the role of B cells in the pathogenesis of G6PI-induced arthritis was a B cell depletion via CD22.<sup>132</sup> Since the antibody they used only reacts with CD22 in strains with the Lyb-8.2 alloantigen they first had to switch to a different mouse strain. They found a similar disease progression with a more chronic course compared to DBA/1 in the strain SJ/L. Immunologic parameters such as immune cell infiltration and the generation of G6PI-specific T cell responses and antibodies was also likewise. The B cell depletion in this strain using their anti-CD22 antibody was long lasting. Lymph nodes, spleens and bone marrow were comprised of fewer cells and B cells were virtually not detectable in secondary lymphoid organs up to 2 weeks. B cell depletion prior to the immunization (at day -6 and day -1 relative to G6PI-immunization) resulted in a delayed onset with a reduced incidence and much lower clinical severity. Also in the induction phase (day 3 and day 8 relative to immunization) absence of B cells resulted in a diminished incidence and a lower disease severity. However, clinical symptoms were already more pronounced than in early treated animals. Most strikingly, a late B cell depletion (day 15 and day 20 relative to the

immunization) had no effect at all demonstrating that B cells are crucial during the early phase but dispensable for the effector stage.<sup>132</sup> A reconstitution of reduced immunoglobulin levels after B cell depletion with serum from G6PI-immunized mice could not restore the disease. Furthermore, G6PI-specific Th cells were almost 10-fold reduced after B cell depletion. Although the remaining G6PI-specific Th cells produced more cytokines the total number of cytokine producing effector T cells was also diminished. Concluding, the major role of B cells is taking place during the induction phase by autoantibody production and via a priming of Th cells.<sup>132</sup>

The next major breakthrough of the model followed in 2010 with a publication by Frey *et al.*<sup>133</sup> They tested the influence of regulatory T cells (Tregs) on the clinical progression of G6PI-induced arthritis. Therefore, DBA/1 mice were treated with anti-CD25 antibodies prior to the immunization with rhG6PI/CFA. This resulted in a reduction of FoxP3<sup>+</sup> Tregs to 10% of normal levels at the time point of immunization. This reduction was at least 50% until day 15 and thereafter Treg frequencies inclined again. After 35 days relative to the immunization the Treg pool was filled again to the normal level. Surprisingly, anti-CD25 treatment did not only deplete the CD25<sup>+</sup> but also CD25<sup>-</sup> Tregs most likely due to the interference with IL-2 signaling in general which is crucial for Treg survival. Recapitulatory, Treg depletion was incomplete and transient. Nevertheless, it had a dramatic effect on the clinical progression of the disease. Anti-CD25 treated mice did not as usual resolve after the maximum until day 40 but remained their clinical symptoms of inflammation for more than 6 weeks. Even worse, they developed heavy deformations and ankylosis. The destructive changes already occurred after 30 days indicating that this was not only resulting from prolonged inflammation. Histologic analysis revealed a denser infiltration of neutrophils, lymphocytes and macrophages. Even after more than 80 days joints were still inflamed by mononuclear cells and the pannus was densely packed with fibroblasts. This pannus had the ability to cover and invade articular cartilage and destroy subchondral bone. Thus, Treg depletion prior to G6PI immunization results in a switch from normally acute, self-limiting to non-remitting, destructive arthritis. Beyond that, anti-G6PI autoantibody titers were also enhanced to maximal at around day 80. The Treg depletion therefore also lead to a prolonged and persistent humoral autoreactivity. The generation of G6PI-specific T cells started much earlier. Already at day 3 post immunization G6PI-specific Th cell frequencies were 4-fold higher in Treg-depleted mice compared to nondepleted counterparts. Additionally, those pathogenic Th cells produced much more cytokines, such as TNF $\alpha$ , IL-2 and RANKL. Considering the increased absolute number of lymph node cells together with the higher frequency of G6PI-specific Th cells that on top showed an enhanced cytokine production one gets a summation of those effects leading to an almost 20-fold enhancement of the G6PI-specific T cell response in Treg-depleted mice at that early time point. Thereafter, the pool of G6PI-specific Th cells was expanding similarly in both experimental animal groups with a maximum around day 9. However, this pool was always larger in Treg-depleted mice. Th cells from both groups produced likewise IL-17, IFN $\gamma$  and GM-CSF. Thereafter, T cell responses slowly reduced indicating that this is not solely the cause of chronicity. G6PI-specific Th cells producing TNF $\alpha$  and RANKL were even detectable in non-immunized, Treg-depleted mice. Thus, Treg-depletion alone is sufficient to mount an autoantigen-driven T cell response. However, this was not strong enough to induce inflammation. To elucidate the role of the pathogenic effector T cells after G6PI-immunization in the course of the chronic arthritis CD4 cells were additionally depleted at different time points relative to the immunization. As before, anti-CD4 treatment before the immunization prevented the disease, both in

nondepleted and Treg-depleted individuals. Remarkably, this CD4 depletion which was usually curative in G6PI-immunized DBA/1 mice after the disease onset turned out to be ineffective in the Treg-depleted subjects. Hence, Th cells are dispensable in the effector phase of the destructive, non-remitting course of G6PI-induced arthritis. On the contrary, a therapeutic depletion of monocyte/macrophage/osteoclast cells using chlodronate liposomes cured the mice regardless of Treg-depletion. Thus, the hypothesized model includes an early burst of pathogenic Th cells enabled by Treg-depletion which causes the activation of an unknown effector cell population which uninfluenced by CD4 depletion and restoration of the Treg pool drives the chronicity of the disease.

### 1.3 FIBROBLAST-LIKE SYNOVIOCYTES

Fibroblast-like synoviocytes (FLS) or Type B synovial cells are mesenchymal, CD45-negative cells found in the intimal lining layer of joints.<sup>134</sup> In normal synovium under physiological conditions those cells serve as providers of nutrients and lubricants for the joint cavity and adjacent cartilage.<sup>134,135</sup> This includes for example the expression of uridine diphosphoglucose dehydrogenase which enables the FLS' expression of hyaluronan, one important component of the synovial fluid and extracellular matrix (ECM).<sup>136</sup> Furthermore, the secretion of lubricin facilitates joint lubrication. Another physiological function of FLS is the regulation of the flux of cells that pass into the synovial fluid space<sup>136</sup> by expressing surface adhesion receptors such as ICAM-1, VCAM-1 and CD44. The architecture of joints and joint homeostasis are (at least partly) mediated by FLS via their ECM remodeling function due to the expression of matrix components like collagen and hyaluronan as well as the expression of matrix-degrading enzymes.<sup>135,137</sup> FLS exclusively express cadherin-11 in the synovial lining<sup>138,139</sup> which is essential for maintaining the integrity of the normal synovium.<sup>140</sup> Mice deficient for cadherin-11 had a hypoplastic synovial lining<sup>138</sup> and cadherin-11 expression in FLS alone was sufficient to induce an organization into a lining layer of synovium-like structure *in vitro*.<sup>139</sup>

In RA patients instead, FLS change their phenotype leading to an expansion of the intimal lining from 1-2 cells to 10-20 cells depth<sup>134</sup> as well as the promotion of inflammation, and cartilage and bone destruction.<sup>140</sup> The following sections will describe some of the most prominent phenotypic and functional changes of FLS in RA patients contributing to the arthritis pathogenesis (see Figure 3).

First of all, the imbalance of proliferation and apoptosis of FLS in the hyperplastic rheumatoid pannus leads to an overabundance of them.<sup>140</sup> Although the increased proliferation of FLS in the RA synovium has not been directly proven yet the appearance of distinct clonal cell lines of cultured RA FLS strongly argues for a substantial growth ability of FLS in the inflamed synovium.<sup>141,142</sup> Furthermore, cultured FLS show an accelerated proliferation *in vitro* upon stimulation with growth factors (e.g. FGF or TGF $\beta$ ), cytokines (e.g. IL-1 or TNF $\alpha$ ), and chemokines (e.g. RANTES).<sup>143,144</sup> The resistance of FLS to apoptosis was shown by several criteria<sup>145</sup> and is even maintained *in vitro*.<sup>146</sup> Stimulation with TNF $\alpha$  as well as the activation of the NF $\kappa$ B pathway could reduce FLS apoptosis via resistance of FasL-induced signaling and upregulation of the expression of anti-apoptotic genes of the Bcl-2 family.<sup>147</sup> The apoptosis resistance together with growth properties like increased migration, reduced contact

inhibition and reduced attachment-dependent growth<sup>136</sup> as well as the ability to spread arthritis to distant joints *in vivo*<sup>148</sup> argue for a tumor-like behavior of RA FLS.

A second very important property of FLS in RA pathology is their ability to invade and destroy cartilage. The usual balance between matrix-degrading enzymes such as MMPs and aggrecanases and their inhibitors such as TIMP-1 is tipped towards the degradation.<sup>140</sup> Moreover, there is a synergy between protease production and adhesion molecule expression. Mice deficient for cadherin-11 for example were shown to be protected from cartilage destruction.<sup>138</sup> Different factors including pro-inflammatory cytokines (especially IL-1 and TNF $\alpha$ ), ROS and RNS as well as growth factors and ECM components can trigger the invasive phenotype of RA FLS in patients.<sup>140</sup> For example, MMP gene expression by FLS can be induced by exposure to IL-1 or TNF $\alpha$ . This can be even enhanced via a synergistic effect of IL-1 or TNF $\alpha$  with the Th17 cytokine IL-17.<sup>149</sup> The ability to erode cartilage is thought to result from intrinsic changes based on the findings in a SCID mouse model.<sup>137</sup> RA FLS were co-implanted with human cartilage under the kidney capsule of SCID mice. Histology revealed FLS-mediated cartilage erosion.<sup>150</sup> But FLS serve not only to destroy cartilage; they also mediate bone erosion by differentiation and activation of osteoclasts.<sup>151,152</sup> Osteoclastogenesis is induced by the binding of RANKL to RANK on the surface of osteoclast precursor cells. At sites of bone erosion, a high expression of RANKL on RA FLS has been shown.<sup>152</sup> The RANKL expression of FLS was further shown to be upregulated by activated T cells.<sup>153</sup> Furthermore, RANKL expression was found to be relatively restricted to sites of bone-erosion whereas the expression of osteoprotegerin (the antagonist of RANKL) was expressed at sites away from erosions. Thus, osteoclast activity is regulated by local expression pattern of those two mediators.<sup>154</sup> An additional effect of RA FLS on bone erosion was just recently found. They were shown to inhibit osteoblast activity via the inhibitor DKK-1.<sup>88</sup> Thus, FLS can actively invade and destroy cartilage and indirectly influence bone erosion by the activation of eroding osteoclasts and the inhibition of bone-forming osteoblasts.

A third change of the phenotype of RA FLS in patients is the alteration of their ability to secrete proinflammatory cytokines, chemokines and proangiogenic factors.<sup>140</sup> FLS are the primary source of IL-6 in the joint implying a therapeutic role for FLS since IL-6 inhibition was shown to decrease disease severity dramatically.<sup>134</sup> The IL-6 production of cultured RA FLS can be increased by stimulation with proinflammatory cytokines like IL-1, IL-17 or TNF $\alpha$ .<sup>155</sup> TGF $\beta$  was shown to induce IL-6 production by RA FLS as well, but also the secretion of VEGF.<sup>156</sup> Colony-stimulating factors, such as M-CSF or GM-CSF, can also be produced by RA FLS and lead to the activation of innate and adaptive immune cells in the RA joint.<sup>140</sup> The chemokine synthesis by FLS in the RA joint determines mainly the cellular composition of the rheumatoid synovium.<sup>134</sup> For example, chemokines MIP-1 $\alpha/\beta$  and RANTES produced by FLS can attract T cells and B cells (harboring CXCR3 and CCR5).<sup>157-159</sup> Numerous other chemokines secreted by RA FLS including RANTES, IP-10, MCP-1 and MIP-1 $\alpha/\beta$  lead to the recruitment of cells of the monocyte/macrophage lineage as well as neutrophils into the joint.<sup>134</sup> The stimulation of FLS in the joints of RA patients is facilitated by multiple mediators produced by other infiltrating cells as well as FLS themselves. Most important here are IL-1 and TNF $\alpha$  produced by macrophages<sup>160</sup>, IL-17 and IFN $\gamma$  secreted by T cells<sup>161</sup>, and TGF $\beta$  and IL-6 sequestered by FLS<sup>162</sup>.

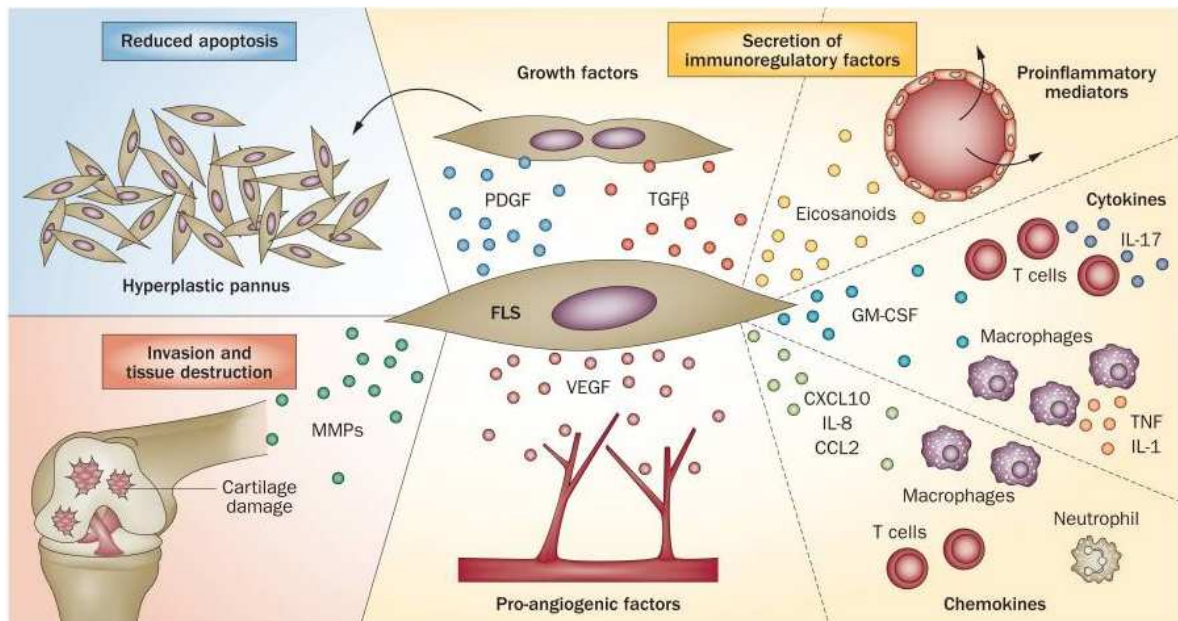


**Figure 3: Diverse role of FLS in RA.**

FLS can contribute to many processes by various kinds of mechanisms. Reduced apoptosis leads to the formation of a pannus. The Invasion and destruction of cartilage is mediated by the secretion of MMPs and other matrix-degrading enzymes. Bone erosion is facilitated by the activation of osteoclasts and the inhibition of osteoblasts. Secreted growth factors serve to enhance angiogenesis and FLS' own growth. The secretion of other immunoregulatory factors induces, maintains and enhances inflammatory responses and chemokines recruit more cells of the innate and adaptive immunity to the joint. (from Bottini and Firestein<sup>140</sup>)

Most of the insights into the role and involvement of FLS contributing to RA pathogenesis arose from studies using isolated FLS from RA patients. Mouse models for those studies are rare. Furthermore, until now there is no other mouse model apart from the G6PI-induced arthritis that allows the comparison of an acute, self-limiting with a destructive, non-remitting course.

Taken together, FLS in rheumatoid arthritis in the literature are nowadays seen as both passive responders to inflammatory stimuli and also active aggressors involved in the maintenance of inflammatory responses as well as contributors to cartilage destruction and bone erosion. However, underlying mechanisms inducing the activated phenotype of RA FLS are still poorly understood. Moreover, it is not known which cells provide those signals and at which stage during the arthritis pathogenesis these changes occur. Most important, it has not yet been addressed and shown if activated FLS alone can drive the chronicity of RA without the help of the adaptive or innate immunity.

## 1.4 AIM OF THIS STUDY

As introduced in 1.2 G6PI can induce an acute, self-limiting course of arthritis in susceptible DBA/1 mice. This can be switched to a non-remitting, destructive one by Treg-depletion prior to the immunization. Furthermore it was shown that B cells and antibodies are necessary for the arthritis induction but alone not sufficient. In the effector phase the B cells seem to play a minor role. An early depletion of CD4<sup>+</sup> cells can prevent the arthritis development in both nondepleted and Treg-depleted animals. However, after the onset of symptoms this CD4<sup>+</sup> cell depletion is ineffective in Treg-depleted mice whereas it rapidly resolves the signs of inflammation in the nondepleted ones. Moreover, Treg-depletion leads to an early burst of G6PI-specific effector T cells with enhanced cytokine production.

Thus, despite an incomplete and transient depletion of Tregs, the obvious independence from CD4<sup>+</sup> cells during the chronic effector phase, and the dispensability of B cells during a later stage of the disease Treg-depleted mice develop a destructive, non-remitting course of G6PI-induced arthritis. Hence, some other cells have to act as effector cells.

The working hypothesis for this study was the following:

The absence of Tregs during the induction phase of the disease allows the differentiation and activation of a large pool of G6PI-specific effector T cells which then instruct resident cells in the joint to become activated effector cells. Those activated effector cells which are most likely FLS gain subsequently independence from the help of adaptive immune cells to autonomously drive the chronicity of the disease.

To test this hypothesis the following topics were addressed:

1. Do FLS from Treg-depleted and nondepleted G6PI-immunized DBA/1 mice display phenotypic and functional differences and do FLS from Treg-depleted animals gain an activated phenotype?
2. If yes, do they also gain independence from the adaptive immunity and can they drive an immune reaction autonomously?
3. If yes, how are those activated FLS instructed?

The long-term goal of the project would then be to translate this information into causative and, in perspective, curative therapeutic strategies.

## 2. MATERIALS

### 2.1 BIOLOGICAL MATERIAL

#### 2.1.1 MICE

Mice of the strains DBA/1 Ola Hsd, DBA/1 DREG, DBA/1 Rag1<sup>-/-</sup> and B6.NQ were used. All mice were bred and maintained in our animal facility. All experiments were approved by the appropriate governmental authority (Thüringer Landesamt für Lebensmittelsicherheit und Verbraucherschutz; registration number 02-002/10) and conducted in accordance with institutional and state guidelines.

Animals were used at the age of 7 – 14 weeks, both male and female. Only one type of sex was used for each experiment.

#### 2.1.2 CELLS

All cultured cells were either primary cultures isolated from murine organs or immortalized cell lines according to Table 2.

**Table 2: Cell cultures**

Cell type	Source
Splenocytes, primary culture	murine spleens
lymphocytes, primary culture	murine lymph nodes
fibroblast-like synoviocytes, primary culture	small joints of the paws and ankle joint
MDCK-C7 cell line	canine kidney epithelial cells

### 2.2 KITS AND CHEMICALS

This section lists chemicals and kits that are not listed in any other section.

**Table 3: Kits**

Kit	Source
Anti-Rat and Anti-Hamster Ig $\kappa$ /Negative Control Compensation Particles Set	BD Biosciences, USA
LIVE/DEAD® Fixable Aqua Dead Cell Stain Kit, 405 nm excitation	life technologies, USA

**Table 4: Chemicals**

Chemical	Source
0,25 % trypsin/EDTA	Sigma-Aldrich, USA
0,4 % trypan blue	Sigma-Aldrich, USA
70 % ethanol	University hospital pharmacy
Mayer's haemalaun	Merck Millipore, Germany
0,9 % NaCl	B.Braun, Germany

## 2.3 ANTIBODIES, STANDARDS AND CYTOKINES

### 2.3.1 *IN VIVO* PROTEINS, ANTIBODIES AND TREATMENTS

**Table 5: List of compounds used for *in vivo* experiments**

Compound	Source
recombinant human G6PI	in house production
Complete Freund's adjuvant	Sigma-Aldrich, USA
diphtheria toxin	Merck Millipore, Germany
anti-IL-17A	in house production, clone MM17F3
IL-1 $\beta$	Peptotech, USA

### 2.3.2 ELISA ANTIBODIES AND STANDARDS

**Table 6: List of ELISA antibodies and standards**

Compound	Source	Concentration
IL-6 capture antibody	ebioscience, USA	4 $\mu$ g/ml
IL-6 detection antibody	ebioscience, USA	1 $\mu$ g/ml
recombinant IL-6 (standard)	Peptotech, USA	5000 – 19,5 pg/ml
Streptavidin-POD	Roche, Switzerland	50 ng/ml

**Table 7: List of ELISA Sets**

Mouse Total MMP-3 DuoSet	R&D Systems, USA
Mouse Total MMP-9 DuoSet	R&D Systems, USA
Mouse TIMP-1 DuoSet	R&D Systems, USA
Mouse CCL3/MIP-1 alpha DuoSet	R&D Systems, USA
Mouse CCL4/MIP-1 beta DuoSet	R&D Systems, USA
Mouse CCL5/RANTES DuoSet	R&D Systems, USA

## 2.3.3 FLOW CYTOMETRY ANTIBODIES

Table 8: DEREg typing staining

Compound	Source	Dilution
CD4 – PacificBlue	in house production, clone GK1.5	1:200
CD25 – Dy647	in house production, clone PC61.5	1:100
anti – CD16/CD32	in house production, clone 2.4G2	1:100
rat IgG	Jackson Immunoresearch, USA	1:200

Table 9: T cell staining

Compound	Source	Dilution
CD4 – APC/Cy7	ebioscience, USA	1:200
CD154 – APC	Miltenyi biotec, Germany	1:40
IL-17 – Alexa488	ebioscience, USA	1:200
IFN $\gamma$ – PE	ebioscience, USA	1:200
TNF $\alpha$ – eFluor450	ebioscience, USA	1:200
anti – CD16/CD32	in house production, clone 2.4G2	1:100
rat IgG	Jackson Immunoresearch, USA	1:200

Table 10: Joint cell staining

Compound	Source	Dilution
CD45 – AF700	Biolegend, USA	1:200
CD4 – PE/Cy7	ebioscience, USA	1:600
CD8 – PE/Cy7	ebioscience, USA	1:300
B220 – PacificBlue	in house production, clone RA3-6B2	1:200
Ly6G – APC	ebioscience, USA	1:200
CD11b – FITC	ebioscience, USA	1:400
CD11c – Pe/Cy5.5	ebioscience, USA	1:500
CD90 – APC eFluor780	ebioscience, USA	1:200
anti – CD16/CD32	in house production, clone 2.4G2	1:100
rat IgG	Jackson Immunoresearch, USA	1:200

Table 11: FLS staining

Compound	Source	Dilution
CD90 – APC/Cy7	ebioscience, USA	1:200
CD11b – AF700	ebioscience, USA	1:800
CD54 – APC	Biolegend, USA	1:300
CD106 – PE/Cy7	Biolegend, USA	1:250
anti – CD16/CD32	in house production, clone 2.4G2	1:100
rat IgG	Jackson Immunoresearch, USA	1:200

### 2.3.4 CELL CULTURE ANTIBODIES, CYTOKINES AND TREATMENTS

**Table 12: List of cell culture compounds**

Compound	Source	Concentration
recombinant human G6PI	in house production	20 µg/ml
anti – CD28	in house production, clone 37.51	3 µg/ml
anti – CD3	in house production, clone 154-2C11	3 µg/ml
Brefeldin A	Sigma-Aldrich, USA	5 µg/ml
IL-1β	Peprotech, USA	10 ng/ml
IL-17A	Peprotech, USA	50 ng/ml
IL-33	Peprotech, USA	50 ng/ml
TNFα	Peprotech, USA	10 ng/ml
poly(I:C)	Sigma-Aldrich, USA	10 µg/ml
peptidoglycan (PGN)	Sigma-Aldrich, USA	1 µg/ml
FGF-2	Peprotech, USA	10 ng/ml
ascorbic acid	Sigma-Aldrich, USA	100 ng/ml

### 2.4 DEVICES, EQUIPMENT AND SOFTWARE

**Table 13: devices**

Device	Model, company
table-top centrifuge	Megafuge 1.0R; Heraeus, Germany
sonicator	Sonopuls HD 60; Bandelin, Germany
mouse restrainer	self-made
ELISA plate washer	Hydroflex 96-well microtiter plate washer; Tecan, Switzerland
ELISA plate reader	Spectra 96-well microtiter plate reader; Tecan, Switzerland
Humidified incubator	Hera cell240; Heraeus, Germany
laminar flow hood	Hera safe, Heraeus, Germany
water bath	julabo U3; julabo, Germany
flow cytometer	LSR II; BD Biosciences, USA
orbital shaker	Easia shaker; Thermo Fisher Scientific (Medgenix diagnostics), USA
bidirectional rotator	HS 260 basic; IKA, Germany
TEER device	EVOM <sup>2</sup> ; WPI, USA
electrophoresis chamber	Mini PROTEAN <sup>®</sup> 3 Cell; Bio-Rad, USA
Power supply	EV261; Consort, Belgium

**Table 14: equipment**

Equipment	Model, company
70 µm cell strainer	BD Falcon, USA
Cell counting chamber	Neubauer chamber; BRAND, Germany
FACS tubes	round-bottom tubes, 5 ml, 12 x 75 mm; BD Falcon, USA
15 ml/ 50 ml tubes	greiner bio-one, Austria
cell culture plates, dishes and flasks	greiner bio-one, Austria
cryo-tubes	greiner bio-one, Austria

Continuation of Table 14: equipment

culture inserts (MATRIN)	BD Falcon, USA
6-well plates (MATRIN)	BD Falcon, USA
ELISA plates	Maxisorp 96-well microtiter plates; Thermo Fisher Scientific, USA
blood lancet	B.Braun, Germany
hematological test tube	Sarstedt, Germany
syringes	Single-use syringes Omnifix®-F, 1ml; B.Braun, Germany Omnican® F Fine dosage syringe, 1 ml; B.Braun, Germany Omnican® 20 Insulin syringe; B.Braun, Germany
needles	Disposable needle 0,50 x 16 mm/25 G x 5/8" (B.Braun, Germany) Disposable needle 1,20 x 40 mm/18 G x 1½" (B.Braun, Germany)
animal disinfectant	Softafept® N, B.Braun, Germany

## 2.6 CELL CULTURE MEDIA, BUFFERS AND SOLUTIONS

### 2.6.1 CELL CULTURE MEDIA

Table 15: Cell culture media

Medium	Components
T cell medium	IMDM with 25 mM Hepes and w/o L-glutamin (Lonza, Switzerland) 10 % FCS (Sigma-Aldrich, USA) 100 U/ml Penicillin/Streptomycin (Jena Bioscience, Germany) 50 µM 2-Mercaptoethanol (Gibco, life technologies, USA)
FLS medium	DMEM with 4,5 g/l glucose, L-glutamine, NaHCO <sub>3</sub> (Sigma-Aldrich, USA) 10 % FCS (Sigma-Aldrich, USA) 100 U/ml Penicillin/Streptomycin (Jena Bioscience, Germany) 10 mM Hepes (Serva, Germany)
MDCK medium	MEM with Earl's salts, L-glutamine and NaHCO <sub>3</sub> (Sigma-Aldrich, USA) 10 % FCS (Sigma-Aldrich, USA) 100 U/ml Penicillin/Streptomycin (Jena Bioscience, Germany) 10 mM Hepes (Serva, Germany)

### 2.6.2 BUFFERS AND SOLUTION

Table 16: Flow Cytometry

Buffer	Components
10x Phosphate buffered saline (PBS)	137 mM NaCl (Carl Roth, Germany) 2,7 mM KCl (Carl Roth, Germany) 1,5 mM KH <sub>2</sub> PO <sub>4</sub> (Merck, Germany) 7,9 mM Na <sub>2</sub> HPO <sub>4</sub> x 2 H <sub>2</sub> O (Applichem, Germany) dissolved in ddH <sub>2</sub> O, diluted to 1x PBS in ddH <sub>2</sub> O

Continuation of Table 16: Flow Cytometry

erythrocyte lysis buffer	0,01 M $\text{KHCO}_3$ (VWR, USA) 0,15 M $\text{NH}_4\text{Cl}$ (Carl Roth, Germany) 0,1 mM EDTA (Sigma-Aldrich, Germany) dissolved in ddH <sub>2</sub> O pH adjusted to 7,5 filter-sterilized
PBA	0,25 % BSA (Albumin Fractin V; Carl Roth, Germany) 0,02 % sodium azide (Sigma-Aldrich, USA) diluted in 1x PBS
4 % PFA stock solution	40 g PFA (Sigma-Aldrich, USA) dissolved in 1 l 1x PBS stirring at 50°C over night cleared with NaOH filter-sterilized diluted to 2 % PFA in 1x PBS
PBA-S	0,5 % saponine (Carl Roth, Germany) diluted in PBA
PBA-E	1 mM EDTA (Sigma-Aldrich, USA) diluted in PBA

Table 17: ELISA

Buffer/Solution	Components
10x PBS	see Table 16
PBS-T	0,05 % Tween 20 (Carl Roth, Germany) dissolved in 1x PBS
blocking solution	2 % BSA (Albumin Fraction V; Carl Roth, Germany) dissolved in PBS
substrate buffer	0,2 M $\text{Na}_2\text{HPO}_4 \times 2 \text{ H}_2\text{O}$ (Applichem, Germany) 0,1 M citric acid (Carl Roth, Germany) dissolved in ddH <sub>2</sub> O pH adjusted to 5,0
substrate solution	10 mg OPD (Sigma-Aldrich, USA) 5 µl of 30% $\text{H}_2\text{O}_2$ (Sigma-Aldrich, USA) dissolved/diluted in 5 ml substrate buffer
stop solution	1,5 M $\text{H}_2\text{SO}_4$ (Carl Roth, Germany) diluted in ddH <sub>2</sub> O
Reagent Diluent (for R&D DuoSets)	1 % BSA dissolved in 1x PBS

Table 18: Zymography

Buffer/Solution	Components
10 % APS	5 g ammonium persulfate (Sigma-Aldrich, USA) dissolved in 50 ml ddH <sub>2</sub> O
4 x separation gel buffer	1,5 M Tris-HCl (Carl Roth, Germany) 0,4 % SDS (Carl Roth, Germany) dissolved/diluted in ddH <sub>2</sub> O pH adjusted to 8,8
4 x stacking gel buffer	0,5 M Tris-HCl (Carl Roth, Germany) 0,4 % SDS (Carl Roth, Germany) dissolved/diluted in ddH <sub>2</sub> O

Continuation of Table 18: Zymography

10x running buffer	250 mM Tris (Tris base; Carl Roth, Germany) 2 M glycine (Carl Roth, Germany) 1 % SDS (Sigma-Aldrich, Germany) dissolved/diluted in ddH <sub>2</sub> O
6x native sample buffer	375 mM Tris (Tris base; Carl Roth, Germany) 12 % SDS (Sigma-Aldrich, Germany) 30 % glycerol (Carl Roth, Germany) 0,001 % bromophenol blue (Applichem, Germany)
washing buffer	2,5 % Triton-X100 ( diluted in ddH <sub>2</sub> O
incubation buffer	100 mM Tris-HCl (Carl Roth, Germany) 30 mM CaCl <sub>2</sub> ( 0,02 % sodium azide (Sigma-Aldrich, Germany) dissolved/diluted in ddH <sub>2</sub> O
Coomassie blue staining	10 % acetic acid 50 % methanol 0,25 % Coomassie blue G250 dissolved/diluted in ddH <sub>2</sub> O
destainer	25 % methanol 7 % acetic acid diluted in ddH <sub>2</sub> O

Table 19: cell culture, *in vivo*, others

Buffer/solution	Component
collagen IV solution	1 mg/ml collagen type IV dissolved in FLS medium
freezing solution	10 % DMSO diluted in FCS (Sigma-Aldrich, USA)
MDCK buffer	0,2 g EDTA 0,2 g KCl (Carl Roth, Germany) 0,2 g KH <sub>2</sub> PO <sub>4</sub> (Merck, Germany) 8 g NaCl (Carl Roth, Germany) 1,15 g Na <sub>2</sub> HPO <sub>4</sub> x 2 H <sub>2</sub> O (Applichem, Germany) dissolved in 1 l ddH <sub>2</sub> O filter-sterilized
MATRIN coating solution	10 µl sodium bicarbonate 20 µl 10x MEM with Earl's salts and l-glutamin 75 µl PureCol
5,5 % formalin solution	125 ml 40 % Formaldehyde (Carl Roth, Germany) 875 ml ddH <sub>2</sub> O 8 g Na <sub>2</sub> HPO <sub>4</sub> x 2 H <sub>2</sub> O (Applichem, Germany) 3,75 g KH <sub>2</sub> PO <sub>4</sub> (Merck, Germany)

## 3. METHODS

### 3.1 METHODS OF CELL BIOLOGY

#### 3.1.1 ISOLATION OF CELLS

##### **3.1.1.1 spleen and lymph nodes**

Spleens and lymph nodes (axillary, brachial, inguinal) were carried in T cell medium after dissection. Afterwards, the organs were smashed through a 70  $\mu$ m cell strainer with a syringe plunger. The strainer was then washed with 10 ml T cell medium. Cells were pelleted by centrifugation at 300 x *g* for 6 min at 4°C. Supernatants were discarded. Spleen cell samples were resuspended in 1 ml erythrocyte lysis buffer and incubated for 4 min at room temperature. Lysis was stopped by the addition of 10 ml T cell medium and cells were centrifuged as above. Cell pellets (both spleen and lymph node) were resuspended in 5 ml T cell medium and counted in a Neubauer chamber using trypan blue for dead cell discrimination. The single cell suspensions were adjusted to the desired cell concentration by the addition of the according volume of T cell medium.

##### **3.1.1.2 blood**

A volume of 100-500  $\mu$ l of mouse blood was mixed with 1 ml erythrocyte lysis buffer and transferred into 5 ml FACS tubes which already contained 1 ml of erythrocyte lysis buffer. The cell suspension was incubated for 4 min at room temperature. Lysis was stopped by the addition of 2 ml PBA. Samples were centrifuged for 6 min at 4°C and 300 x *g*. The supernatants were discarded. Samples were washed twice by centrifugation as above with 1 ml PBA and used for further experiments.

##### **3.1.1.3 joint cells**

The skin as well as muscle tissue and tendons of dissected fore and hind limbs were removed. The foremost toe segment was removed by overexpansion of the interphalangeal joint. Paws were retrieved by overexpansion and torsion of the ankle joint. Extreme care was taken not to damage the bone. Paws were stored in ice cold PBS until all samples were prepared. Subsequently, paws were digested in collagen IV solution for 90-100 min in a 37°C water bath with vigorous stirring. Last, the solution was transferred to 50 ml tubes and centrifuged at 250 x *g* for 10 min at room temperature. Cell pellets were resuspended in FLS medium and plated for culture.

### 3.1.2 CELL CULTURE

All cell culture work was performed under sterile conditions. All tools and materials were autoclaved before usage. Additionally, tools were sprayed with 70 % ethanol prior to their usage. All work was performed under a sterile laminar flow hood. All cells were cultured at 37°C and 5% CO<sub>2</sub> in their appropriate cell culture media.

#### 3.1.2.1 *In vitro* restimulation of G6PI-specific T cells

Single cell suspensions of spleens and lymph nodes were adjusted to 5 x 10<sup>6</sup> cells /ml in T cell medium. 1 ml of the cell suspension was plated into 24-well plates. Samples were stimulated with 20 µg/ml of rhG6PI and 3 µg/ml of anti-CD28. Remaining samples were pooled and used as positive and negative controls. The negative control was only stimulated with 3 µg/ml of anti-CD28. The positive control was additionally stimulated with 3 µg/ml of anti-CD3. All samples were incubated for 2 h in a humidified incubator at 37°C and 5% CO<sub>2</sub>. Subsequently, 5 µg/ml of Brefeldin A was added to each sample to block the secretion of cytokines by the ER-golgi system. After additional 4 h incubation time, samples were harvested for further analysis.

#### 3.1.2.2 Culture of fibroblast-like synoviocytes

Fibroblast-like synoviocytes were plated in FLS medium in 15 cm petri dishes with periodic medium exchange based on the medium's indicator. Cells were grown until confluence was reached. Then, cells were splitted 1:2 by removal of the old medium, flushing the plate with prewarmed PBS and detaching the cells using trypsin/EDTA. After washing the cells by centrifugation at 250 x *g* for 10 min at room temperature cells were plated again und cultured further. After the third passage FLS were detached as described and cell pellets were resuspended in FCS with 10% DMSO. Cell solutions were transferred into cryo-freezing tubes and stored for two days at -80°C. Finally, tubes were transferred into liquid nitrogen tanks and stored for future experiments.

For restimulation analysis FLS were counted and adjusted to 10<sup>5</sup> cells/ml. 1 ml of the cell suspension was seeded into the wells of a 24-well plate. Stimuli were added according to Table 12. Cultures were incubated for 24 h and supernatants were harvested for further analysis.

#### 3.1.2.3 Culture of MDCK-C7 cells

MDCK-C7 cells were cultured in T75 flasks in MDCK medium until confluence was reached. Then, cells were splitted 1:10 by incubation in MDCK buffer for 45 min at 37°C, detachment by incubation in trypsin/EDTA for additional 5 min and washed by centrifugation in MDCK medium.

### 3.1.3 FLOW CYTOMETRY

All flow cytometry measurements were conducted on a BD LSR II flow cytometer with proper compensation using the Anti-Rat and Anti-Hamster Ig  $\kappa$  /Negative Control Compensation Particles Set. The flow cytometer was regularly calibrated using the instrument's software (BD FACS Diva 5) for baseline calibration (four times per year) and performance check (monthly) as well as maintained according to the manufacturer's advice (cleaning of the whole system). Analysis of the recorded samples was performed using the FlowJo VX software and calculations have been made with Microsoft Excel 2010. The generation of graphs was done with SigmaPlot 12.5.

#### 3.1.3.1 Determination of G6PI-specific T cells

For the determination of G6PI-specific T cells the expression of CD154 on *in vitro* G6PI-restimulated splenocytes and lymph node cells was measured. Therefore, restimulated samples were harvested into labeled 5 ml FACS tubes containing 1 ml of PBS. After a centrifugation at 300 x *g* for 6 min at 4°C supernatants were discarded. Pellets were resuspended in the remaining liquid. LIVE/DEAD® Fixable Aqua Dead Cell Stain was diluted 1:250 in PBS and 25  $\mu$ l of the dilution was added to each sample. After an incubation of 30 min at 4°C in the dark samples were washed twice by centrifugation in PBS. Subsequently, samples were fixed for 20 min in 200  $\mu$ l of 2 % PFA on ice followed by an additional washing step. Then, cells were stored up to 3 days in the fridge. Thereafter, samples were washed twice in 1 ml PBA-S by centrifugation to permeabilize the cell membrane. Next, unspecific binding was blocked by the addition of anti-CD16/CD32 and rat IgG in PBA-S for 10 min at 4°C followed by the staining of the samples with anti-CD4, anti-CD154, anti-IL17A, anti-IFN $\gamma$  and anti-TNF $\alpha$  in PBA-S for 20 min at 4°C. At last, samples were washed and resuspended in 200 – 500  $\mu$ l PBA for analysis on the flow cytometer.

#### 3.1.3.2 Staining of fibroblast-like synoviocytes

Cells isolated directly from the joints as well as cultured FLS were washed twice in PBA-E by centrifugation at 250 x *g* for 10 min at room temperature. Afterwards, samples were blocked with anti-CD16/CD32 and rat IgG and stained with anti-CD90, anti-CD11b, anti-CD45, anti-CD4, anti-CD8, anti-Ly6G, anti-CD54 and anti-CD106 in PBA-E for 20 min at 4°C in the dark. Last, samples were washed once by centrifugation in PBA-E and resuspended in 500  $\mu$ l PBA-E for analysis on the flow cytometer.

### 3.1.4 CARTILAGE ATTACHMENT ASSAY

To determine the ability of FLS to attach to wild type articular cartilage femoral head cartilages ("caps") were dissected as described by Stanton *et al*<sup>163</sup>. Prepared caps were placed in the wells of a 96-well u-bottom plate and incubated for 24 h in FLS medium supplemented with 100  $\mu$ g/l ascorbic acid at 37°C and 5% CO<sub>2</sub>. After three washing steps with serum-free FLS medium cartilages were incubated additional 24 h in serum-free FLS medium

supplemented with 1 ng/ml IL-1 $\beta$  at 37°C and 5% CO<sub>2</sub>. Subsequently, the medium was removed and replaced by 200  $\mu$ l fresh FLS medium containing 6 x 10<sup>5</sup> FLS. Samples were incubated for 2 h at 37°C with rotation (160 rpm) on an orbital shaker. Thereafter, an additional incubation of 12 h at 37°C and 5% CO<sub>2</sub> was done. Next, the medium was removed and samples were fixed in 4 % PFA for 20 min at room temperature. Last, samples were washed three times with PBS and stained with Mayer's haemalaun for 1 min at room temperature. After several washing steps with tap water, samples could be analyzed under a stereo microscope. Pictures were taken at several z-layers with a camera and stacked for a complete picture using the ProgRes Capture Pro v2.8.0 software. Those pictures were then used to count attached FLS.

### 3.1.5 MATRIX-ASSISTED TRANSEPITHELIAL RESISTANCE INVASION (MATRIN) ASSAY

To measure the destructive potential of FLS the MATRIN assay was performed as described by Wunrau *et al*<sup>164</sup>. Cell culture inserts for 6-well plates were incubated for 90 min at 37°C and 5% CO<sub>2</sub> after apical coating with MATRIN coating solution. Next, inserts were placed upside-down onto petri dishes and 500  $\mu$ l of MDCK-C7 cell solution were applied on the basal side of the cell culture inserts and incubated for 4 h at 37°C and 5% CO<sub>2</sub>. Afterwards, cell culture inserts were placed back into the 6-well plate and filled with 2,5 ml MDCK medium. The wells of the 6-well plate were also filled with 2,5 ml MDCK medium. The plates were kept in a humidified incubator with daily medium exchange until the electrical resistance on the membrane of the cell culture insert reached at least 2,5 k $\Omega$ . At that time, FLS were diluted in FLS medium to 1,2 x 10<sup>6</sup> cells/ml and 500  $\mu$ l of medium in the cell culture insert was replaced by 500  $\mu$ l of FLS suspension. Thereafter, no more medium exchange was possible due to the sensitivity of the system. The transepithelial electrical resistance (TEER) was measured with the EVOM<sup>2</sup> and the according electrode every 4-5 h for up to 5 days. Therefore, the electrode was sterilized with 70% ethanol and stored in 0,9% NaCl while not in use. The 0,9% NaCl solution was also used to determine the blank. The values were noted and TEER break-down was calculated using SigmaPlot 12.5.

## 3.2 METHODS OF MOLECULAR BIOLOGY

### 3.2.1 ENZYME-LINKED IMMUNOSORBENT ASSAY (ELISA)

For all ELISA experiments supernatants were used that had been stored at -20°C. All supernatants were never thawed and frozen again but were only for single use.

The IL-6 ELISA was performed using matching-pair antibodies. Therefore, NUNC maxisorb 96-well plates were coated over night at 4°C with the IL-6 capture antibody diluted in PBS. Then, plates were washed three times with an automated plate washer using PBS-T. Next, plates were blocked for 2 h at room temperature with 200  $\mu$ l/well of PBS with 2% BSA followed by three washing steps. Standard (recombinant murine IL-6) as well as samples were diluted in FLS medium and filled in a total volume of 50  $\mu$ l as duplicates into the wells. Plates were incubated for 2 h at room temperature. After additional three washing steps the

detection antibody diluted in PBS-T with 1% BSA was applied into the wells and incubated for 2 h at room temperature. Again, plates were washed three times as before and incubated for 40 min with 100  $\mu$ l/well of streptavidin-POD in PBS-T with 1% BSA at room temperature. Then, plates were again washed three times. Last, 50  $\mu$ l/well of substrate solution was added and the reaction was stopped after 2-5 min with 100  $\mu$ l/well of 1,5 M  $\text{H}_2\text{SO}_4$ . Finally, the absorbance at 492 nm with a reference wavelength of 620 nm was recorded using a TECAN microplate reader with the Magellan software. Calculations were done with Microsoft Excel 2010 and graphs were plotted using SigmaPlot 12.5.

The chemokine and MMP ELISA experiment were performed using R&D Systems ELISA DuoSets. Basically, all steps were similar to the IL-6 ELISA with some exceptions. Incubation with the capture antibody was not at 4°C but at room temperature. Blocking of the plates was only 1 h in PBS with 1% BSA. Detection antibody was diluted in PBS with 1% BSA. As conjugate a streptavidin-HRP provided by the kits was used at a 1:200 dilution in PBS with 1% BSA and incubated for only 20 min. The incubation with the substrate solution was done for 5-10 min. Measurement and analysis of the samples was exactly the same as for the IL-6 ELISA.

### 3.2.2 LUMINEX MULTIPLEX ASSAY

The cytokine levels in the supernatants of cultured FLS were measured using the Luminex-based multiplex technology by collaboration partners from Hannover (Prof. Chr. Falk). The assay was performed according to the manufacturer's instructions. Briefly, 25  $\mu$ l of culture supernatant was diluted with 25  $\mu$ l of sample diluent and incubated with color-coded beads covered with capture antibodies for the respective cytokines and chemokines. After 1 h incubation and washing, bead-bound cytokines were quantified by biotinylated detection antibodies followed by streptavidin-PE staining. Concentrations were measured by parallel standard curves for each parameter and the 5 parameter logistic plot for linear regression based on the MFI of 50-100 beads per cytokine per sample using the BioPlex Manager 6.1 software. Data was plotted using SigmaPlot 12.5.

### 3.2.3 GELATIN-ZYMOGRAPHY

For gelatin zymography a separation gel and a stacking gel were prepared according to the Table 20. The water was supplemented with 2 mg/ml gelatin; final concentration in the gel was 0,8 mg/ml. A volume of 10  $\mu$ l of supernatants was mixed with 2  $\mu$ l of 6x native sample buffer and pipetted into the slots of the stacking gel. A molecular weight marker was run in one lane. Electrophoresis was run at 15 mA/gel until the 50 kDA band of the molecular weight marker reached the end of the gel. Afterwards, the gel was washed twice for 20 min on a bidirectional rotator in 2,5% Triton-X100. Gels were incubated in incubation buffer overnight at 37°C. The next day, gels were stained with Coomassie blue staining solution for 45 min on a bidirectional rotator. Finally, gels were destained until white bands were visible, dried in a frame and scanned for analysis. Quantification of the bands was conducted using the ImageJ software and Microsoft Excel 2010. Plots were generated with SigmaPlot 12.5.

**Table 20: Zymography gels**

<b>Gel</b>	<b>Components</b>
8 % separation gel	4,7 ml ddH <sub>2</sub> O/gelatin solution 2,7 ml Rotiphorese Gel 30 (Carl Roth, Germany) 2,5 ml 4x separation gel buffer 100 µl 10 % APS 8 µl TEMED
5 % stacking gel	1,16 ml ddH <sub>2</sub> O/gelatin solution 0,33 ml Rotiphorese Gel 30 (Carl Roth, Germany) 0,5 ml 4x stacking gel buffer 10 µl 10 % APS 1 µl TEMED

### 3.3 ANIMAL EXPERIMENTS

#### 3.3.1 BLEEDING OF ANIMALS

Mice were held at the neck skin fold with the thumb and the forefinger and the tail was gripped between the third finger and the ball of the thumb. The facial vein was pricked with a lancet. Blood was collected into EDTA-containing hematological test tubes.

#### 3.3.2 GENOTYPING OF DEREK MICE

Blood was used to genotype DBA/1 DEREK mice and prepared for staining as described above. Cells were stained with anti-CD4 and anti-CD25 antibodies for 20 min at 4°C. Afterwards, cells were washed by centrifugation at 300 x *g* for 6 min at 4°C and resuspended in 200 µl PBA. Analysis of the cells was performed on a BD LSR II flow cytometer recording at least 20000 cells. The fluorescence of eGFP by CD4<sup>+</sup> CD25<sup>+</sup> cells was used to determine the genotype of the mice. Transgene positive animals showed an eGFP fluorescence in the CD4<sup>+</sup> CD25<sup>+</sup> cell compartment whereas transgene negative ones did not.

#### 3.3.3. IMMUNIZATION OF MICE

For immunization of mice a standard emulsion containing 400 µg/ml rhG6PI in CFA was prepared. Therefore, rhG6PI resuspended at a concentration of 4 mg/ml in PBS was emulsified at a ratio of 1:1 with CFA by sonification (70 % power, 70 % cycles). The emulsion was filled into a syringe using a 18 G x 1½" needle. Then, the needle was exchanged to 25 G x 5/8". Mice were firmly placed into a mouse restrainer. The tail base was disinfected with Softasept® N. A total volume of 200 µl of the emulsion was injected each left and right of the tail base subcutaneously. Afterwards, the tail base was cleaned from remaining emulsion and disinfected again. Thus, all mice received 400 µg of rhG6PI in CFA.

### 3.3.4 INTRAPERITONEAL TREATMENT OF MICE

The administration of DTx or anti-IL-17A was performed intraperitoneally in PBS. Therefore, mice were held in a supine position. The syringe was inserted into the abdomen almost parallel to the vertebral column and pushed in at an approximate angle of 10°.

The DTx treatment was done 2 and 1 days before as well as 4 and 5 days after the immunization. Each mouse received 0,5 µg of DTx in a total volume of 50 µl per injection

The anti-IL-17A was administered in 100 µl at a concentration of 3 mg/ml. Preventively treated animals received injections at day 0, 3 and 6. Therapeutically treated mice received injections at day 10, 13 and 16.

### 3.3.5 CLINICAL SCORING OF MICE

For clinical scoring of G6PI-immunized DBA/1 mice each paw was divided into three sections a, b, and c. Section a includes the fingers/toes. Section b comprises the middle region of the paw, i.e. the region from the metacarpophalangeal (MCP) joints including metacarpals and metatarsophalangeal (MTP) joints including metatarsi. Section c is the region around the carpal-metacarpal/tarsal-metatarsal joints (see Figure 4).

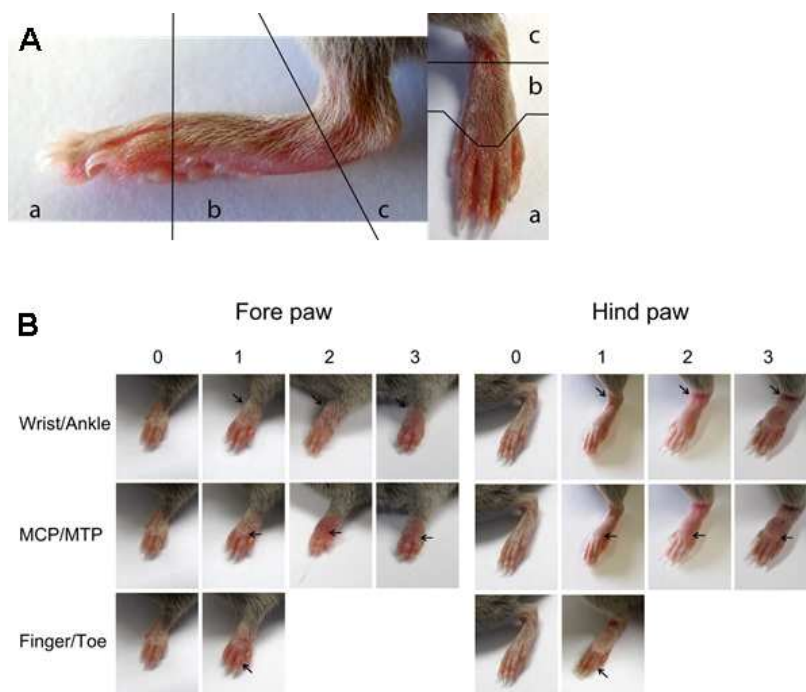


**Figure 4: Clinical scoring of inflammation in the paws.**

A) Hind paw showing the three sections for clinical scoring; namely a for finger/toe region, b for MCP/MTP and c for wrist/ankle. B) Inflammation in the joints of fore and hind paws, reflected by swelling and redness, can be graded according to a macroscopical score ranging from 0-3 for Wrist/Ankle and MCP/MTP joints. Furthermore, the absolute number of fingers and toes with inflamed phalangeal joints is determined.

In section a swollen toes/fingers were counted. Each swollen toe/finger got a score of 0,5. The score of all four paws was summated. In sections b and c there was a discrimination of three steps. Redness and mild swelling received 1 point, medium to strong swelling got 2 points and severe swelling with edema was scored with 3 points. Again, the values of all four paws were summated. At the end, the scores of all three regions were added up, and plotted using SigmaPlot 12.5.

### 3.3.6 DISSECTIONS

Mice were sacrificed by cervical dislocation and disinfected with 70% ethanol.

For the dissection of spleens and lymph nodes animals were fixed in a supine position on a soft plate with needles through the paws. The peritoneum was opened with a scissor and inguinal, brachial and axillary lymph nodes as well as the spleen were prepared with forceps.

For FLS isolation all four extremities were prepared. Therefore, the skin was cut at the ankle joint and peeled off in proximal direction. The limbs were amputated and stored in FLS medium until cell isolation.

For the cartilage attachment assay femoral head cartilage was dissected as described by Stanton *et al*<sup>163</sup>. Briefly, the skin was removed from the leg and the hip joint. Muscle tissue was removed around the hip joint and the femoral head was gently pulled out from the joint. The cartilage cap was then lifted with a forceps and placed into a 96-well plate.

### 3.3.7 TRANSFER OF FIBROBLAST-LIKE SYNOVIOCYTES INTO KNEE JOINTS OF RECIPIENTS

Fibroblast-like synoviocytes from the third passage were cultured as described before. Cells were *in vitro* restimulated with anti-IL-17/anti-TNF $\alpha$  for 24 h (concentrations as described in Table 12). During the same time, knee joints of the DBA/1 Rag1<sup>-/-</sup> mice were pretreated with 100 ng IL-1 $\beta$ . Thereafter, cultured FLS were detached as described before using PBS and trypsin/EDTA. Cells were counted with trypan blue for dead cell discrimination in a Neubauer chamber and adjusted to  $1,3 \times 10^7$  cells/ml. A total volume of 37,5  $\mu$ l (equating to  $5 \times 10^5$  cells) was injected into the right knee joint of the animals. The left knee joint was treated with PBS only as a control. After 2 weeks, mice were sacrificed and knee joints were dissected. After an incubation of 24 h in 5% formalin solution and a transfer to sterile water, samples were shipped to a collaborator in Erlangen (Prof. G. Schett) for histological analysis.

### 3.3.8 HISTOLOGY OF KNEE JOINTS

All histological experiments were conducted by collaboration partners at the University hospital Erlangen (Prof. G. Schett). Knee joints were decalcified in EDTA (Sigma-Aldrich). Serial paraffin sections (2 $\mu$ m) were stained with hematoxylin-eosin or for tartrate-resistant

acid phosphatase (TRAP) using a Leukocyte Acid Phosphatase Kit (Sigma) according to the manufacturer's instructions. All analyses were performed using a microscope (Nikon) equipped with a digital camera and an image analysis system for performing histomorphometry (Osteomeasure; OsteoMetrics). Scoring was done by an experienced investigator (Prof. G. Schett) blinded to the treatment groups. At least three sections were scored for each individual animal. Synovitis was scored on hematoxylin-eosin stained knee sections and graded according to the intensity of synovial inflammation (0, normal synovium, no inflammation; 1, mild inflammation with small and localized synovial infiltrates; 2, moderate inflammation with diffuse synovial infiltrates; 3, severe inflammation with synovial infiltrates and hyperplasia). Presence or absence of osteoclasts and bone erosions was assessed on TRAP-stained tissue sections.

## 4. RESULTS

### 4.1 SWITCH FROM ACUTE, SELF-LIMITING TO CHRONIC, NON-REMITTING ARTHRITIS AFTER TREG-DEPLETION IN THE DEREK MOUSE MODEL

Immunization of susceptible DBA/1 mice with the ubiquitously expressed glycolytic enzyme glucose-6-phosphate isomerase (G6PI) emulsified in complete Freud's adjuvant (CFA) induces a severe polyarthritis characterized by joint and paw swelling starting at day 9 after immunization. Following a rapid aggravation the clinical signs reach a maximum after about 2 weeks and then slowly resolve<sup>123</sup>. However, it has been previously reported that treatment with anti-CD25 antibodies prior to the immunization leads to an incomplete and transient depletion of regulatory T cells (Tregs), thereby switching the normally self-limiting course of arthritis to a chronic, non-remitting one<sup>133</sup>. Nevertheless, the application of anti-CD25 can potentially itself also interfere with the IL-2 signaling in general thereby affecting effector Th cells expressing the IL-2R $\alpha$  chain.

To circumvent this problem one can make use of the DEREK mouse model. Those mice are genetically altered in a way that they harbor a diphtheria toxin receptor and an eGFP construct under the control of the FoxP3 promoter on a BAC<sup>165</sup>. This transgenic mouse model was previously only available on the (non-susceptible) C57BL/6 background. In order to use this Treg-depletion system with the (susceptible) DBA/1 strain the DEREK construct was introduced into DBA/1 wild type mice by speed congenic breeding with C57BL/6 DEREKs. Afterwards it was tested, if the Treg-depletion with DTx in DBA/1 DEREK mice is consistent to the published data for Treg-depletion with anti-CD25 in DBA/1 wild type mice.

Wild type DBA/1 mice as well as DBA/1 DEREK mice were immunized with 400  $\mu$ g G6PI in CFA s.c. at day 0. Prior to the immunization one group of wild type DBA/1 mice received two injections of 500  $\mu$ g anti-CD25 at day -11 and day -8. One group of DBA/1 DEREK mice was treated with 0,5  $\mu$ g DTx at days -2, -1, 4, and 5. The appearance of clinical symptoms was monitored from day 8 until day 54. The Treg-depletion was measured in the blood of animals by flow cytometric analysis of FoxP3<sup>+</sup> cells. The appearance of G6PI-specific Th cells was analyzed from spleen and lymph nodes.

As depicted in Figure 5A the clinical progression did not differ between anti-CD25 treated wild type DBA/1 and DTx treated DEREK mice. As expected, all groups showed an increase of symptoms characterized by redness, swelling and erythema starting at day 9 after immunization and peaking at around day 14. The nondepleted control group recovered until around day 30 whereas animals from both Treg-depleted groups did not. They still showed arthritic symptoms after more than 50 days. Furthermore, the severity of arthritis was much higher in the Treg-depleted animals compared to the nondepleted counterparts. Differences between the nondepleted group and the Treg-depleted groups started to be highly significant ( $p < 0,001$ ) after approximately two weeks post immunization. Further observations that were made but do not appear in the clinical score are the malformation of the joints during the chronic phase of the Treg-depleted animals which were generally not seen in the nondepleted ones. Those Treg-depleted animals suffered from a symptom typical for rheumatoid arthritis patients called ulnar deviation, where the swelling of the metacarpophalangeal joints induces

a displacement of the fingers/toes towards the ulna. In addition to that, the ankle joints were stiff later than 30 days after immunization in some cases.

As already published by our group for the anti-CD25 model<sup>133</sup>, also the Treg-depletion with DTx is only transient and incomplete. At the time of immunization Treg-frequencies are reduced to approximately 0,5 % of CD4<sup>+</sup> T cells whereas in the nondepleted animals Treg-frequencies are about 8 % throughout the whole time course (Figure 5Bi). The reduction of Tregs in DERE mice is transient and already at day 2 the frequency is increasing again. Therefore, a second depletion step at days 4 and 5 was included. Regarding the FoxP3 staining Tregs are repopulating the pool of T cells until day 8 when they reach levels equal to the nondepleted animals. Though, comparing FoxP3 stainings and analysis of eGFP in CD4<sup>+</sup> T cells in the DERE animals reveals a difference in Treg frequencies. Whereas the FoxP3<sup>+</sup> CD4<sup>+</sup> cells recover early until day 8, the eGFP<sup>+</sup> CD4<sup>+</sup> cells remain reduced in the blood of those mice until day 18 (Figure 5Bii). Thus, the DTx treatment efficiently depletes the transgenic Tregs but the Treg pool is quickly repopulated by nontransgenic FoxP3<sup>+</sup> CD4<sup>+</sup> cells. Nevertheless, the Treg-depletion with DTx in DERE mice is also transient and incomplete and leads to the switch from acute, self-limiting to chronic, non-remitting arthritis as already published using the anti-CD25 depletion. The reduced presence of Tregs is associated with an early burst of G6PI-specific Th cells in the depleted animals (Figure 5C). To determine their number and frequency some of the animals of each group were sacrificed at day 3 after immunization. Spleens and draining lymph nodes were *ex vivo* analyzed for the presence of antigen-specific Th cells by an *in vitro* restimulation with G6PI and the flow cytometric measurement of CD154 expressing T cells as a marker for antigen-specificity<sup>166</sup>. Thus, it was found that already non-immunized animals have a certain proportion (less than 0,2 % in spleens and less than 0,05 % in lymph nodes) of T cells that are specific for G6PI, probably due to the fact that this is an auto-antigen. However, immunization of non-depleted DBA/1 mice lead to an enhancement of this proportion to approximately 0,4 % in spleens and 0,2 % in lymph nodes (Figure 5C). The Treg-depletion further allowed the generation of even more G6PI-specific Th cells of almost 1 % in spleens and 0,6 % in lymph nodes. The same could be seen regarding the absolute numbers of G6PI-specific Th cells in the spleen and draining lymph nodes. Immunized mice showed a higher number than non-immunized ones but the highest cell number of CD154 expressing CD4<sup>+</sup> T cells was achieved by the Treg-depletion. Thus, the missing regulation by Tregs allowed an elevated generation and clonal expansion of Th cells specific for the antigen G6PI.

Those findings proof that the DTx-treated DBA/1 DERE mice showed a similar behavior regarding their immune response and clinical progression as the anti-CD25 treated DBA/1 wild type animals. This makes the DBA/1 DERE mouse model a valuable tool to examine the role of FLS in the contribution to the chronicity of arthritis in the G6PI-induced arthritis mouse model without affecting effector Th cells.

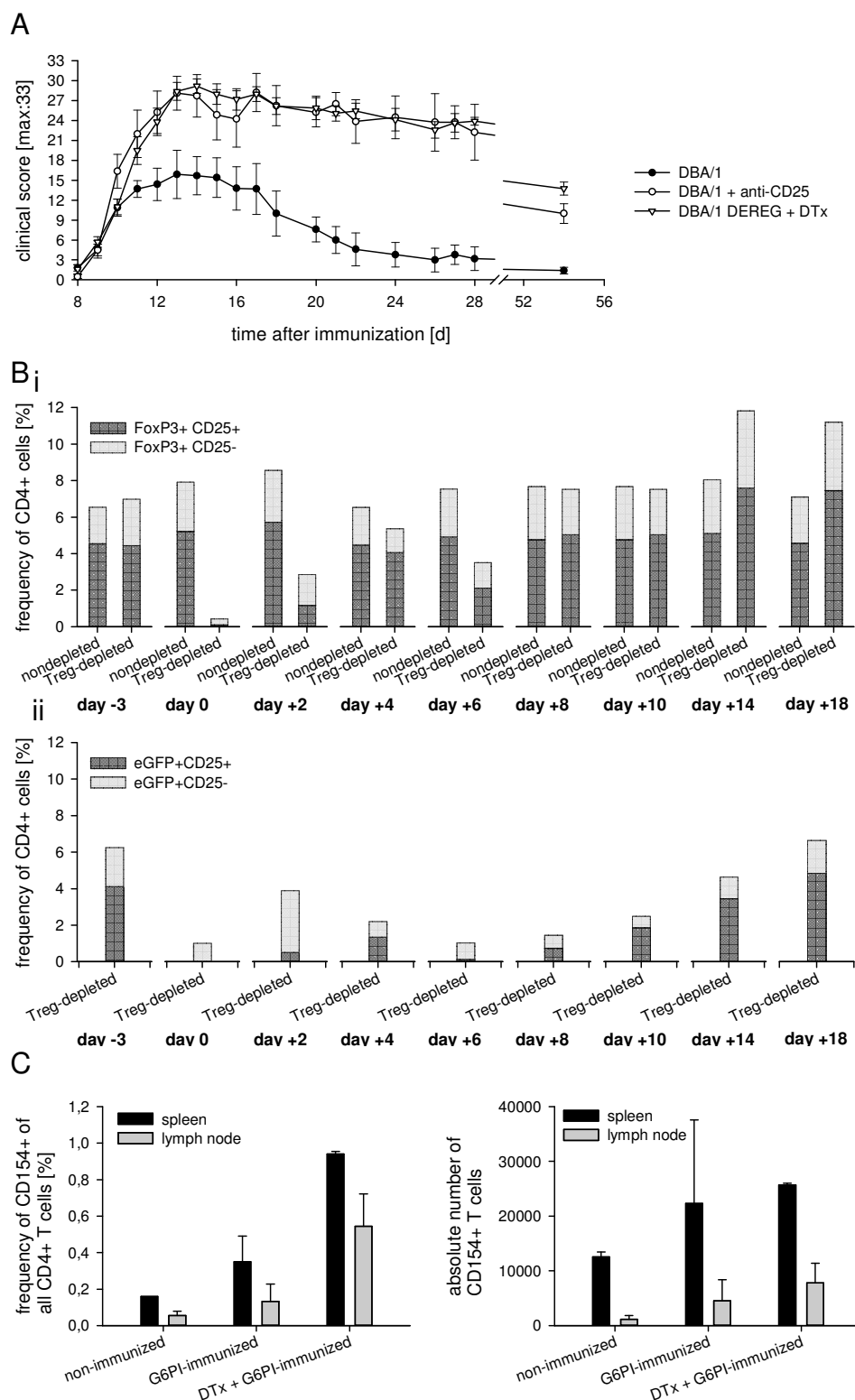


**Figure 5: The G6PI-arthritis model in DBA/1 DEREG mice.**

A) Clinical score of G6PI-immunized DBA/1 wild type mice without (●) or with (○) anti-CD25 treatment prior to immunization compared to DTx treated DBA/1 DEREG mice (▽). Each group consists of at least 5 animals and the experiment has been repeated 3 times. B) Treg-kinetic of DTx treated and untreated DBA/1 DEREG mice. Blood was drawn at the indicated days from at least 6 animals of each group. Tregs were analyzed by FoxP3 staining (i) and eGFP expression (ii) C) Early burst of G6PI-specific Th cells after DTx treatment in comparison to non-immunized and G6PI-immunized, nondepleted animals 3 days after immunization. Both frequency and absolute cell number of CD154<sup>+</sup> T cells were determined in samples from organs of 3 animals per group. This experiment has been performed twice.

## 4.2 CHARACTERIZATION OF MURINE FIBROBLAST-LIKE SYNOVIOCYTES

### 4.2.1 CELLS IN THE JOINT DURING ARTHRITIS PROGRESSION

To analyze the role and contribution of resident cells in the joint to the chronicity of the Treg-depleted, G6PI-immunized mice in this model phalangeal, metatarsal/metacarpal as well as ankle joints were digested at several time points during the disease progression both from nondepleted and Treg-depleted animals. Those cellular isolates were used for further experiments.

To elucidate which cell types are present in the joint during disease progression cells of inflamed joints from immunized as well as Treg-depleted, immunized animals were flow cytometrically analyzed.

Approximately a third of the isolated cells in the joints were positive for CD90 (Figure 6A). This marker has been suggested by Armaka *et al* to be characteristic for FLS<sup>167</sup>. The frequency was about 30 % of all isolated cells during the whole time course with one exception. There was a drop of CD90<sup>+</sup> cells during the peak of clinical symptoms at day 14 to almost 10 %. At the same time, CD11b<sup>+</sup> cells that were usually only present to an extent of less than 10 % did rise to almost 50 % of all cells during that time (Figure 6B). Thus, there is a shift of the proportion of cells in the joint during the disease's peak from CD90<sup>+</sup> to CD11b<sup>+</sup> cells. To further investigate what type of cells those CD11b expressing ones are, this population was analyzed for their hematopoietic origin by staining for CD45 and for the expression of Ly6G which is characteristic for neutrophils in combination with CD11b (Figure 6C and D). Indeed, almost all of the CD11b<sup>+</sup> cells were originating from hematopoietic stem cells expressing CD45. Approximately 10 % of them were neutrophils. Remarkably, at day 14 when the frequency of CD11b<sup>+</sup> cells peaked, the expression level of Ly6G increased from the usual 10-15 % to more than 60 % representing a massive infiltration of the joints by neutrophils. CD90 is also known to be expressed by CD4<sup>+</sup> and CD8<sup>+</sup> T cells. Thus, the CD90<sup>+</sup> cells were also further analyzed for the expression of CD45 (Figure 6E and F). Here, only a small proportion of the CD90 expressing cells were from hematopoietic origin (5-10 %). Only in the sample from Treg-depleted animals at day 14 there was an increase to almost 20 %. This minor population of CD45 expressing CD90<sup>+</sup> cells was further analyzed for the expression of CD4 or CD8. It is noticeable that the appearance of T cells in the joint follows the clinical progression. Whereas only 25-30 % of CD90<sup>+</sup> CD45<sup>+</sup> cells were expressing the T cell surface molecules CD4 and/or CD8 at day 0, this amount increased until day 14 to more than 50 % but dropped again to the initial level at the late time point (day 56).

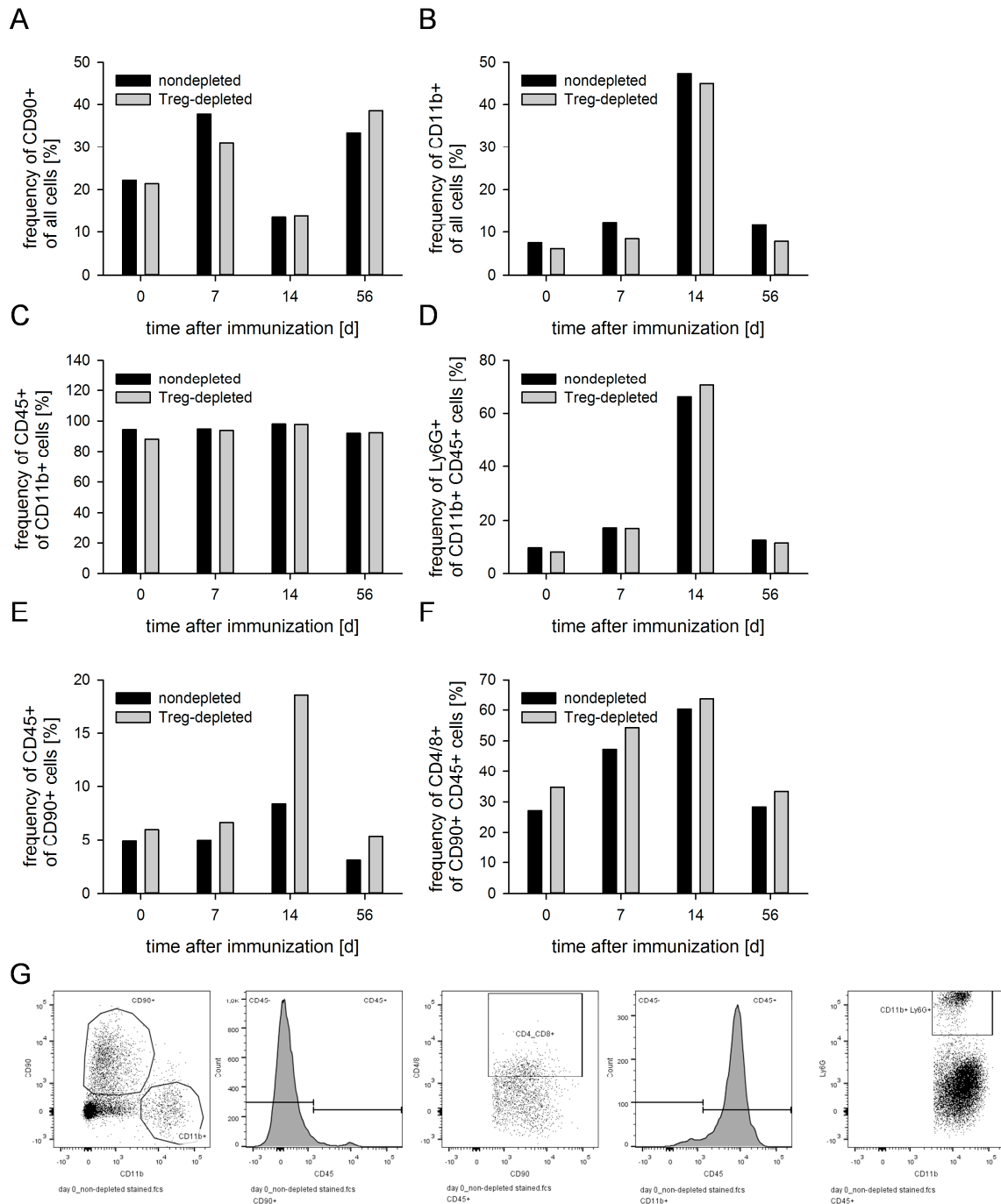


**Figure 6: Cells isolated by joint digestion.**

Representative graphs of flow cytometric analysis of freshly isolated cells from small joints of arthritic paws at several time points after immunization. The experiment has been repeated at least 3 times. CD11b<sup>+</sup> cells (A) were further analyzed for the presence of CD45 (B) and subsequently for Ly6G (C). The frequency of CD90<sup>+</sup> cells was determined (D) and further analyzed for presence CD45 (E). The CD45<sup>+</sup> CD90<sup>+</sup> cells were more closely analyzed for the surface expression of CD4 and CD8 (F). A representative example of the gating is shown in panel G.

Summarizing, the majority of cells in the joints were CD90<sup>+</sup> the number of which dropped at day 14 and was replaced by infiltrating neutrophils. A minor population was comprised of T cells whose presence follows the clinical progression. In general, there was no difference between nondepleted and Treg-depleted animals with one exception. The frequency of CD45 expressing CD90<sup>+</sup> cells was double as high in samples from Treg-depleted mice compared to

the counterparts from nondepleted ones at day 14 resembling the missing control by Tregs during the inflammatory response.

#### 4.2.2 CULTURES OF FIBROBLAST-LIKE SYNOVIOCYTES

Cells from the joints were isolated and cultured over three passages and further analyzed for their characteristic expressions of surface molecules. In their isolation protocol Armaka *et al* suggest that the majority of FLS carries the CD90, ICAM-1 and VCAM-1 on their surface<sup>167</sup>. CD11b<sup>+</sup> cells should be less than 10 % (personal correspondence with Armaka M<sup>167</sup>).

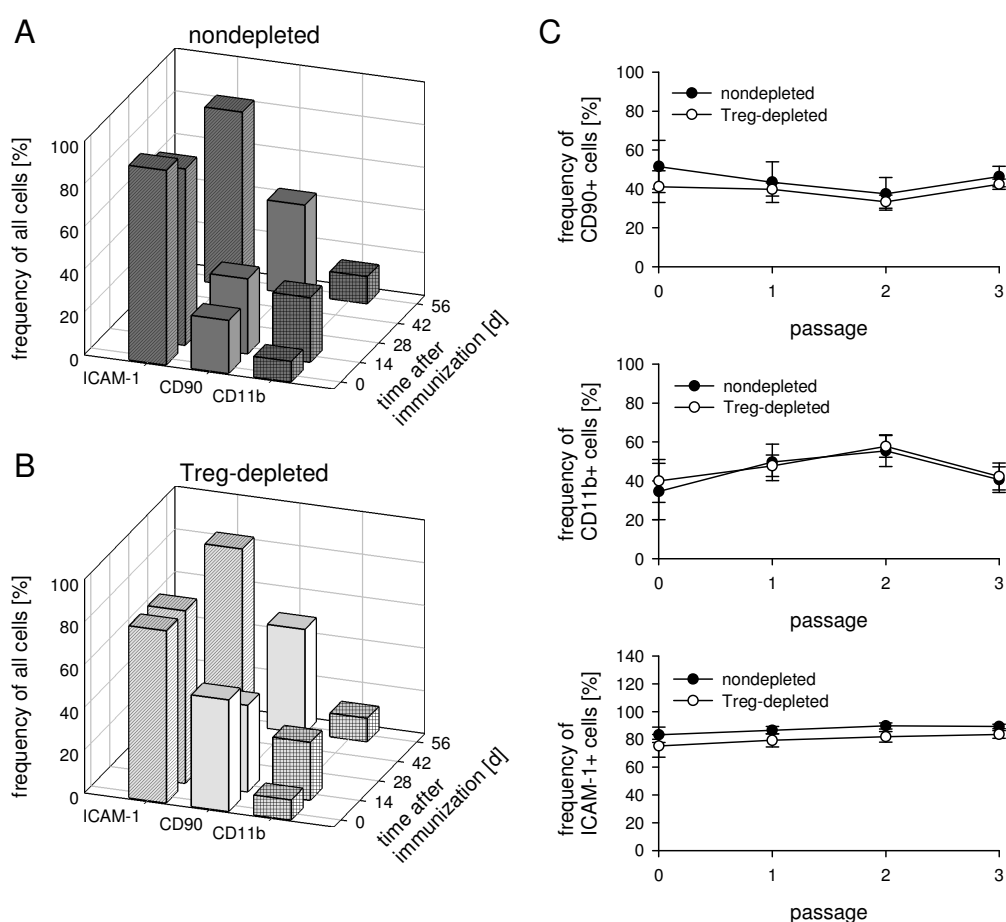


**Figure 7: Fibroblast-like synoviocytes in culture.**

Flow cytometric analysis of cultured FLS from several isolation time points. The cultures from nondepleted (A) and Treg-depleted (B) animals were stained for common markers such as ICAM-1, CD90 and CD11b. The stability of those was determined over the three passages shown in a samples from day 14 (C).

As expected, the major population of cells in the cultures expressed CD90 (Figure 7A and B). Those cells were exclusively CD45<sup>-</sup> (data not shown). Nevertheless, there was a population of CD11b<sup>+</sup> cells, which was almost as frequent as the CD90<sup>+</sup> ones at day 14 but negligible at day 0 and day 56 (Figure 7A and B). None of the CD11b<sup>+</sup> cells expressed markers characteristic for macrophages, namely F4/80 and MHC class II (data not shown). The surface

molecule ICAM-1 was expressed on almost all of the cells in the culture, regardless of the expression of CD90 or CD11b. However, the expression of VCAM-1 was very inconsistent between independent experiments. Mostly, the expression levels were about 50-100 % of all cells but in some cases it was not detected at all. Therefore, VCAM-1 was regarded as not specific for FLS. Again, there was no difference between cultures from nondepleted and Treg-depleted animals. Yet, there was a slight tendency of a somewhat higher frequency of CD90 expressing cells in the samples from Treg-depleted animals.

The stability of the cellular composition of the isolates was monitored over the three passages. The expression of all analyzed markers was stable from the time of isolation until the end of the third passage (Figure 7C). The initially isolated cells (passage 0) consisted of the same amount of CD90<sup>+</sup> cells (approximately 40-50 %) and CD11b<sup>+</sup> cells (approximately 30 %) as they did in the following passages 1, 2 and 3. Likewise, the frequency of ICAM-1 expressing cells did not change and was approximately 80 % over the whole culture. A difference between samples from nondepleted and Treg-depleted mice was not found.

During a Bachelor's thesis by Anne Machate under the supervision of the present study performed in this institute also working with FLS it was found that the cellular composition of isolates and the expression pattern of surface molecules did not change after cryo-freezing as well as after stimulation with cytokines and/or growth factors. CD90, CD11b and ICAM-1 were found with similar frequencies after the storage in liquid nitrogen for several weeks as well as after stimulations with different cytokines (i.e. IL-1, IL-17, IL-33, and TNF $\alpha$ ) and growth factors (i.e. TGF $\beta$  and EGF) for 6 – 48 h.

### 4.3 PROPERTIES OF FIBROBLAST-LIKE SYNOVIOCYTES DETERMINED BY *IN VITRO* EXPERIMENTS

#### 4.3.1 PHENOTYPIC ANALYSIS

##### 4.3.1.1 The secretion of cytokines

The isolated FLS cultures from nondepleted and Treg-depleted DBA/1 mice were further used to examine them for differences between the two groups. First, their inflammatory potential was of interest since it has been published that FLS can possess immunomodulatory and inflammatory functions<sup>135</sup>.

A common read-out for the inflammatory capacity of FLS is the measurement of secreted cytokines. Therefore, FLS from nondepleted and Treg-depleted, immunized mice were isolated at several time points and stimulated with numerous cytokines, growth factors and TLR ligands. The supernatants were then subjected to the analysis by sandwich ELISA and luminex assay.

Several publications have shown that stimulation with TLR ligands<sup>168-170</sup> as well as cytokines<sup>161,171,172</sup> and growth factors<sup>173</sup> can induce the secretion of different inflammatory mediators by RA FLS via different pathways. Hence, different single and double stimulations were tested to induce the secretion of cytokines and chemokines by the FLS from acute and chronic arthritic mice at different time points during the disease progression.

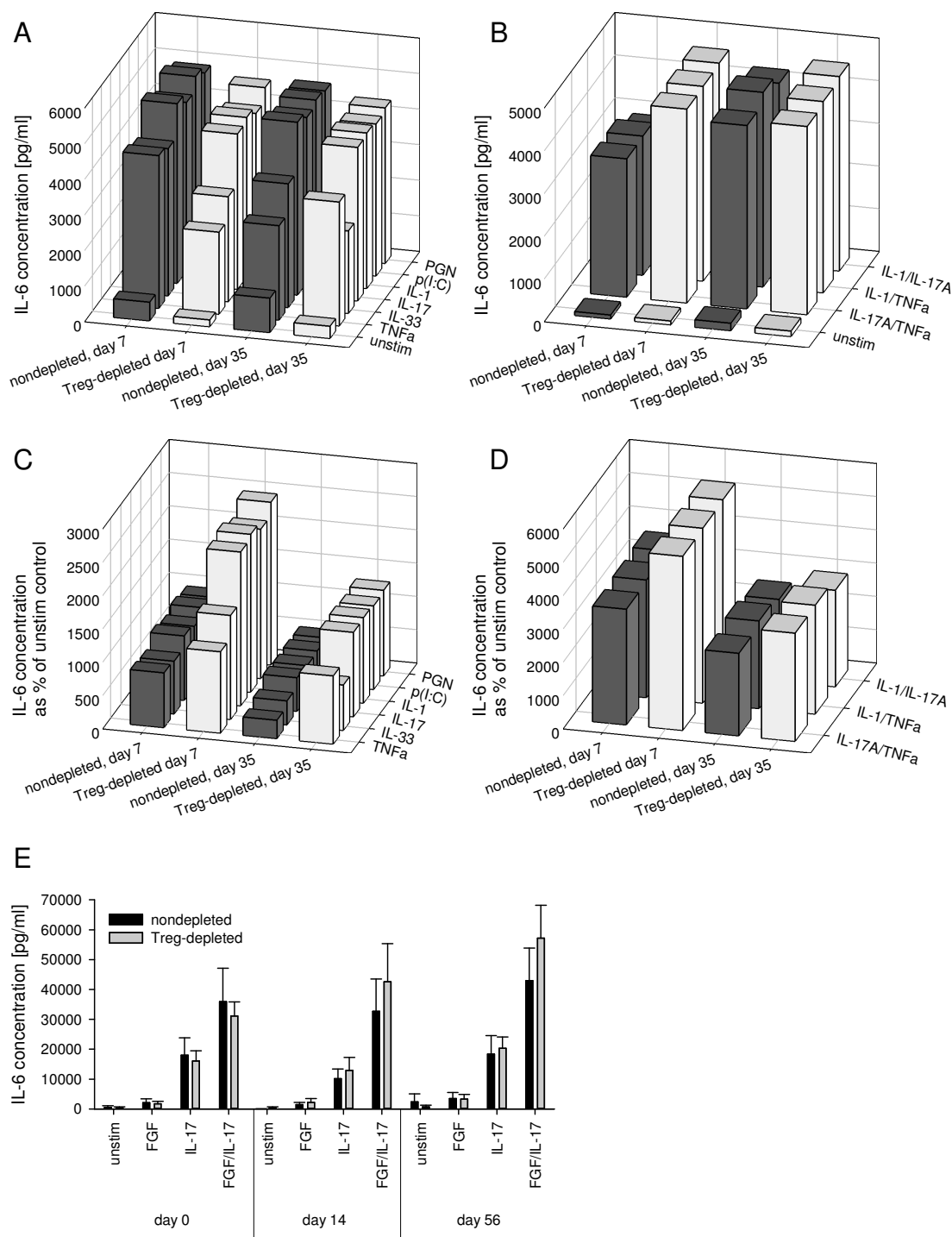


**Figure 8: Inflammatory phenotype of fibroblast-like synoviocytes.**

Phenotypic analysis of FLS from early (day 0, 7 or 14) and late (day 35 or 56) isolation time points. A) Secretion of IL-6 after single stimulations. B) Secretion of IL-6 after double stimulations with cytokines. C) Increase of secretion of IL-6 after single stimulation with cytokines. D) Increase of secretion of IL-6 after double stimulations with cytokines. E) Secretion of IL-6 after stimulation with FGF-2 and/or IL-17A. All experiments have been done in triplicates and at least 3 times.

The Toll-like receptors (TLRs) 2 and 3 were stimulated with peptidoglycan and poly(I:C) respectively. For cytokine-induced stimulations the cytokines IL-1, IL-17A, IL-33 and TNF $\alpha$  were chosen based on published data. As a model growth factor for fibroblasts FGF-2 was used. Double stimulations of IL-1/IL-17A, IL-1/TNF $\alpha$ , IL-17A/TNF $\alpha$  as well as FGF-2/IL-17A were also applied. Supernatants were collected after a 24 h stimulation period.

Figure 8A and B show that stimulation with TLR ligands as well as cytokines and combinations of them could potentially induce the secretion of proinflammatory IL-6 by the FLS in general. There was a massive increase of IL-6 in the supernatants from only some hundred pg/ml in unstimulated controls to some thousand pg/ml in the stimulated ones. However, neither at early (day 7) nor at late time points (day 35) there was a significant difference in the concentration of secreted IL-6 between samples from nondepleted and samples from Treg-depleted mice. Moreover, there was also no difference between day 7 and day 35, the levels of IL-6 in the supernatants were all similar. This applies both for single and double stimulations. Nevertheless, the comparison of stimulated samples with the unstimulated control revealed some differences (Figure 8C and D). IL-6 levels were elevated in samples from nondepleted individuals to 800 – 900 % of unstimulated controls at day 7 and approximately 400 – 500 % at day 35. In comparison to that those IL-6 secretion levels were enhanced to more than 2000 % of unstimulated control at day 7 and approximately 1000 % at day 35 in samples from Treg-depleted subjects. There were just two exceptions, namely IL-33 and TNF $\alpha$ , which did not induce such a dramatic increase in samples from Treg-depleted mice but still caused a stronger elevation of secreted IL-6 compared to the nondepleted counterparts (Figure 8C). Thus, at day 7 the ability to respond to stimulation was 1,5 and 2 times higher in TNF $\alpha$  and IL-33 stimulated samples from Treg-depleted animals compared to their nondepleted equivalents, respectively. In all other tested single stimulations from the early time point there was a more than 2-fold higher stimulatability of the FLS from Treg-depleted mice than in those from nondepleted ones. Similar observations were made with the samples from day 35. FLS from Treg-depleted mice were at least 2-fold more stimutable than the ones from the nondepleted animals. The double stimulations with cytokines had an even stronger effect on the stimulatability (Figure 8D). In the samples from day 7 from nondepleted subjects the IL-6 production was elevated to approximately 3000 % of unstimulated control. That was even more pronounced in the Treg-depleted samples with more than 5000 % of the initial value. Although there was a drop of those values at the later time point (day 35), there was still an enhancement of approximately 2500 % and 3500 % in samples from nondepleted and Treg-depleted mice, respectively. Thus, the stimulation properties were always about 1,5-fold higher in supernatants generated by FLS from Treg-depleted mice compared to the ones from the nondepleted under those conditions.

In an additional approach, the effect of the costimulation of a relevant cytokine with a growth factor was of interest. Here, FGF-2 and IL-17A were used at very low concentrations either alone or in combination (Figure 8E). FGF-2 as a growth factor was chosen because it is known that this growth factor can act in an autocrine loop on FLS<sup>135</sup>. The single stimulation with FGF-2 had almost no effect on the secretion of IL-6 in all samples. None of the samples showed a remarkable increase of IL-6 in the supernatant. As expected and seen before, the single stimulation with IL-17A was a potent inducer of IL-6 secretion in all samples. Strikingly, this induction could be boosted by the double stimulation using FGF-2 and IL-17A to more than twice as much secreted IL-6 than under IL-17A single stimulation conditions. However, there was no significant difference between samples from nondepleted and Treg-depleted animals. There was just a small tendency showing a slightly stronger effect of the double stimulation on samples from Treg-depleted mice.

At the same time, supernatants were also screened for other mediators that could be relevant for the inflammatory and immunomodulatory role of FLS. There was one more protein found to be secreted by the isolated FLS under stimulatory conditions, which was VEGF. However,

this was only found at very low levels with no difference between time point of isolation and group of experimental animal. Additional tested molecules including IL-1, IL-4, IL-5, IL-12, IL-13, IL-15, IL-17, IL-23, IFN $\gamma$ , TNF $\alpha$ , SCF and RANKL were not detected in an ELISA. To enhance the sensitivity of the measurement supernatants from IL-17A/TNF $\alpha$  stimulated samples were subjected to a luminex multiplex assay by collaboration partners from the Hannover Medical School (Prof. Chr. Falk). This revealed an upregulation of the secretion of IL-1, IL-2, IL-3, IL-5, IL-6, IL-9, IL-10, IL-12, IL-13, Eotaxin, G-CSF, GM-CSF, IFN $\gamma$  and TNF $\alpha$  into the culture medium of stimulated FLS compared to unstimulated ones. However, this enhancement was very minor and did not show any difference between isolation time points or samples from FLS of nondepleted and Treg-depleted mice.

Summarizing, the stimulation of FLS isolated at different time points during arthritis progression from nondepleted and Treg-depleted mice lead to an enhanced secretion of IL-6 both with single and double stimulatory regimen. Although there was no difference in the absolute concentration of IL-6 in the supernatants between samples from nondepleted and Treg-depleted animals there was a difference in the stimulatability. FLS isolated from Treg-depleted mice were more susceptible to the tested stimulations than the corresponding ones from nondepleted subjects.

Since IL-17A and TNF $\alpha$  in combination turned out to be potent stimuli and those cytokines have been described as relevant molecules during arthritis pathogenesis, this double stimulation was further used in subsequent experiments.

#### 4.3.1.2 The secretion of chemokines

As mentioned above, supernatants from FLS isolated at different time points from Treg-depleted and nondepleted arthritic mice were screened in a luminex assay at the Hannover Medical School. Two independent experiments showed that the secretion of three chemokines was highly elevated after stimulation with IL-17A/TNF $\alpha$ , namely CCL3 (MIP-1 $\alpha$ ), CCL4 (MIP-1 $\beta$ ) and CCL5 (RANTES) (Figure 9A). Those three chemokines are known to attract and activate monocytes, macrophages and NK cells as well as eosinophils and basophils<sup>174-176</sup>. In the unstimulated controls those chemokines were barely measurable. Upon stimulation the secretion was highly increased in all cases. There was a tendency of a higher chemokine secretion in samples isolated at day 56 from Treg-depleted animals in comparison to those from the nondepleted ones.

Therefore, additional experiments were conducted in ELISA approaches to find if this tendency was significant or not (Figure 9B). The luminex results could be confirmed. The stimulation of FLS supernatants with IL-17A/TNF $\alpha$  was able to induce the secretion of CCL3, CCL4 and CCL5. Furthermore, there was still the same tendency of an elevated secretion by FLS isolated from Treg-depleted animals. However, these differences did not reach statistical significance.

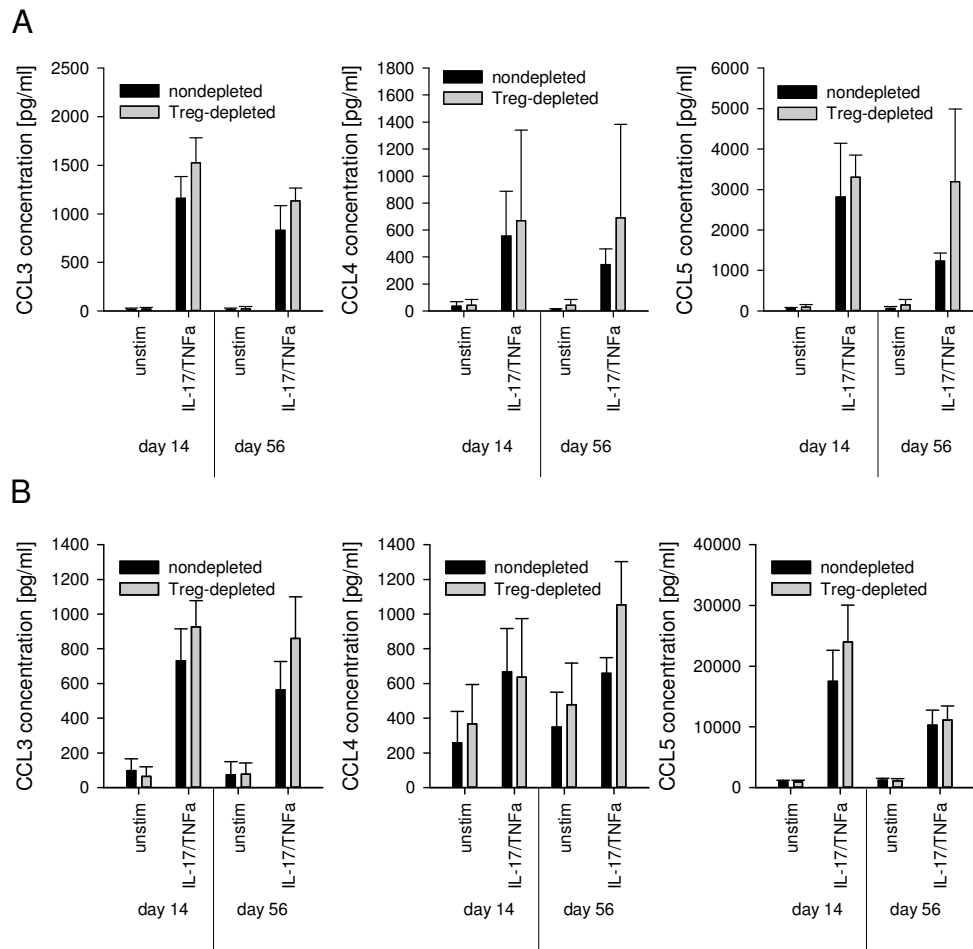


**Figure 9: Chemokine-secretion by fibroblast-like synoviocytes.**

Phenotypic analysis of FLS from early (day 14) and late (day 56) isolation time points. Secretion of chemokines after double stimulation with IL-17A/TNF $\alpha$  in a luminex assay (A) and sandwich ELISA (B). All experiments have been done in triplicates and at least 2 times.

#### 4.3.1.3 The secretion of Matrix-metalloproteinases

A major function of fibroblast-like synoviocytes in healthy individuals is the modulation of extracellular matrix and the maintenance of internal joint homeostasis by e.g. providing nutrients to chondrocytes and by the secretion of matrix degrading enzymes, such as matrix metalloproteinases (MMPs)<sup>137</sup>. However, a dysregulation in the secretion of those proteins during joint inflammation contributes to the pathogenicity of rheumatoid arthritis<sup>134,135</sup>. Therefore, the secretion of MMPs was examined after stimulation of isolated FLS from Treg-depleted and nondepleted, G6PI-immunized mice in several ELISA studies. Additionally, gelatin-zymography was performed to determine the biological activity of the gelatinases MMP-2 and MMP-9.

In ELISA experiments the stromelysin MMP-3, the gelatinase MMP-9 and the inhibitor TIMP-1 as representative examples for the long list of MMPs were measured. Both MMP-3 and TIMP-1 were secreted already at high levels of about 50 – 70 ng/ml in the unstimulated controls whereas MMP-9 was almost undetectable (Figure 10A-C). The stimulation with IL-17A/TNF $\alpha$  caused a very strong increase of the MMP-3 and MMP-9 secretion to about 550 – 750 ng/ml and 20 – 30 ng/ml respectively in all samples. In contrast, the secretion of

TIMP-1 was barely induced upon stimulation and reached only 1,5-fold higher levels than in unstimulated controls.

A difference between the samples from nondepleted and Treg-depleted arthritic animals was not ascertainable. Both unstimulated controls as well as IL-17A/TNF $\alpha$  stimulated samples contained similar concentrations of secreted MMP-3, MMP-9 and TIMP-1. Furthermore, no differences were found between samples that were isolated at different time points after arthritis induction.

However, the ELISA assay only allows the detection of MMPs by their structure and does not account for biological activity. MMPs are initially generated as inactive forms harboring a pro-peptide domain that has to be cleaved off before the enzyme is active<sup>177</sup>. Most ELISA antibodies do not distinguish between active enzyme and inactive pro-form. Therefore, a gelatin-zymography was conducted. Using gelatin as a substrate in a native SDS-PAGE allows the detection of the two gelatinases MMP-2 (72 kDa) and MMP-9 (92 kDa). It has been published that MMP-2 is constitutively expressed in FLS and the synovium<sup>178</sup>. Also here, MMP-2 was found to be highly secreted by all tested samples. In fact, the secretion and biological activity was so high that a quantitation of the digestion bands in the gel was not possible. Therefore, MMP-2 has been excluded from the analysis. Nevertheless, the digestion of gelatin by MMP-9 could be visualized and quantified in the separate samples. Since it turned out that the gelatin-zymography is not sensitive enough to detect MMP-9 activity in unstimulated samples only IL-17A/TNF $\alpha$  stimulated FLS supernatants were further used for analysis. Both FLS from nondepleted and Treg-depleted mice isolated at day 14 and day 56 showed an enzymatic activity for MMP-9 after the stimulation (Figure 10D). This clearly showed that the detected MMP-9 in the ELISA exhibits a biological activity. Furthermore, there were differences between the samples from nondepleted and Treg-depleted animals. The relative amount of active MMP-9 was higher in the samples from Treg-depleted subjects at day 14 and with significance at the late FLS isolation time point (day 56).

As for the cytokines, also for MMPs it was of interest, if the combination of a cytokine and a growth factor, namely IL-17A and FGF-2, could influence the secretion of them (Figure 10E). Regarding MMP-3 IL-17A stimulation alone resulted in just a minor increase of its secretion to about 1,5-fold of the unstimulated control. FGF-2 alone was more potent to do so but the difference to the unstimulated control was still not large. Here, the induction was approximately 3-fold. In contrast, the double stimulation enhanced the secretion of MMP-3 to more than 6-fold. Again in the unstimulated controls, there was almost no MMP-9 detectable. The stimulation with IL-17A alone resulted in a likewise minor induction of MMP-9 secretion as for the MMP-3. Also, the single stimulation with FGF-2 was a little more potent but still not striking. The double stimulation had by far the strongest effect on the secretion of MMP-9 with FGF-2 and IL-17A. The secretion of TIMP-1 was not affected at all, neither by the single stimulation with IL-17A or FGF-2 nor by the double stimulation of them. TIMP-1 stayed at the same level in the supernatants as in unstimulated controls.

Nonetheless, it has to be stated that there were again no differences observable between neither the different isolation time points of the FLS nor the two different experimental groups of animals. In all cases, the effects of the stimulation on the secretion of MMPs were similar on FLS isolated at early and late time points from nondepleted and Treg-depleted, G6PI-immunized mice.

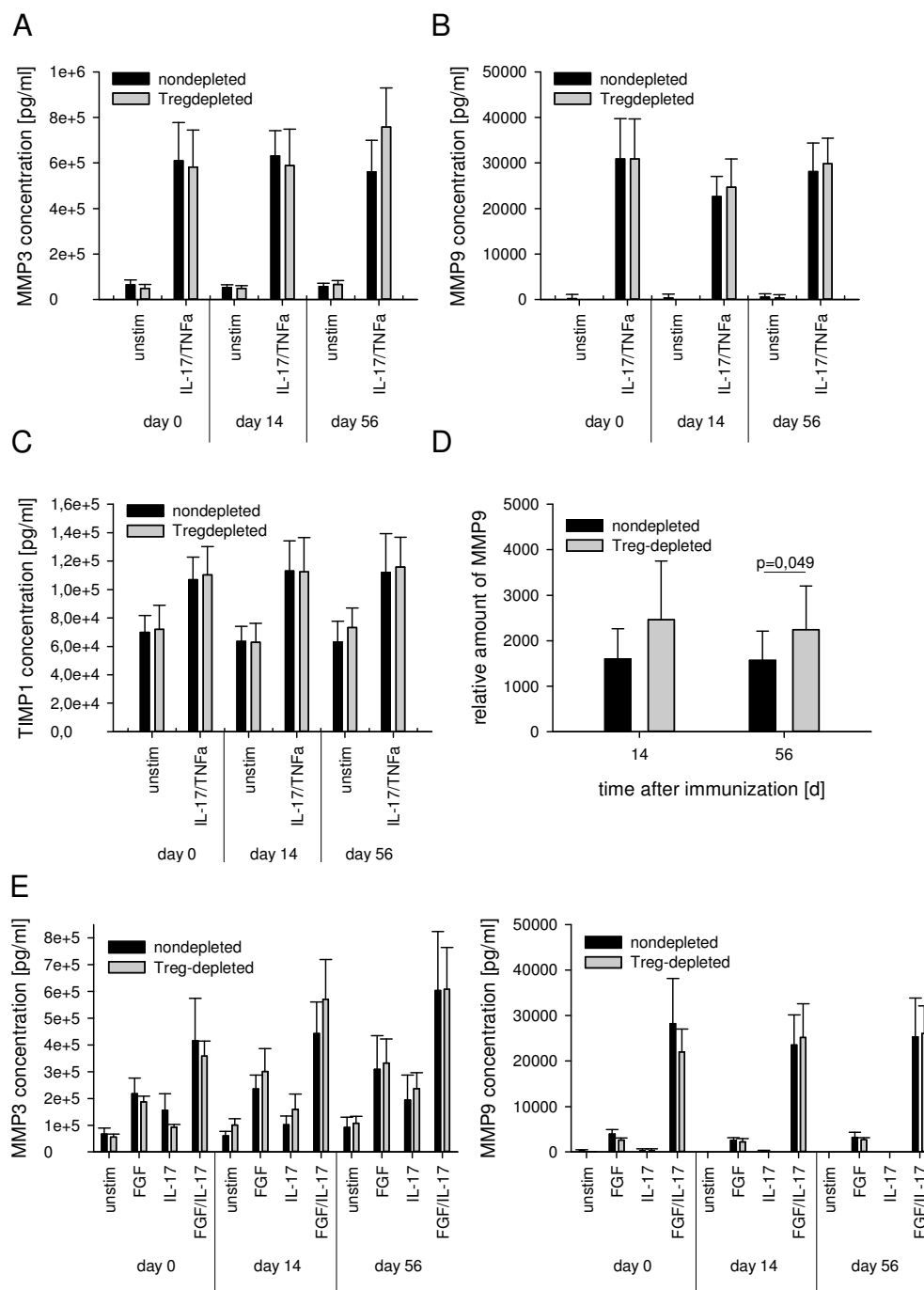


**Figure 10: Destructive phenotype of fibroblast-like synoviocytes.**

Phenotypic analysis of FLS from several isolation time points. A) – B) Secretion of collagenases MMP3 and MMP9 after stimulation with IL-17A/TNFα. C) Secretion of the inhibitor of matrix metalloproteinases TIMP1 after stimulation with IL-17A/TNFα. D) Relative amount of active MMP9 after IL-17A/TNFα stimulation determined by gelatin-zymography. E) Secretion of the collagenases MMP3 and MMP9 after stimulation with FGF-2 and/or IL-17A. All experiments have been done in triplicates and at least 3 times.

#### 4.3.2 FUNCTIONAL ANALYSIS

Since the phenotypic analyses showed a tendency to a more proinflammatory and destructive phenotype of FLS from Treg-depleted animals compared to FLS from nondepleted ones it was of great interest if the FLS differ in other functions. Therefore, the invasive and destructive

potential of the different FLS samples were tested in two different *in vitro* approaches. First, the attachment of FLS to wild type femoral head cartilage was measured. Second, the destruction of an artificial cartilage matrix in the MATRIN assay was assessed.

#### 4.3.2.1 Attachment of fibroblast-like synoviocytes

Cartilage destruction *in vivo* involves two compartments, the cartilage on the one hand and the synovial membrane on the other hand. To analyze this interaction *in vitro* FLS isolated at different time points from nondepleted and Treg-depleted mice were applied to wild type femoral head cartilage pretreated with IL-1 as published by Korb-Pap *et al*<sup>179</sup>. This allows to determine the potential to invade and eventually destroy cartilage and subchondral bone.

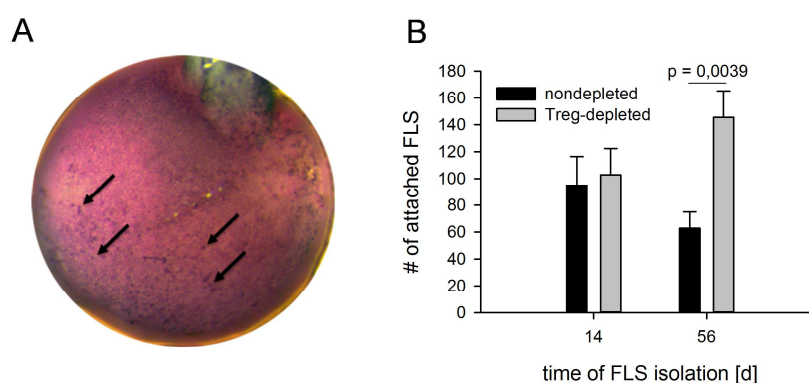


**Figure 11: Attachment of fibroblast-like synoviocytes to wild type cartilage.**

The potential of FLS to invade cartilage was determined by an attachment assay. A) Representative image of a wild type femoral head cartilage with attached FLS isolated at day 14 from nondepleted DBA/1 mice. B) Number of FLS from different isolation time points attached to wild type femoral head cartilage. The experiment has been performed with n=6 in 5 independent runs. Significance was determined by Mann-Whitney-U-Test.

After femoral head cartilages had been pretreated with IL-1 to induce a proteoglycan loss which is necessary for FLS to attach<sup>179</sup> different FLS were applied on them. After an incubation time of 14 h the cartilage caps were stained with Mayer's hemalaun to make the attached FLS countable under a stereo microscope. Since the femoral head cartilage has a large 3-dimensional structure several Z-stacks were aligned to produce a complete picture for the counting of the cells (Figure 11A). As depicted in Figure 11B FLS isolated at day 14 from nondepleted and Treg-depleted mice attached equally good. In both cases approximately 100 cells were counted on the cartilage cap. In contrast, at the late time point of isolation (day 56) FLS from the Treg-depleted group attached much better to the wild type cartilage than the ones from the nondepleted animals. This difference in the ability to attach to cartilage is highly significant ( $p=0.0039$ ). Thus, the invasive potential of the FLS resembled the clinical progression of both experimental groups. During the peak of inflammation both types of FLS had an equal potential to invade. While this potential decreased in the samples from nondepleted mice it increased with the FLS from the Treg-depleted animals.

#### 4.3.2.2 Destructive potential of fibroblast-like synoviocytes

Although the attachment assay reveals the invasive potential of FLS it cannot tell if the cells are really invading or destroying the cartilage. Therefore, another *in vitro* method using artificial cartilage resembled by a collagen matrix was performed. Briefly, the matrix-assisted transepithelial resistance invasion (MATRIN) assay uses the breakdown of electrical resistance on a semipermeable membrane of a cell culture insert coated with a collagen gel on the inner side and an epithelial cell layer (MDCK-C7 cells) on the outer side to test the destructiveness of cells (Figure 12A).

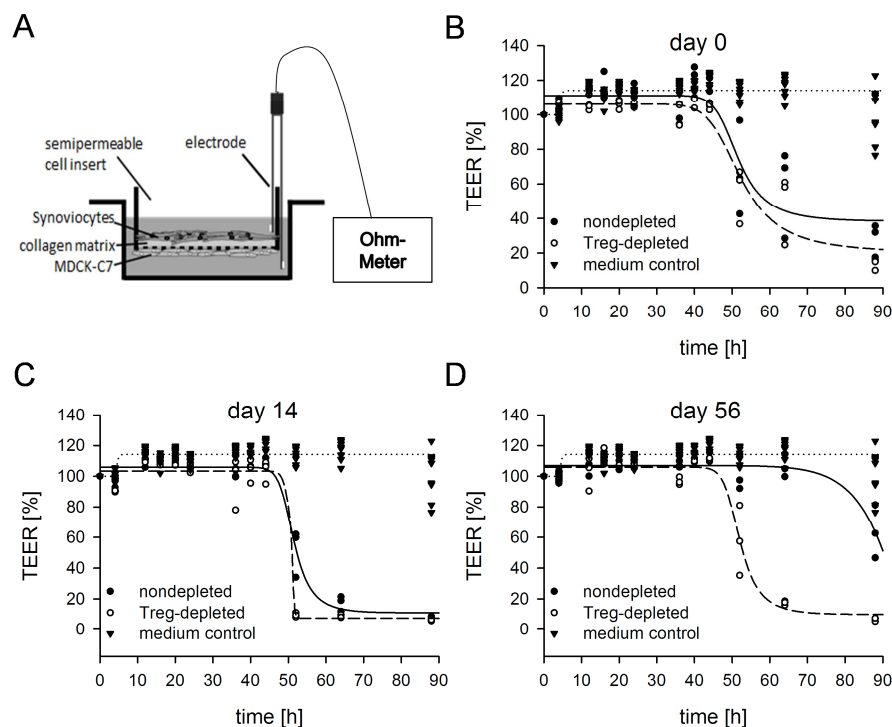


**Figure 12: Functional analysis of fibroblast-like synoviocytes' destruction of cartilage.**

The destructive potential of FLS to degrade cartilage was determined by the MATRIN assay A) Schematic of the experimental setup of the MATRIN assay. B) – D) Transepithelial electrical resistance (TEER) in the MATRIN assay using FLS from different isolation time points. Shown is one representative experiment with at least triplicates of the samples. This MATRIN assay has been performed 4 times with independent FLS isolates.

The initial high electrical resistance between inner and outer chamber results only partly from the collagen-matrix and is mainly produced by the MDCK-C7 cell layer which is an epithelial cell line harboring extremely “tight” tight junctions due to the lack of endogenous claudin-2<sup>180</sup>. If the cells of interest are destructive they will first degrade the artificial cartilage layer on the inner side of the membrane. Subsequently, eventually produced cytokines can then induce the upregulation of claudin-2 expression in the MDCK-C7 cells<sup>181</sup> resulting in “leaky” tight junctions and/or facilitate their internalization<sup>182</sup>. This leads in the end to a breakdown of the transepithelial electrical resistance (TEER) representing the destructiveness of the applied cells, here the FLS. Two factors stand for the destruction, first the time point of the breakdown and second the steepness.

Comparing the FLS isolated from naive (day 0) or G6PI-immunized (day 14 and day 56) either nondepleted or Treg-depleted DBA/1 mice in the MATRIN assay revealed some

important differences. At day 0 FLS from both experimental groups were similarly destructive. Both induced the TEER breakdown approximately 50 h after the start of the experiment with the same intensity (represented by the steepness of the decline) (Figure 12B). This started to change already at the early time point during disease progression, day 14. Whereas the induction of the TEER breakdown was again similar at around 50 h after FLS application, the intensity differed. FLS from Treg-depleted mice created a steeper decline than FLS from the nondepleted ones (Figure 12C). Strikingly, at the late time point during the chronic phase, FLS from both experimental groups were completely different in their ability to destroy cartilage (Figure 12D). Fibroblast-like synoviocytes from Treg-depleted individuals were still almost as destructive as on day 14. The TEER breakdown started again at about 50 h post FLS addition and the decline was almost as steep as during the disease's peak. In contrast to that, the FLS from nondepleted mice showed a much lower cartilage destruction potential. The TEER breakdown began later than 80 h after the FLS addition and with a decreased decline of the slope. In fact, those FLS were even less destructive than the ones from naive mice at day 0. After 90 h of measurement the experiment had to be stopped due to the fact that the method allows no medium exchange and eventually the MDCK-C7 cells lack nutrients and start to die off.

Thus, the MATRIN assay revealed an aggressive, destructive phenotype of FLS from Treg-depleted mice during the chronic phase which was not seen by FLS from nondepleted animals. Instead, those seemed to fall into some kind of a hypoactive state.

#### 4.4 *IN VIVO* ANALYSES OF FIBROBLAST-LIKE SYNOVIOCYTES

The functional *in vitro* studies demonstrated a significant difference between FLS from nondepleted and Treg-depleted mice during the late stage of the disease progression (d56 after immunization) when the clinical data also diverged. The synovial fibroblasts isolated from Treg-depleted animals displayed an aggressive, destructive phenotype which allowed them to invade and destroy wild type cartilage. This aggressiveness was also seen by FLS from nondepleted animals during the inflammatory stage at around day 14 but was lost again later on in the course of disease progression.

Furthermore, this study hypothesizes that the FLS from the Treg-depleted animals gain an independence from the adaptive immunity and become the drivers of the chronicity. To ultimately test this, FLS isolated from both experimental groups before the immunization (day 0), during the peak of the disease severity (day 14) and at a late stage of disease progression (day 56) were transferred into the knee joint of *rag1*-deficient DBA/1 mice lacking mature B and T cells. 2 weeks later, knee joints were dissected and histologically analyzed for inflammation and cartilage- as well as subchondral bone destruction.

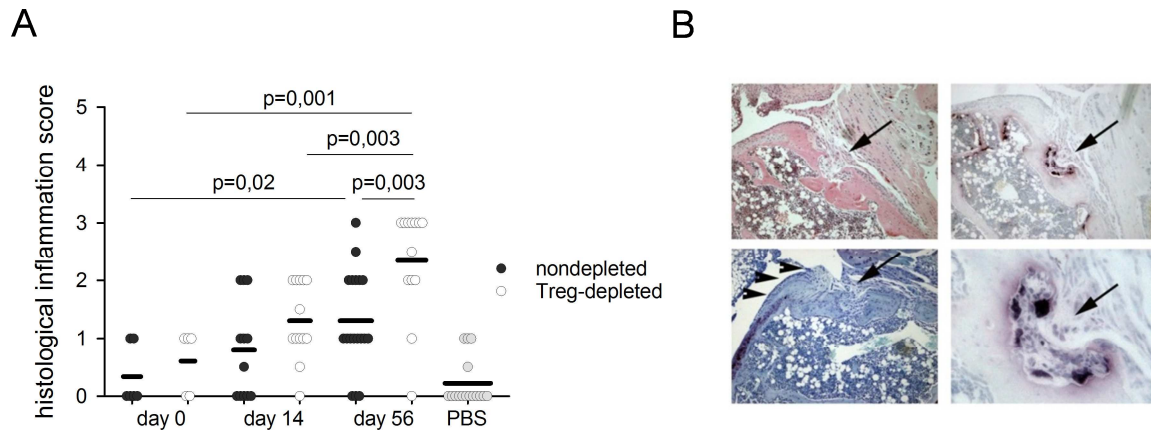


**Figure 13: *In vivo* function of fibroblast-like synoviocytes.**

FLS isolated at different time points were transferred into the knee joint cavity of DBA/1 *rag1*-deficient recipients and histologically analyzed for inflammation and destruction after 2 weeks. A) Histological inflammation score of analyzed knee joints. Shown are the mean values of at least 7 animals per time point and group obtained in 3 independent experiments. B) Representative histology slide of cartilage (left) and subchondral bone (right) destruction in a sample with FLS from Treg-depleted animals isolated at day 56 (chronic phase).

The histological scoring of the inflammation in the joint demonstrated that FLS from arthritic mice are in general able to induce an inflammation in the joint of the recipient (Figure 13A). FLS from naïve mice (day 0) induced almost no inflammation in the joint. The histological value was comparable to that of the PBS control. The transfer of FLS isolated at day 14 from both experimental groups resulted in a histological score between 0.8 and 1.3. This demonstrated that the FLS from this early peak phase of the disease progression can induce infiltration of leukocytes into the knee joint of the *rag1*-deficient recipient without the help of the adaptive immunity. However, at this stage there was no difference between samples from nondepleted and Treg-depleted animals. That changed in the later stages. Though there was a higher histological score observable for both FLS from nondepleted and Treg-depleted mice from day 56 the difference between day 14 and day 56 samples was not significant for the nondepleted group but highly significant for the Treg-depleted one. Moreover, the highest inflammation score (approximately 2.5) was caused by the transfer of day 56 FLS from Treg-depleted animals. That score was significantly lower in the case of transferred day 56 FLS from nondepleted animals. Thus, the by far strongest inflammatory infiltration of the knee joint of DBA/1 *Rag1*<sup>-/-</sup> was generated by FLS isolated at day 56 from Treg-depleted donor mice. Ultimately, destruction of the cartilage and subchondral bone was exclusively seen in samples from recipients that received FLS from Treg-depleted animals isolated at day 56 during the chronic stage of the arthritis progression (Figure 13B) most likely due to the secretion of MMPs (Figure 13B left panel) and the induction of osteoclasts (Figure 13B right panel).

#### 4.5 INSTRUCTION OF FIBROBLAST-LIKE SYNOVIOCYTES TO OBTAIN AN AGGRESSIVE, DESTRUCTIVE PHENOTYPE

The experiments in the previous chapters revealed that FLS from Treg-depleted, G6PI-immunized DBA/1 mice obtained an aggressive phenotype characterized by the elevated potential to invade and destroy cartilage *in vitro* and the ability to potently induce joint inflammation and destruction (cartilage and bone) *in vivo* in a B and T cell independent manner. That gives rise to the question how are those aggressive FLS instructed.

Published data<sup>124,133,161</sup> as well as results from this study have demonstrated that IL-17 plays an important role in the G6PI-induced arthritis model. It is highly produced by antigen-specific T cells before the onset of symptoms<sup>133</sup> and is a potent inducer of IL-6 production by FLS both alone and in combination with other cytokines and growth factors. Furthermore, IL-17 is a cytokine that is not exclusively expressed by CD4 T cells but also  $\gamma\delta$  T cells, NK cells, NKT cells and mast cells. Hence, it was of interest if IL-17 is in any way involved in the instruction of FLS during the pathogenesis of the chronic (Treg-depleted) G6PI-arthritis. Therefore, clinical data using IL-17A blocking antibodies was collected. Furthermore, FLS were isolated from G6PI-immunized animals that were either nondepleted or Treg-depleted. A subgroup of the animals of both groups received either a preventive (day 0, 3, 6) or therapeutic (day 10, 13, 16) anti-IL17A treatment. Those FLS were then subjected to the MATRIN assay to assess their destructive potential and clarify if the IL-17A treatment possibly could reverse the aggressiveness and destructive potential.

The influence of the anti-IL-17A treatment is depicted in Figure 14A and B representing preventive and therapeutic administration respectively. The preventive treatment of nondepleted DBA/1 mice resulted in a lower peak score and a faster resolution of the disease. In the Treg-depleted animals the symptoms were not completely resolved by the preventive anti-IL-17A administration but the overall score was significantly lower after the peak of the disease until the end of measurement. Moreover, the significant difference between nondepleted and Treg-depleted animals from around day 20 on was also observable between both preventively IL-17A-treated groups. Thus, the preventive treatment could ameliorate the disease course in both experimental groups but was not sufficient to cure the Treg-depleted ones. The therapeutic injection of anti-IL17A into nondepleted and Treg-depleted DBA/1 mice lead to a drop of the clinical score right after the treatment had started (day 10-13). Since the peak of the severity is usually reached at around day 14, such treated mice did not develop a clinical arthritis score peak as high as the untreated ones. Instead the maximum was lower and the resolution earlier. Nevertheless, the maximum of Treg-depleted mice was still higher compared to nondepleted ones also when they were therapeutically treated with anti-IL-17A. Furthermore, the decrease of clinical symptoms happened slower and to a lower extent. Thus, anti-IL-17A treated, Treg-depleted mice had a clinical score lower than the untreated, Treg-depleted ones but still higher than the nondepleted mice until the end of measurement. Nonetheless, the difference between nondepleted and Treg-depleted animals is again significant from day 30 on also in the therapeutically anti-IL-17A treated individuals.

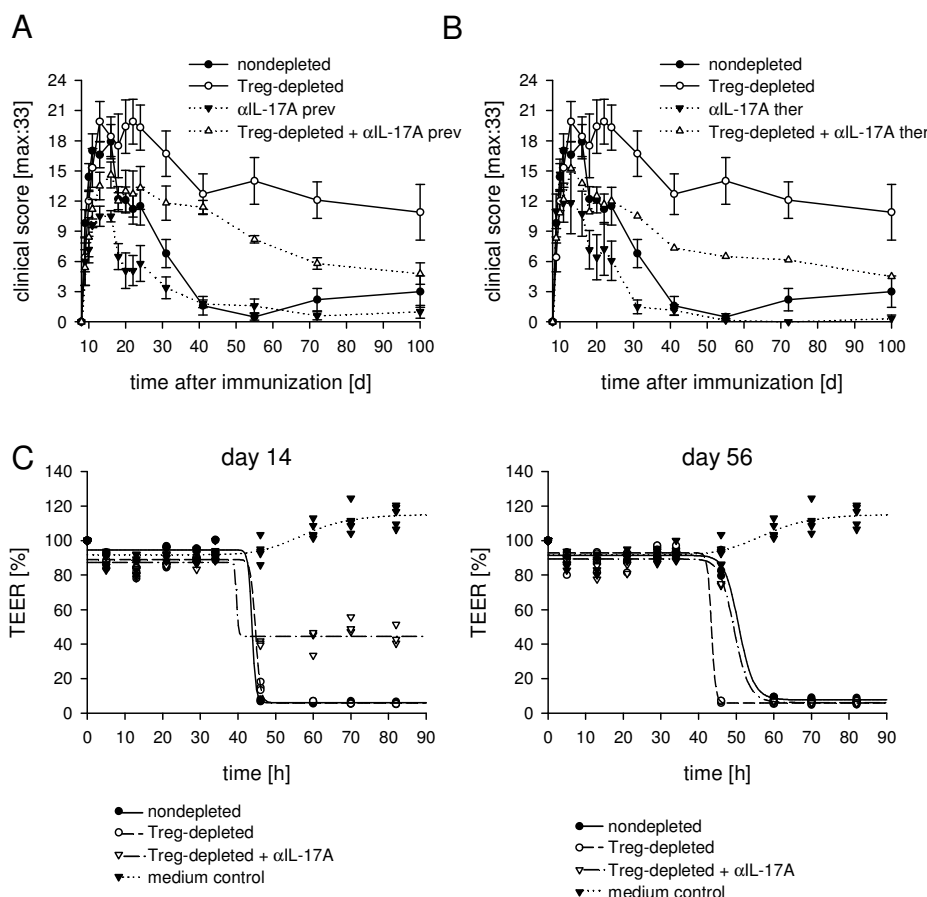


**Figure 14: Anti - IL-17A treatment.**

Clinical progression after preventive (A) and therapeutic (B) treatment of G6PI-immunized mice with anti - IL-17A as well as a the measurement of the destructive potential by MATRIN assay from FLS isolated at day 14 and day 56 from untreated and therapeutically  $\alpha$ IL-17A treated animals (C). Clinical analysis has been repeated three times and the MATRIN assay has been done twice.

To assess if the changes/differences in the clinical course after the treatment with anti-IL-17A could also have an influence on the FLS, cells isolated early (day 14) or late (day 56) from therapeutically anti-IL-17A treated animals were subjected to the MATRIN assay (Figure 14C). As seen before (in 4.3.2.2 Destructive potential of fibroblast-like synoviocytes), FLS from nondepleted and Treg-depleted animals were similarly destructive when isolated at the early time point (day 14) but not during the later stage (day 56). Then, FLS from Treg-depleted animals showed a higher destructive potential. However, the therapeutic administration of anti-IL-17A was able to affect the destructive behavior of FLS from Treg-depleted animals. The change is already observable in samples from day 14. Whereas the time point of the TEER breakdown and the slope of the curve were similar to those from untreated nondepleted and Treg-depleted mice, the overall extent of the destruction was less. The measurement of samples from untreated animals resulted in a TEER after the breakdown of less than 10% compared to the initial value. In contrast, the TEER in the wells with the FLS from anti-IL-17A treated mice was just going down to approximately 40 % of the initial value. Thus, the destruction of the collagen as well as the breakage of the integrity of the MDCK-C7 cell layer were not as complete as seen with the FLS from nontreated mice. Furthermore, the therapeutic anti-IL-17A treatment could cause the reverse of the functional phenotype of FLS from Treg-depleted animals to that of nondepleted ones during the late phase (day 56).

The time point of the TEER breakdown as well as the slope of the decline of FLS from Treg-depleted, anti-IL-17A treated mice are no longer equal to the ones from untreated, Treg-depleted animals but to that from nondepleted individuals. The TEER breakdown happened later and the decline was more moderate. Thus, the FLS from the Treg-depleted animals that were therapeutically treated with anti-IL-17A resemble the functional phenotype of the nondepleted, acute arthritic mice rather than the Treg-depleted, chronic ones.

#### 4.6 OUTLOOK: G6PI-INDUCED ARTHRITIS IN OTHER MOUSE STRAINS

As already shown by Schubert *et al*<sup>123</sup> only DBA/1 mice are susceptible to G6PI-induced arthritis due to their H2-haplotype q. There have been other publications showing that the G6PI-induced arthritis mouse model also works in other strains like SJL<sup>132</sup> and B10.Q<sup>183</sup>. However, on all those backgrounds only a few knockout strains are available. This makes functional *in vivo* studies of genetically manipulated mice very difficult in the G6PI-induced arthritis model. The only solution so far is the back-crossing and breeding of susceptible DBA/1 mice with knockout animals from other strains. Since this is a very time consuming and often error-prone procedure one would wish to have the possibility to induce arthritis with G6PI in more commonly used mouse strains such as C57BL/6 or BALB/c. However, those strains do not have the H2-haplotype q but H2-b and -d, respectively. Thus, they are not susceptible<sup>123</sup>.

Recently, a new strain has been generated by cross-breeding approaches by collaboration partners from the Karolinska Institute in Stockholm (Prof. R. Holmdahl). This strain is on the C57BL/6N background (an NIH subline from C57BL/6 from 1951) but harbors the H2-haplotype q originating from B10.Q mice. It was therefore named B6.NQ. Those mice were tested in the present study to check if they were applicable for the future experiments on functional involvements using knockout animals.

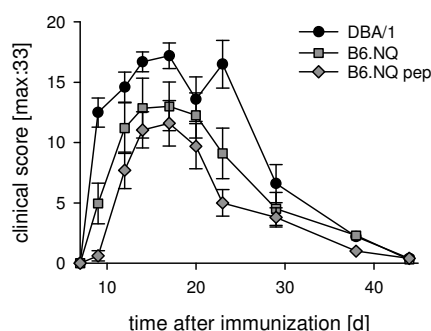


**Figure 15: G6PI-arthritis in B6.NQ mice.**

Wild type DBA/1 mice as well as B6.NQ mice were immunized with 400  $\mu$ g G6PI in CFA. Additionally, B6.NQ mice were also immunized with 10  $\mu$ g of a G6PI peptide (as 325-339) as suggested by Holmdahl (personal correspondence). Animals were clinically scored for arthritis severity.

For the comparison, DBA/1 wild type mice as well as B6.NQ mice were immunized with 400 µg of G6PI in CFA intradermally. Additionally, a group of B6.NQ mice was immunized with 10 µg of G6PI peptide 325-339 in CFA as suggested by Holmdahl (personal correspondence). The immunization of B6.NQ mice both with the full-length G6PI protein as well as the G6PI peptide induced a polyarthritis similar to that seen in DBA/1 wild type animals (Figure 15). Symptoms started to appear around day 10 and increased until 2 weeks post immunization. Afterwards, clinical signs decreased and arthritis resolved. It made no difference if B6.NQ mice were immunized with the full-length protein or the G6PI peptide. However, the severity of arthritis in B6.NQ mice did not reach the level of DBA/1 wild type animals. While DBA/1 mice had a clinical score of approximately 25 at their peak the B6.NQ mice had a maximum of about 13.

Summarizing, B6.NQ mice can be immunized with G6PI to induce arthritis. The clinical progression is similar to the one in DBA/1 but the severity is milder. That makes the B6.NQ strain a G6PI-susceptible strain which might be useful for further knockout studies. However, it has to be tested if the arthritis progression in B6.NQ mice can be switched from acute, self-limiting to chronic, non-remitting by Treg-depletion.

## 5. DISCUSSION

### 5.1 REGULATORY T CELLS CONTROL THE SWITCH FROM ACUTE, SELF-LIMITING TO CHRONIC, NON-REMITTING ARTHRITIS IN THE G6PI-INDUCED ARTHRITIS MOUSE MODEL

At the beginning of this study a new mouse model for the depletion of regulatory T cells on the DBA/1 background was tested for its suitability to study the impact of fibroblast-like synoviocytes on the chronicity of arthritis. The so called DBA/1 DERE mice were obtained by a speed congenic approach from the previously published C57BL/6 DERE mice<sup>184</sup> at the Hannover Medical School (Prof. T. Sparwasser). Those mice had been generated by the introduction of a bacterial artificial chromosome (BAC) containing a diphtheria toxin receptor – eGFP construct under the control of a *foxp3* promoter into fertilized C57BL/6 oocytes. Thus, all regulatory T cells express the diphtheria toxin receptor at high levels which allows their specific depletion by the administration of DTx. The eGFP serves as a reporter protein both to genotype the mice and monitor the depletion.

The G6PI-induced arthritis mouse model was first published by Schubert *et al*<sup>123</sup> as a model for rheumatoid arthritis with an acute, self-limiting course of clinical signs and symptoms in 2004 in the DBA/1 mouse strain. In 2010 Frey *et al*<sup>133</sup> published that a depletion of regulatory T cells with an anti-CD25 antibody could switch that course to a chronic, non-remitting one. However, since an immunization with an antigen in CFA induces the generation of effector T cells which also carry the CD25 surface molecule it could not be excluded that the anti-CD25 treatment also affected the Th cells although the treatment happened prior to the immunization. More important, targeting CD25 to deplete Tregs is not possible close to or after the immunization. This regimen only allows the administration of anti-CD25 several days before immunizing the mice. Therefore, one would prefer to use the more specific and time point-independent depletion of Tregs in the DERE mice. This allows the determination of the impact of Treg-depletion both prior and post immunization during different phases of the disease, i.e. induction, effector or chronic phase. However, the present project was still focused on the Treg-depletion before immunization. DTx treatment at later time points is currently under investigation in other projects. Additionally, the DBA/1 DERE depletion system allows the identification and tracking as well as sorting of Tregs due to the simultaneous expression of the eGFP reporter.

Initial experiments were done to exclude general differences in the properties of the G6PI-induced arthritis of anti-CD25 treated DBA/1 wild type and DTx treated DBA/1 DERE mice. The clinical progression of DTx treated animals was very much similar to the situation seen by anti-CD25 administration confirming the results by Frey *et al*<sup>133</sup>. It is indeed the Treg-depletion that switches the clinical course of arthritis from acute to chronic and leads to the prolonged inflammation in the joints. In the same publication<sup>133</sup> the authors showed that the Treg-depletion with anti-CD25 was incomplete and transient but still sufficient to induce the clinical switch. That is why in this work the Treg-depletion with DTx in DBA/1 DERE mice was also measured both by intranuclear staining for FoxP3 and by the endogenous expression of eGFP in the transgenic Tregs. It turned out that the first depletion prior to the immunization lasted only until about day 4 and that Tregs were already repopulating after that short period. In this case mice did not develop a chronic, non-remitting disease course

(data not shown). Therefore, a second depletion after the immunization was introduced. This caused a longer depletion of Tregs and the clinical switch. However, differences emerged when comparing the frequencies of cells positive in the intranuclear FoxP3 staining and frequencies of endogenous eGFP expressing cells. While the frequency of eGFP expressing CD4<sup>+</sup> CD25<sup>+</sup> cells in the blood of DTx treated DBA/1 DERE mice remained reduced the frequency of FoxP3<sup>+</sup> CD4<sup>+</sup> CD25<sup>+</sup> cells increased much faster. Moreover, most of the FoxP3<sup>+</sup> CD4<sup>+</sup> CD25<sup>+</sup> cells occurring in the DTx treated DERE mice did not express eGFP anymore. Thus, after the depletion the Treg pool is repopulated by nontransgenic Tregs that cannot be depleted any more by a second DTx administration. Such a phenomenon was recently published using the DERE mouse model in an infection experiment by Berod-Sparwasser *et al* as well<sup>185</sup>. Reasons that explain this finding are just speculative. It is possible that the DBA/1 DERE mice produce nontransgenic cells from the beginning due to the loss/excision of the BAC from the murine genome by an unknown mechanism. Thus, there would be a population of Tregs that has no DTx receptor. This population must be rather small compared to the transgenic ones since genotyping of the mice did not reveal such a population. However, the treatment with DTx could serve as a selective advantage for the nontransgenic Tregs allowing them to expand in the absence of the transgenic counterparts. Another, more likely possibility is the presence of Tregs with a very low FoxP3 expression. This extremely low FoxP3 expression is then insufficient to induce the *foxp3* promoter of the transgene resulting in transgene negative Tregs. Upon DTx depletion of the transgene positive Tregs, the transgene negative ones are rapidly filling the niche. However, there are hints that those repopulating Tregs are not fully suppressive<sup>165</sup>. This competition of eGFP<sup>+</sup> and eGFP<sup>-</sup> Tregs for the Treg niche in both described scenarios is supported by the fact that the proportion of eGFP<sup>-</sup> FoxP3<sup>+</sup> Tregs is again decreasing further on in the disease progression (data not shown). In fact, the reason for the emergence of transgene negative Tregs after the DTx treatment of DBA/1 DERE mice cannot be concluded from the present experiments. This phenomenon must be further studied to elucidate the origin and/or generation of those eGFP<sup>-</sup> FoxP3<sup>+</sup> cells. Nevertheless, for the present project this fact can be disregarded since the incomplete and transient Treg-depletion is still sufficient to switch the clinical course from self-limiting to non-remitting. Moreover, the absence of Tregs before the onset of symptoms leads to an early burst of G6PI-specific T cells in the DTx treated DBA/1 DERE mice in a similar manner as shown by Frey *et al*<sup>133</sup> for the anti-CD25 treatment. Both in spleen and lymph nodes the frequency and cell number of G6PI-specific T cells are enhanced after the Treg-depletion. These pathogenic effector T cells are hypothesized to instruct resident cells in the joint to drive the chronic progression. This is supported by the published data from Frey *et al*<sup>133</sup> showing that an early CD4 depletion (before the onset of symptoms) but not a late one (around the peak of the disease) can ameliorate the disease progression in Treg-depleted animals. Accordingly, CD4 cells play an important role during early disease progression but not later on.

The present experiments showed that the properties of the disease progression as well as the inflammation in DBA/1 DERE mice are very similar to DBA/1 wild type mice when the Tregs were depleted either with DTx or with anti-CD25 respectively. Due to the advantages of the DERE system described earlier in this section all following experiments were performed using the Treg-depletion via DTx in the DBA/1 DERE mice.

In general, Tregs are able to suppress T cell effector functions and are crucial to maintain peripheral tolerance.<sup>186</sup> The absence of Tregs was shown to lead to fatal autoimmune

disorders both in human and in mice.<sup>187-190</sup> In the scurfy mouse the gene of the master transcription factor of Tregs (FoxP3) is mutated leading to the absence of FoxP3 in those mice.<sup>188</sup> The result is a lack of Tregs which finally leads to a lymphoproliferative disorder due to the lack of immune regulation.<sup>189</sup> Those mice display an early lethality (after 3-4 weeks of age) due to extensive multi-organ infiltration and enhanced cytokine production, both mediated by uncontrolled CD4<sup>+</sup> T cells. The human equivalent of that disease was phenotypically and functionally identified as the X-linked neonatal diabetes mellitus, enteropathy and endocrinopathy syndrome (IPEX).<sup>190</sup> A possible discussed general mechanism by which Tregs can prevent autoimmunity and maintain peripheral tolerance is the expression of self-reactive T cell receptors on Tregs.<sup>191</sup> Mice deficient for FoxP3 were shown to house a lot of activated T cells with self-reactive TCRs usually expressed by Tregs.<sup>192</sup> Thus, in the absence of FoxP3 most cells expressing (self-reactive) Treg-associated TCRs are not deleted and instead enter the normal T cell pool. Furthermore, most of the self-reactive T cells escaping negative selection are turned into Tregs under normal conditions.<sup>193</sup> This could in fact explain the early burst of G6PI-specific Th cells after Treg-depletion in the DBA/1 mice. Hypothetical it is possible that the absence of Tregs allows that a usually negatively selected autoreactive T cell against the ubiquitous enzyme G6PI escapes thymic and peripheral selection. Under normal physiological conditions however, Tregs would be suspected to express the TCR against the self-peptide(s) of G6PI and thereby inhibit G6PI-specific Th effector cells. To clarify this hypothesis one would have to determine if Tregs in wild type DBA/1 mice (either immunized or non-immunized) indeed express G6PI-specific TCRs. The present project was not addressing this question and thus, the molecular mechanism remains unknown.

The current literature suggests either an impaired suppressive capacity of Tregs or resistance of effector cells against Treg modulation is taking place in the inflamed joints of RA patients (see 1.1.2 Pathogenesis of the disease). A similar scenario is conceivable in the mouse model of the present study. Despite the recurrence of Tregs after the depletion animals still develop a chronic course of the disease. This could be at least partly due to the reversal of Treg suppression by T cell- and macrophage-derived TNF $\alpha$  and IL-7 during the early phase and FLS-derived IL-6 during the chronic progression. Ongoing experiments are aiming to elucidate the interplay between FLS and Tregs and the role of Tregs in the instruction of the FLS' aggressive phenotype seen in chronic arthritic mice. Additionally, it is also thinkable that activated, aggressive FLS can influence Tregs as shown by the conversion of CD25<sup>low</sup> FoxP3<sup>+</sup> Tregs into Th17-like cells in an IL-6 dependent manner in autoimmune arthritis.<sup>194</sup>

## 5.2 THE ROLE OF FIBROBLAST-LIKE SYNOVIOCYTES FOR THE CHRONICITY OF ARTHRITIS

Having the DBA/1 DREG mouse model at hand, it was now possible to study differences between nondepleted and Treg-depleted animals at the cellular level. The main focus was the elucidation of phenotypic and functional properties of resident cells in the joint, namely fibroblast-like synoviocytes, as potent candidates for drivers of the chronicity. Those cells are known to exhibit immunomodulatory as well as cartilage and bone remodeling/resorbing functions in the pathogenesis of arthritis<sup>134</sup>. However, little is known about their impact on the chronification of this autoimmune disease. Therefore, FLS from nondepleted and Treg-

depleted mice were isolated at different time points during the disease and compared concerning phenotype and functions *in vitro* as well as immunogenicity *in vivo*.

### 5.2.1 CELLULAR COMPOSITION OF ISOLATES AND PURITY OF FLS CULTURES

Until now, there is almost no reliable and often controversial data on specific surface markers for FLS in mice<sup>167,195-197</sup>. Publications on FLS in murine arthritis models often only rely on their appearance under the microscope as fibroblast-like shaped cells. Some groups have tried to identify specific markers for the FLS but published data is contradictory. Since the isolation method of FLS for the present project was based on the published protocol by Armaka *et al*<sup>167</sup> their suggestion for markers was applied in this study as well. They showed that their FLS isolated from the knee joints of C57BL/6 mice were predominantly CD90<sup>+</sup> and CD11b<sup>-</sup>. In a personal correspondence with Armaka it turned out that up to 10% of the isolated cells can express CD11b. Moreover, the majority of their FLS expressed the adhesion molecules ICAM-1 and VCAM-1. Another group compared an invasive murine fibroblast cell line (LS48) with conventional noninvasive 3T3 fibroblasts and found that the LS48 cells also predominantly expressed CD90<sup>195</sup>. However, they also found CD11b expressing cells. Additionally, they showed that VCAM-1 but not ICAM-1 was highly expressed on the invasive fibroblasts. The expression of CD90 by FLS has been further described by other groups<sup>134,196</sup>. Additionally, the genetic profile of FLS has been shown to be stable *in vitro* at early passages (passage 2-5) and during freezing but seems to be altered if FLS are used at later passages (after passage 7)<sup>197</sup>. Therefore, cells isolated from the joint as well as cultured isolates were flow cytometrically analyzed for the expression of CD90, CD11b, ICAM-1 and VCAM-1. Furthermore, cells were monitored for their surface marker expression after each passage.

Differences in the composition of isolated cells from nondepleted and Treg-depleted mice were not found. The cellular composition of the joints of arthritic mice consisted mainly of nonhematopoietic CD90<sup>+</sup> cells and to a minority of hematopoietic CD11b<sup>+</sup> ones. During the peak of the disease there was an infiltration of the joint by neutrophils and T cells which afterwards decreased again. However, the cell isolations were very stable regarding cell frequencies from experiment to experiment.

After culturing the cells it was important to ensure that the FLS cultures were pure and that the cellular composition was stable over time. The majority of cells expressed again CD90 and a minority was CD11b<sup>+</sup>. One would initially suspect those CD11b<sup>+</sup> cells to be macrophages. However, stainings both for F4/80 and MHC class II were negative but almost all of them stained positive for CD45. Thus, it is likely that the CD11b<sup>+</sup> cells are blood-born fibrocytes, a newly emerged leukocyte subpopulation<sup>198</sup>. This cell population has already been described to play a role in arthritis pathogenesis<sup>199</sup>, other diseases<sup>200</sup> and wound healing processes<sup>201,202</sup>. It was also shown that they express the surface molecules CD45 and CD11b<sup>198,203</sup>. After all, the frequency of CD90<sup>+</sup>, CD11b<sup>+</sup> and ICAM-1<sup>+</sup> cells in the cultures did not change during the passages. Therefore, it was concluded that the FLS cultures are a heterogeneous population as described by others before with the majority of CD90<sup>+</sup> fibroblasts and a minority of CD11b<sup>+</sup> fibrocytes. Thus, FLS isolated for this project could serve as reliable material since no fluctuations in the cellular composition were found. Unfortunately, the lack of a specific surface marker for FLS excludes this possibility as a

mutual target for anti-FLS therapy. The importance of targeting FLS in rheumatoid arthritis will be discussed more detailed in some of the following sections.

### 5.2.2 IMPACT OF PHENOTYPIC PROPERTIES OF FIBROBLAST-LIKE SYNOVIOCYTES

After the clarification that FLS cultures were stable regarding cellular composition cells were studied for differences between nondepleted and Treg-depleted experimental groups.

The initial focus lay on the elucidation of the inflammatory properties of the FLS and if there are differences in the susceptibility to stimulation and/or the secretion of inflammatory mediators which could explain the chronic progression in Treg-depleted animals. Therefore, several stimuli were tested based on published data. The most common read-out for the inflammatory phenotype of FLS is the measurement of secreted IL-6.

Both the stimulation with TLR ligands as well as with cytokines known to activate FLS (see 1.3 FIBROBLAST-LIKE SYNOVIOCYTES) could induce a massive IL-6 secretion by them. However, no major differences between samples from nondepleted and Treg-depleted mice were observed.

The same could be found in an additional approach using FGF-2, IL-17A or the combination of both for stimulation. The amount of secreted IL-6 did not differ between FLS from nondepleted and Treg-depleted mice. Yet, this experiment showed something else, namely the synergistic effect of a growth factor together with a cytokine. FGF-2 alone was not able to induce an IL-6 secretion but in combination with IL-17A there was an enhancement of the secreted IL-6 concentration induced by IL-17A alone. It was published that FLS can express FGF-2 themselves which then acts in an autocrine manner<sup>204</sup>. Thus, it is possible that the basal expression of FGF-2 by the FLS serves as a platform to boost the effect of inflammatory cytokines (such as IL-17A) when an inflammation in the joint is ongoing. Thereby, the expression of FGF-2 by FLS could be further enhanced since FLS harbor several receptors for FGFs<sup>205</sup>. Moreover, FGF-2 is also involved in bone destruction processes by the induction of osteoclast maturation. It was shown that FGF-2 can induce the expression of RANKL on FLS in a heparan sulfate proteoglycan-dependent manner<sup>206</sup>.

Taken together, IL-6 can be highly produced both by FLS from nondepleted and Treg-depleted arthritic mice. However, since there is no significant difference in the capability to secrete this proinflammatory cytokine it is most likely not the relevant factor leading to the switch from acute, self-limiting to chronic, non-remitting arthritis.

Fibroblast-like synoviocytes are not only able to produce and secrete cytokines but also chemokines<sup>174-176</sup>. Therefore, the secretion of several chemokines was screened in a luminex approach and with ELISA. Three candidates, namely CCL3, CCL4 and CCL5, were highly secreted upon IL-17A/TNF $\alpha$  stimulation. In general, it is widely accepted that the chemokine expression by FLS is to a certain extent responsible for the cellular composition of the rheumatoid synovium.<sup>134</sup> For instance, the here shown secretion of CCL3 and CCL5 allows for the recruitment of CD4<sup>+</sup> T cells since those express the specific receptors CXCR3 and CCR5.<sup>134</sup> As already described in the introduction, FLS can secrete an array of chemokines, three of which are the here tested CCL3, CCL4, and CCL5, that are responsible for recruiting cells of

the monocyte/macrophage as well as the granulocyte lineage.<sup>134</sup> Here, it was found that CCL3, CCL4 and CCL5 are equally high secreted by FLS from nondepleted and Treg-depleted animals both at early and late stages in the arthritis progression. This implies an equal ability to attract and retain other immune cells to and in the inflamed joints. Thus, those chemokines play for sure an important role for joint infiltration by other leukocytes during the inflammation but are probably also not alone leading to the chronicity.

In normal, healthy tissue FLS as well as other resident cells in the joint function during joint homeostasis by maintaining ECM integrity. This changes during arthritis development and progression leading to cartilage degradation and bone erosion<sup>134,137</sup>. This is at least partly mediated by the overproduction of matrix metalloproteases (MMPs) and the reduction of their specific inhibitors, tissue inhibitors of metalloproteases (TIMPs). Therefore, it was also tested in the present study if there were changes in MMP and TIMP secretion between FLS samples from nondepleted and Treg-depleted mice.

The ELISA experiments revealed a very strong upregulation of MMP-3 and -9 but not TIMP-1 secretion after *in vitro* stimulation with IL-17A/TNF $\alpha$ . However, there were again no significant differences between samples from nondepleted and Treg-depleted animals, regardless from which time point. Nevertheless, the fact that the stimulation of FLS increases the MMP secretion very strong and is almost not affecting the TIMP-1 secretion strengthens the role of MMPs during arthritis progression. Moreover, ELISA antibodies do often not distinguish between inactive pro-form and active form of the MMP. To circumvent this issue a gelatin-zymography was performed. Gelatin is the major substrate of the two gelatinases MMP-2 and MMP-9<sup>207</sup>. However, since it is known that MMP-2 is constitutively expressed in the synovium<sup>178</sup> and less important for joint invasion and cartilage degradation<sup>178,208</sup> only the secreted MMP-9 was quantified. It was found that FLS from Treg-depleted animals secreted significantly more active MMP-9 when isolated during the chronic stage (day 56) of the disease. This is a first hint of a difference between FLS from nondepleted, acute arthritic and Treg-depleted, chronic arthritic mice. Of note, it is known that RA FLS upregulate adhesion molecules such as VCAM-1 upon binding to the ECM.<sup>209</sup> This interaction in turn can then trigger intracellular signaling cascades regulating the cell cycle and the expression of MMPs. Thus, it is possible that full MMP activity cannot be provoked by such a simple *in vitro* experiment and needs a more complex milieu to mirror the *in vivo* situation.

Here again, an additional experimental step was included to determine the synergistic effect of cytokine and growth factor stimulation on the secretion of MMPs. While FGF-2 alone was already able to induce an increase of MMP-3 and -9 secretion by FLS, IL-17A alone could not. However, the double stimulation with FGF-2/IL-17A heavily boosted this secretion. Those findings taken together with the IL-6 secretion after FGF-2/IL-17A stimulation demonstrate an immunological concept seen in other inflammatory processes as well, namely the synergistic effect of a growth factor and a cytokine<sup>210-213</sup>. Normal dermal fibroblasts from rabbit or human were shown to boost the upregulation of MMP-9 when stimulated with PDGF or FGF-2 in combination with IL-1 or TNF $\alpha$ .<sup>211</sup> MMP-1, MMP-3 and MMP-9 are also synergistically induced in dermal fibroblasts after IL-1/TGF $\alpha$  stimulation.<sup>212</sup> Studies on synergistic effects of cytokines and growth factors on FLS however are very rare. One study described the synergistic effects of PDGF or TGF $\beta$  in combination with IL-1 or TNF $\alpha$  on the secretion of MMP3 and other proinflammatory mediators in RA FLS.<sup>213</sup> The present study elucidated that IL-17A stimulation alone could induce the secretion of proinflammatory IL-6 but not the matrix degrading MMPs. In contrast, the single stimulation with FGF-2 did not

affect the IL-6 secretion but was able to enhance the secretion of MMPs. Both factors together elevated both the secreted IL-6 and MMP-3/-9 concentrations to a very high extent. This demonstrates that FGF-2 might act as a basal inducer of MMPs, IL-17A as a basal inducer of cytokines and that both together work in a synergistic manner supporting their important role for inflammatory and destructive processes during the arthritis progression. This concept of boosting the FLS' response to inflammatory cytokines by growth factors may provide a therapeutic approach by targeting fibroblast-specific growth factors.

Summarizing the phenotypical analyses it has to be stated that differences in the inflammatory and destructive phenotype of FLS isolated from nondepleted and Treg-depleted animals at different time points during the disease course were just marginal and did not reach statistical significance in most cases. Only the secretion of active MMPs by FLS from Treg-depleted animals at day 56 was significantly enhanced. Thus, looking at inflammatory cytokines, chemokines and matrix-degrading enzymes one by one does not elucidate the impact and role of FLS for the switch to and the maintenance of chronicity in this arthritis mouse model. However, it is still possible that the interplay of the measured factors as well as other additional ones not included in this project may make a difference in FLS phenotype and function.

### 5.2.3 IMPACT OF FUNCTIONAL PROPERTIES OF FIBROBLAST-LIKE SYNOVIOCYTES

To further investigate the role of FLS during the chronic phase of arthritis in a more complex and comprehensive setup functional assays were performed. This allows the study of the FLS' properties in a broader context not only looking at single molecules, mediators and effects one by one.

Two compartments are involved in cartilage (and subsequent bone) destruction/erosion *in vivo*<sup>99,179</sup>, the cartilage itself and the synovial membrane consisting of macrophage-like (type A) and fibroblast-like (type B) cells<sup>99</sup>. In order to achieve destruction in the joint, cells from the synovial membrane need to attach to and invade into the articular cartilage.

The present study made use of two *in vitro* methods to study this interaction. The first approach was a cartilage attachment assay as published by Korp-Pap *et al*<sup>179</sup>. Wild type femoral head cartilage was incubated with isolated FLS and the number of attached FLS could be counted. This allowed the determination of the FLS' capacity to attach to cartilage as a first step of joint invasion. The experiment showed that FLS from nondepleted and Treg-depleted animals have the same capacity to attach to wild type cartilage when isolated during the peak of the disease (day 14). It changes dramatically using FLS from the late, chronic phase. While FLS from nondepleted mice lose their attachment capacity the FLS from Treg-depleted ones gain an even higher ability of attaching to wild type articular cartilage. This difference between both experimental groups is highly significant. The capability of the FLS to attach to the wild type femoral head cartilage is the first requirement to damage a joint<sup>209</sup>. The more cells attach to articular cartilage the higher the possibility to eventually invade the cartilage and subsequently erode it. Since the attachment of FLS to cartilage is facilitated by cell surface adhesion molecules<sup>209</sup> it is likely that FLS from Treg-depleted mice upregulate their adhesion molecules stronger than those from nondepleted ones. However, this method does not elucidate if the FLS are really destructive. Yet, in connection with the data about MMPs

after *in vitro* stimulation one would suspect that the attached FLS will all invade the cartilage. So far, previous publications have shown that FLS from hTNFtg mice (a transgenic mouse model spontaneously developing chronic arthritis<sup>119</sup>) are able to attach and eventually invade wild type articular cartilage.<sup>179</sup> However, the focus there lay on the elucidation of prerequisites that have to be fulfilled on the cartilage side in order to allow FLS attachment. Moreover, until now there is no evidence that FLS from chronic arthritic animals or RA patients show a higher ability for potential cartilage destruction than those from acute arthritic mice or OA patients, respectively. Therefore, this is the first time showing an improved cartilage invading potential represented by enhanced attachment to cartilage of FLS when they acquired their activated phenotype in a chronic disease progression directly compared to counterparts from acute arthritic subjects.

To clarify if the enhanced capacity of FLS from Treg-depleted mice to attach to cartilage is resulting in stronger destruction the MATRIN assay<sup>164</sup> was performed. This assay uses the measurement of the breakdown of an electrical resistance on a barrier when destroyed by the cells of interest, in this case the FLS. The barrier is comprised of a collagen-matrix on the one side of a semipermeable cell insert and an epithelial cell layer on the other side. This allows the indirect measurement of the destructive potential of the FLS. The first step of the breakdown is the destruction of the collagen-matrix, most likely due to the secretion of MMPs. If the collagen is degraded it allows other mediators secreted by the FLS to migrate through the semipermeable membrane to disintegrate the epithelial cell layer. This is facilitated by secreted cytokines and MMPs acting on the epithelial cells. The epithelial cells used in this assay are MDCK-C7 cells, a variant of Madin-Darby canine kidney cells that has especially “tight” tight junctions due to the lack of endogenous claudin-2 expression<sup>180</sup>. After encountering cytokines, those cells however start to express claudin-2 which then leads to the replacement of the “tight” tight junctions by “leaky” tight junctions<sup>181</sup>. Moreover, it also induces their internalization<sup>182</sup>. Those events result in the breakdown of the transepithelial electrical resistance (TEER). Thus, if the FLS are destructive, the resistance will break down. There are two parameters of the measurement that are most important. First, the time point after which the breakdown happens represents the destructive potential in general. Second, the steepness of the decrease represents the continuous production of MMPs and cytokines and thereby the speed of destruction by the FLS. Comparing the destructive capacity of FLS from nondepleted and Treg-depleted mice in the MATRIN assay revealed that FLS in general have the potential to destroy cartilage. Already the FLS from naïve, non-immunized animals induced a breakdown of the TEER, regardless if isolated from nondepleted or Treg-depleted mice. Yet, that potential increased using FLS isolated during the peak of the disease being most prominent with the FLS from Treg-depleted mice. The most dramatic change and difference was observed with FLS isolated during the late stage of the disease. While FLS from Treg-depleted animals remained almost as destructive as during the peak phase, the ones from nondepleted mice seemed to lose their initial destructive capacity being less destructive than the naïve ones. These results demonstrate two very important findings: 1) FLS from chronic arthritic mice gain an aggressive phenotype which remains stable throughout the whole disease course being completely in contrast to the FLS from the acute arthritic animals. 2) FLS from acute arthritic mice seem to fall in some kind of a refractory/repressed phase after an initial activation having a lower activity for cartilage destruction than naïve FLS. Those findings are very important for explaining the switch from acute to chronic arthritis after Treg-depletion. It clearly demonstrates that the FLS in the Treg-depleted mice gain an aggressive phenotype which persists over the whole time of investigation. However, the

underlying mechanism by which the FLS from Treg-depleted animals gain this aggressiveness remains unclear. From the *in vitro* stimulation experiments regarding cytokine, chemokine and MMP secretion one would expect that FLS from nondepleted and Treg-depleted mice are likewise destructive. However, those ELISA approaches only look at one phenomenon at a time. The functional examination of the FLS in the attachment and MATRIN assay have a much more complex setup allowing the interplay of several factors that could contribute to the pathogenicity. For example, it has been published that the attachment of FLS to cartilage induces MMP expression and secretion<sup>209</sup> through cell surface adhesion molecules which interact with signaling cascades resulting in MMP expression enhancement<sup>209,214</sup>. This can just not be mimicked in the *in vitro* stimulation assay for the measurement of cytokines, chemokines and MMPs which might explain the lack of differences between FLS from nondepleted and Treg-depleted arthritic mice in those assays. In the cartilage attachment assay and the MATRIN assay instead FLS have access to wild type cartilage or artificial cartilage, respectively. This might possibly result in the activation of intracellular signaling via their surface molecules leading to the observed results.

One important notion of these MATRIN experiments results from the fact that FLS from acute arthritic mice (which resolve the disease) show a much less destructive capacity than their naïve counterparts. Accounting for the fact that FLS are thought to be one of the major cell types involved in cartilage destruction and induction of bone erosion in RA patients one would wish to elucidate the mechanism by which the FLS from the nondepleted animals gain this refractory/repressed behavior. Thereby, it would eventually be possible to discover targets to trigger this “switch-off” and reverse the phenotype of the aggressive ones to nonaggressive. RA patients could highly benefit from it since anti-inflammatory therapies as applied nowadays do not prevent cartilage and bone erosion. Unfortunately, such a phenomenon has not been seen in any earlier experiment and therefore never been addressed. It could be a very valuable aim of research in order to really cure patients from rheumatic diseases.

#### 5.2.4 TRANSFER OF ARTHRITIS BY *IN VIVO* FLS-TRANSFER

To ultimately test if the FLS in the present chronic arthritis mouse model gain an independent, aggressive phenotype acting autonomously without the help of the adaptive immunity to become the drivers of the inflammation, isolated and *in vitro* restimulated FLS from nondepleted and Treg-depleted arthritic mice were transferred into knee joints of *rag1*-deficient recipients. After 2 weeks of incubation the knee joints were histologically analyzed for inflammation and cartilage/bone erosion by a simple H&E and TRAP staining in cooperation with Prof. G. Schett from Erlangen. This allowed the pathological quantification of inflammation/synovitis and an estimation of cartilage destruction as well as bone erosion.

There had been earlier approaches by several researchers using an engraftment model in SCID mice as an *in vivo* model for cartilage destruction<sup>150,215,216</sup>. Synovial tissue or fibroblasts from RA patients were implanted together with normal human cartilage under the renal capsule or subcutaneously. Afterwards, cartilage erosion was examined by light and electron microscopy as well as histology. As a result the researchers found that RA synovial cells can erode normal human cartilage in this *in vivo* system. However, the implantation of human

material into a murine host makes the setup rather artificial. Moreover, the incubation time was comparatively long; depending on the study between 60 and 100 days. Furthermore, there were no signs of inflammation detected; indicating that the implant was its own closed, isolated system in a host organism. Thus, those previous studies were able to show erosion and cartilage invasion by RA synovial cells into normal human cartilage and did not indicate a transfer of arthritis *in vivo*. This engraftment SCID mouse model for RA is therefore a nice tool to study certain properties of RA synoviocytes regarding cartilage destruction but it is unable to give a comprehensive view of the RA synoviocyte's capabilities in the arthritic inflammatory context. In contrast, the transfer of FLS into *rag1*-deficient mice enables the examination of a broader range of functions and properties of the transferred cells simultaneously in a living organism. Instead of having a closed, isolated system this transfer allows a comprehensive view on the role and importance of the FLS during arthritis pathogenesis.

The FLS-transfer experiments showed that it is possible to transfer arthritis by simply injecting isolated FLS from arthritic mice into *rag1*-deficient recipients. The transfer of naïve FLS (from day 0) was not inducing an inflammatory reaction in the joint but FLS isolated at day 14 and day 56 from nondepleted or Treg-depleted mice lead to an infiltration of the joint by innate immune cells, most likely monocytes/macrophages and neutrophils. However, while FLS from nondepleted mice were just marginally immunogenic, the ones from Treg-depleted subjects induced heavy synovitis. Especially the FLS isolated at day 56 from the Treg-depleted mice were very potent inducers of immune cell infiltration. Moreover, those FLS from the chronic phase were exclusively able to induce cartilage and bone erosion, most likely by the secretion of MMPs and the differentiation and induction of osteoclasts. Undoubtedly, FLS are capable of secreting MMPs which results in the degradation of cartilage<sup>178,217</sup>. Additionally, it has also been published that fibroblast-like cells can itself resorb bone independently of osteoclasts by the secretion of acidic components<sup>218</sup>. Moreover, fibroblasts from RA patients as well as FLS from mouse models are known to express RANKL, the inducer of osteoclastogenesis<sup>20,219,220</sup>. Furthermore, IL-6 which is highly produced by FLS can induce RANKL expression by other resident cells in the joint, e.g. osteoblasts<sup>220</sup>. In line with those findings, the inhibition of the IL-6R can inhibit the formation of osteoclasts *in vitro* and *in vivo*<sup>221</sup>. Additionally, osteoclast formation/differentiation as well as activation can also be achieved independent of RANKL<sup>222,223</sup>.

Taken together, a possible mechanism of action in this setup is the recruitment of innate immune cells to the joint by aggressive, destructive FLS (derived from day 56 Treg-depleted mice) via the secretion of chemokines and cytokines, the degradation of cartilage and erosion of bone by the FLS itself via the secretion of MMPs and the release of acidic components<sup>218</sup>, and the induction of bone resorbing osteoclasts by RANKL expression and IL-6 secretion. Until now, this is the first time showing that FLS from chronic arthritic mice alone can drive an immune reaction and lead to cartilage as well as bone erosion in a B- and T-cell independent manner which makes them autonomous drivers of the arthritis. The remaining question is how those FLS are instructed and why the Treg-depletion can induce this switch of the FLS phenotype. Nevertheless, these experiments underline the importance to expand the therapies for RA patients from only anti-inflammatory also to anti-FLS treatments.

### 5.3 INSTRUCTION OF FIBROBLAST-LIKE SYNOVIOCYTES BY IL-17

In the past years there have been several publications from different research groups showing that IL-17 plays an important role for arthritis pathogenesis. It was found to be highly abundant in the synovium of RA patients<sup>29</sup> being a potent stimulator for osteoclastogenesis<sup>224,225</sup>. On the one hand, IL-17 can induce the expression of RANKL on fibroblasts and osteoblasts<sup>224</sup>, on the other hand it also serves as a stimulus for the secretion of proinflammatory cytokines such as IL-6 and TNF $\alpha$  by fibroblast-like and endothelial cells<sup>161,226</sup>. IL-17 is also able to induce osteoclastogenesis independent of RANKL by osteoblasts and synoviocytes<sup>225</sup>. Initially, the main source of IL-17 was always believed to be the Th17 cells. Animal models for arthritis, including the G6PI-induced arthritis mouse model, have shown an important role for Th17 cells<sup>123,124,227</sup>. However, little was known about the origin of IL-17 in the RA synovium. In fact, it has been found that mast cells in the synovium of RA patients were the major source of that cytokine demonstrating the importance of the innate immunity for arthritis pathogenesis<sup>71</sup>. Nevertheless, IL-17 is up to now thought to be mainly responsible for the osteoclastogenesis, either directly or indirectly. So far, there have been no efforts to elucidate the role and impact of IL-17 on the phenotype and function of FLS. Yet, there was a recent publication by Wu L *et al* showing an importance of IL-17A for fibroblasts in a mouse model of inflammatory dilated cardiomyopathy (DCMi)<sup>228</sup>. They demonstrated earlier that IL-17A is the essential factor to develop DCMi after a myocarditis<sup>229</sup> but the mechanism was unclear. Now, they found that IL-17A could potentially induce chemokine and cytokine secretion by cardiac fibroblasts being a critical step in the development of DCMi. Thus, a similar mechanism could be acting here in the setup of G6PI-induced arthritis to lead to the aggressive, destructive phenotype of FLS.

It turned out that both preventive as well as therapeutic treatment of nondepleted and Treg-depleted, G6PI-immunized mice with anti-IL-17A antibodies could ameliorate the disease. In the case of the preventive treatment it seems rational since the original publication about the G6PI-induced arthritis mouse model as well as the report about the Treg-dependent switch from acute to chronic arthritis showed the involvement of Th17 cells during the induction phase<sup>123,133</sup>. Moreover, the preventive administration of anti-CD4 antibodies prohibited the disease<sup>133</sup>. Yet, this anti-CD4 treatment was no longer curative when administered after the onset of symptoms in the Treg-depleted mice suggesting the participation of other immune cells apart from Th17 cells as the source of IL-17. It is very likely that those IL-17 producing cells during later stages of the disease are mast cells since they have been shown to be a major source of IL-17 in the synovium of RA patients<sup>71</sup>. Unfortunately, there is no antibody or compound available to specifically deplete mast cells for a clinical investigation. Besides, a more elegant way to study the role of mast cells as IL-17 producing cells would be the use of an inducible mast cell knockout. Sadly, there is not such a mouse strain available, especially not on the DBA/1 background. Another possible cell type producing IL-17 are the  $\gamma\delta$  T cells<sup>230,231</sup>. They have been shown to be the predominant source of IL-17 in another arthritis mouse model<sup>232</sup>. Thus, one would also wish to perform a clinical study with G6PI-immunized mice depleting the  $\gamma\delta$  T cells preventively or therapeutically to determine their role for the disease progression. There is an antibody, called GL3, available against the T cell receptor of  $\gamma\delta$  T cells. Unfortunately, this antibody does not deplete the cells but rather makes them invisible by triggering TCR internalization<sup>233</sup>. This does not necessarily mean that IL-17 production by  $\gamma\delta$  T cells is thereby inhibited. The production of IL-17 by  $\gamma\delta$  T cells has been

reported to be largely independent of their TCR activation<sup>231</sup>. This is probably also the reason why a conducted experiment in the scope of this project with preventive and therapeutic GL3 administration showed no effect on arthritis progression (data not shown). Thus, a “depletion” using the GL3 antibody is not a useful tool for this issue. In the end, the source of IL-17 after the onset of symptoms in this mouse model remains unknown.

Further studies isolating FLS from the therapeutically anti-IL-17 treated mice shed some light on the instruction of those joint resident cells. In the MATRIN assay the FLS from Treg-depleted, chronic arthritic animals were shown to be still highly aggressive and destructive at the late stage of the disease as seen in earlier experiments. This was completely in contrast to the FLS from the nondepleted animals. But, this aggressive, destructive behavior could be reduced and even reverted to normal levels by the therapeutic treatment of the Treg-depleted animals with anti-IL-17A. Those findings demonstrate that IL-17A (from which source ever) is one major important factor to transform the FLS to the destructive drivers of the arthritis. Yet, it remains to be elucidated if the IL-17 is acting directly or indirectly on the FLS. However, clarifying the role of IL-17 on the FLS’ instruction provides another possible target to interfere with for a feasible therapy.

## 5.4 CONCLUSION AND OUTLOOK

Based on the previously published findings from Schubert *et al*<sup>123</sup> and Frey *et al*<sup>133</sup> together with the results of the present study the following model can be postulated:

The absence of Tregs during the early phase of the disease progression enables the generation of a larger population of G6PI-specific effector T cells with a Th17-like phenotype which is able to instruct resident cells in the joint, most likely fibroblast-like synoviocytes, at least partly by the secretion of IL-17. This instruction leads to a transformation of the FLS’ phenotype towards a more aggressive, destructive one with the capability to autonomously drive the arthritis progression without the help of the adaptive immunity and facilitate cartilage and bone erosion directly and indirectly via osteoclast induction.

This knowledge should be taken into account when designing novel therapies for RA patients. So far, RA patients are mostly treated with compounds or antibodies to suppress the inflammation (such as TNF $\alpha$  antagonists), induce anti-inflammatory proteins (e.g. via glucocorticoid administration), slow down the joint damage (by biological DMARDs) and improve the patients daily life (e.g. by pain relievers). However, all therapies used up-to-date aim only at reducing the symptoms and the inflammation and are not directed against the causes of them because those are still largely unknown. Therefore, it is important to intensify the research efforts to clarify the certain roles of adaptive and innate immune cells as well as resident cells in the joint to develop new combinatorial treatment strategies.

Despite the fact that the present study revealed some interesting facts about FLS and shed more light on their independent role during arthritis progression in the G6PI-induced arthritis mouse model there are still open questions that need to be addressed in future experiments.

It remains unclear if and how the Tregs are influencing the FLS indirectly or directly. Ongoing experiments using coculture approaches with FLS and Tregs are aiming to elucidate if the Tregs can suppress the aggressive, destructive phenotype (using the MATRIN assay) and if the FLS in turn can push the Tregs towards a more Th17-like phenotype as indicated by published data from Komatsu *et al*<sup>194</sup>. Moreover, *in vivo* experiments by colleagues showed that reconstituting Treg-depleted, G6PI-immunized mice with isolated Tregs from naïve animals during the chronic phase is able to ameliorate the disease severity.

Also, the source of IL-17 during the different stages of the disease (i.e. before the onset of symptoms, during the peak phase and during the late, chronic progression) remains to be elucidated. Therefore, depletion experiment using antibodies against potential cell types could be used. However, not in all cases specific antibodies are available. A more elegant way would be the utilization of cell-type specific (ideally inducible) knock-out animals for IL-17 and/or IL-17 receptors. For the present project only complete IL-17 knock-out mice were available. But as expected, they hardly developed any symptoms of arthritis (data not shown). Unfortunately, on the rarely used DBA/1 background only a few more knock-out strains are available. In contrast, on the widely used C57BL/6 background almost all desirable knock-out strategies have been already generated. The newly available B6.NQ mice harbor the H2-haplotype q, thereby making those mice susceptible to G6PI-induced arthritis. This strain could serve as a very valuable tool to conduct further knock-out studies, not only restricted to the role of IL-17. Yet, it has to be tested if the disease progression of these mice can be switched from acute, self-limiting to destructive, non-remitting by Treg depletion as well.

Last but not least, the cellular mechanisms that induce the aggressive, destructive phenotype in the FLS need to be decoded in order to develop efficient and specific treatments. Ultimately, those results could lead to the treatment of RA patients not only improving the patient's daily life but actually really eliminating the causes of the symptoms so that a long time, continuous medication is no longer necessary and complete remission is achieved.

## ABBREVIATIONS

ACPA	anti-citrullinated protein antibody
APC	antigen-presenting cell
APRIL	a proliferation-inducing ligand
APS	ammonium persulfate
BAC	bacterial artificial chromosome
BAFF	B cell activating factor
Bcl-2	B-cell lymphoma 2
BSA	bovine serum albumin
CaCl <sub>2</sub>	calcium chloride
CCL	CC chemokine ligand
CCR	C-C chemokine receptor
CD	cluster of differentiation
CFA	complete Freund's adjuvant
CO <sub>2</sub>	carbon dioxide
CTLA4	cytotoxic T-lymphocyte-associated protein 4
CXCR	C-X-C chemokine receptor
DAMP	danger associated molecular pattern
DC	dendritic cell
DCMi	inflammatory dilated cardiomyopathy
ddH <sub>2</sub> O	double-distilled water
DEREG	depletion of regulatory T cells
DMARD	disease modifying anti-rheumatic drug
DMEM	Dulbecco's modified Eagle's medium
DMSO	dimethyl sulfoxide
DTx	diphtheria toxin
e.g.	exempli gratia (for example)
ECM	extra cellular matrix
EDTA	ethylenediaminetetraacetic acid
eGFP	enhanced green fluorescent protein
ELISA	enzyme-linked immunosorbent assay
ER	endoplasmic reticulum
<i>et al</i>	et alii (and others)
FACS	fluorescence-activated cell sorting
FasL	Fas ligand
FCS	fetal calve serum
FGF	fibroblast growth factor
FLS	fibroblast-like synoviocytes
FoxP3	forkhead box P3
<i>g</i>	acceleration
G6PI	glucose-6-phosphate isomerase
GM-CSF	granulocyte/macrophage colony-stimulating factor
GZMB	granzyme B
H <sub>2</sub> O <sub>2</sub>	hydrogen peroxide
H <sub>2</sub> SO <sub>4</sub>	sulfuric acid
HCl	hydrogen chloride

HLA	human leukocyte antigen
hTNFtg	human TNF transgenic
i.e.	id est (that is)
<i>i.p.</i>	intraperitoneal
ICAM-1	intercellular adhesion molecule 1
IFN $\gamma$	interferon gamma
Ig	immunoglobulin
IL	interleukin
IL-1R	IL-1 receptor
IL-1ra	IL-1 receptor agonist
IL-1RacP	IL-1R accessory protein
IL-6R	IL-6 receptor
IMDM	Iscoves' modified Dulbecco's medium
IPEX	immunodysregulation polyendocrinopathy enteropathy X-linked syndrome
KCl	potassium chloride
KH <sub>2</sub> PO <sub>4</sub>	potassium dihydrogen phosphate
KHCO <sub>3</sub>	potassium hydrogen carbonate
LFA-1	lymphocyte function-associated antigen 1
LT $\beta$	lymphotoxin beta
mAb	monoclonal antibody
MATRIN	matrix-associated transepithelial resistance invasion
MCP	metacarpophalangeal
MCP-1	monocyte chemotactic protein 1
M-CSF	macrophage colony stimulating factor
MDCK	Madin-Darby canine kidney cell
MEM	minimal essential medium
MFI	mean fluorescence intensity
MHC	major histocompatibility complex
MIP-1 $\alpha/\beta$	macrophage inflammatory protein 1 $\alpha/\beta$
MLS	macrophage-like synoviocytes
MMP	matrix metalloprotease
MTP	metatarsophalangeal
Na <sub>2</sub> HPO <sub>4</sub>	disodium hydrogen phosphate
NaCl	sodium chloride
NaHCO <sub>3</sub>	sodium hydrogen carbonate
NaOH	sodium hydroxide
NF $\kappa$ B	nuclear factor kappa-light-chain-enhancer of activated B cells
NH <sub>4</sub> Cl	ammonium chloride
NK cell	natural killer cell
NLR	NOD-like receptor
NO	nitric oxide
OA	osteoarthritis
OPD	o-phenylenediamine
PAGE	polyacrylamide gel electrophoresis
PAMP	pathogen associated molecular pattern
PBMC	peripheral blood mononuclear cell
PBS	phosphate buffered saline

PFA	paraformaldehyde
PGN	peptidoglycan
POD	peroxidase
PRKCQ	protein kinase C theta
PTPN22	protein tyrosine phosphatase, non-receptor type 22
RA	rheumatoid arthritis
rag	recombination activating gene
RANK	receptor activator of nuclear factor $\kappa$ B
RANKL	receptor activator of nuclear factor kappa-B ligand
RANTES	regulated on activation, normal T cell expressed and secreted
rhG6PI	recombinant human G6PI
RNS	reactive nitrogen species
ROS	reactive oxygen species
rpm	revolutions per minute
s.c.	subcutaneous
SCF	stem cell factor
SCID	severe combined immunodeficiency
SDS	sodium dodecyl sulfate
TCR	T cell receptor
TEER	transepithelial electrical resistance
TEMED	tetramethylethylenediamine
TGF $\beta$	transforming growth factor beta
Th	T helper cell
TIMP	tissue inhibitor of metalloproteinases
TLR	Toll-like receptor
TNF	tumor necrosis factor
TNFAIP3	tumor necrosis factor, alpha-induced protein 3
TRAP	tartrate-resistant acid phosphatase
Treg	regulatory T cell
unstim	not stimulated
VCAM-1	vascular cell adhesion molecule 1
VEGF	vascular endothelial growth factor

## ACKNOWLEDGEMENT

I hereby want to thank Prof. Thomas Kamradt for the provision of an interesting immunological project and his supervision. I am also thankful for numerous opportunities to present my data at different international meetings and for the ability to participate in immunological schools and seminars.

I also want to thank all the members of the Institute of Immunology at the University Hospital Jena for nicely introducing me into the group, helping me with experimental issues and supporting me in hard times. Thanks also for the fun during social events.

I am also thankful for all the help from our collaboration partners, including Prof. Georg Schett from Erlangen, Prof. Thomas Pap, Dr. Adelheid Korb-Pap and Dr. Christina Wunrau-Koers from Münster, Prof. Christine Falk from Hannover, Prof. Rikard Holmdahl from Stockholm, Dr. Sylvia Heink from Munich and my friend Dr. Hyun-Dong Chang from the German Rheumatology Research Center in Berlin. Thank you for providing me valuable experimental methods, inspiring ideas and critical questions during progress reports.

Thanks go also to our animal care takers for the provision of their services and a good cooperation.

Special thanks go to Dr. Ingo Irmeler and Dr. Sebastian Drube for not only a lot of help in the lab but also becoming good friends, for fun during drinking and movie nights, barbeques and a lot of discussions about the issues of the world.

Many thanks to “Fachimmunologe” Dr. D for all the morning and afternoon coffees, talks on intellectual and also brainless topics, for (heated) debates about movies, cars, traffic, women, drinks, research habits and many more as well as fun times during parties. Special thanks to super hero Dr. D for the provision of a Master thesis project to Romy which in the end definitely improved my personal, private life.

I also want to thank my girlfriend Romy for the personal support in times of stress, anger and frustration about the work.

Last but not least I thank my family for always supporting me in any possible way.

## LIST OF TABLES

Table 1: Biological DMARDs in clinical use	12
Table 2: Cell cultures	23
Table 3: Kits	23
Table 4: Chemicals	24
Table 5: List of compounds used for <i>in vivo</i> experiments	24
Table 6: List of ELISA antibodies and standards	24
Table 7: List of ELISA Sets	24
Table 8: DEREg typing staining	25
Table 9: T cell staining	25
Table 10: Joint cell staining	25
Table 11: FLS staining	25
Table 12: List of cell culture compounds	26
Table 13: devices	26
Table 14: equipment	26
Table 15: Cell culture media	27
Table 16: Flow Cytometry	27
Table 17: ELISA	28
Table 18: Zymography	28
Table 19: cell culture, <i>in vivo</i> , others	29
Table 20: Zymography gels	35

## LIST OF FIGURES

Figure 1: Schematic view of a normal joint (a) and a joint affected by RA (b)	8
Figure 2: Clinical course and histopathology of G6PI-induced arthritis.	16
Figure 3: Diverse role of FLS in RA.	21
Figure 4: Clinical scoring of inflammation in the paws.	36
Figure 5: The G6PI-arthritis model in DBA/1 DEREg mice.	41
Figure 6: Cells isolated by joint digestion.	43
Figure 7: Fibroblast-like synoviocytes in culture.	44
Figure 8: Inflammatory phenotype of fibroblast-like synoviocytes.	46
Figure 9: Chemokine-secretion by fibroblast-like synoviocytes.	49
Figure 10: Destructive phenotype of fibroblast-like synoviocytes.	51
Figure 11: Attachment of fibroblast-like synoviocytes to wild type cartilage.	52
Figure 12: Functional analysis of fibroblast-like synoviocytes' destruction of cartilage.	53
Figure 13: <i>In vivo</i> function of fibroblast-like synoviocytes.	55
Figure 14: Anti – IL-17A treatment.	57
Figure 15: G6PI-arthritis in B6.NQ mice.	58

## REFERENCES

- 1 Lee, D. M. & Weinblatt, M. E. Rheumatoid arthritis. *Lancet* **358**, 903-911, doi:10.1016/s0140-6736(01)06075-5 (2001).
- 2 Charles-Schoeman, C. Cardiovascular disease and rheumatoid arthritis: an update. *Current rheumatology reports* **14**, 455-462, doi:10.1007/s11926-012-0271-5 (2012).
- 3 Listing, J., Gerhold, K. & Zink, A. The risk of infections associated with rheumatoid arthritis, with its comorbidity and treatment. *Rheumatology (Oxford)* **52**, 53-61, doi:10.1093/rheumatology/kes305 (2013).
- 4 Scrivo, R., Vasile, M., Muller-Ladner, U., Neumann, E. & Valesini, G. Rheumatic diseases and obesity: adipocytokines as potential comorbidity biomarkers for cardiovascular diseases. *Mediators of inflammation* **2013**, 808125, doi:10.1155/2013/808125 (2013).
- 5 Alamanos, Y. & Drosos, A. A. Epidemiology of adult rheumatoid arthritis. *Autoimmunity reviews* **4**, 130-136, doi:10.1016/j.autrev.2004.09.002 (2005).
- 6 Oliver, J. E. & Silman, A. J. Risk factors for the development of rheumatoid arthritis. *Scandinavian journal of rheumatology* **35**, 169-174, doi:10.1080/03009740600718080 (2006).
- 7 Klareskog, L., Malmstrom, V., Lundberg, K., Padyukov, L. & Alfredsson, L. Smoking, citrullination and genetic variability in the immunopathogenesis of rheumatoid arthritis. *Seminars in immunology* **23**, 92-98, doi:10.1016/j.smim.2011.01.014 (2011).
- 8 McInnes, I. B. & Schett, G. The pathogenesis of rheumatoid arthritis. *N Engl J Med* **365**, 2205-2219, doi:10.1056/NEJMra100496510.7748/phc2011.11.21.9.29.c8797 (2011).
- 9 De Almeida, D. E. *et al.* Immune dysregulation by the rheumatoid arthritis shared epitope. *J Immunol* **185**, 1927-1934, doi:10.4049/jimmunol.0904002 (2010).
- 10 Gregersen, P. K., Silver, J. & Winchester, R. J. The shared epitope hypothesis. An approach to understanding the molecular genetics of susceptibility to rheumatoid arthritis. *Arthritis Rheum* **30**, 1205-1213 (1987).
- 11 Weyand, C. M., Hicok, K. C., Conn, D. L. & Goronzy, J. J. The influence of HLA-DRB1 genes on disease severity in rheumatoid arthritis. *Annals of internal medicine* **117**, 801-806 (1992).
- 12 Weyand, C. M. & Goronzy, J. J. Disease-associated human histocompatibility leukocyte antigen determinants in patients with seropositive rheumatoid arthritis. Functional role in antigen-specific and allogeneic T cell recognition. *The Journal of clinical investigation* **85**, 1051-1057, doi:10.1172/jci114535 (1990).
- 13 Genome-wide association study of 14,000 cases of seven common diseases and 3,000 shared controls. *Nature* **447**, 661-678, doi:10.1038/nature05911 (2007).
- 14 Silman, A. J. *et al.* Twin concordance rates for rheumatoid arthritis: results from a nationwide study. *British journal of rheumatology* **32**, 903-907 (1993).
- 15 Symmons, D. P., Barrett, E. M., Bankhead, C. R., Scott, D. G. & Silman, A. J. The incidence of rheumatoid arthritis in the United Kingdom: results from the Norfolk Arthritis Register. *British journal of rheumatology* **33**, 735-739 (1994).
- 16 Uhlig, T., Hagen, K. B. & Kvien, T. K. Current tobacco smoking, formal education, and the risk of rheumatoid arthritis. *The Journal of rheumatology* **26**, 47-54 (1999).
- 17 Klareskog, L., Padyukov, L. & Alfredsson, L. Smoking as a trigger for inflammatory rheumatic diseases. *Current opinion in rheumatology* **19**, 49-54, doi:10.1097/BOR.0b013e32801127c8 (2007).
- 18 Padyukov, L., Silva, C., Stolt, P., Alfredsson, L. & Klareskog, L. A gene-environment interaction between smoking and shared epitope genes in HLA-DR provides a high risk of seropositive rheumatoid arthritis. *Arthritis Rheum* **50**, 3085-3092, doi:10.1002/art.20553 (2004).

- 19 Klareskog, L. *et al.* A new model for an etiology of rheumatoid arthritis: smoking may trigger HLA-DR (shared epitope)-restricted immune reactions to autoantigens modified by citrullination. *Arthritis Rheum* **54**, 38-46, doi:10.1002/art.21575 (2006).
- 20 McInnes, I. B. & Schett, G. Cytokines in the pathogenesis of rheumatoid arthritis. *Nature reviews. Immunology* **7**, 429-442, doi:10.1038/nri2094 (2007).
- 21 Choy, E. Understanding the dynamics: pathways involved in the pathogenesis of rheumatoid arthritis. *Rheumatology (Oxford)* **51 Suppl 5**, v3-11, doi:10.1093/rheumatology/kes113 (2012).
- 22 Girard, J. P. & Springer, T. A. High endothelial venules (HEVs): specialized endothelium for lymphocyte migration. *Immunology today* **16**, 449-457 (1995).
- 23 Shiozawa, S., Shiozawa, K. & Fujita, T. Morphologic observations in the early phase of the cartilage-pannus junction. Light and electron microscopic studies of active cellular pannus. *Arthritis Rheum* **26**, 472-478 (1983).
- 24 Kobayashi, I. & Ziff, M. Electron microscopic studies of the cartilage-pannus junction in rheumatoid arthritis. *Arthritis Rheum* **18**, 475-483 (1975).
- 25 Kamradt, T. & Frey, O. Arthritis: where are the T cells? *Arthritis Res Ther* **12**, 122, doi:10.1186/ar3008 (2010).
- 26 Panayi, G. S. Even though T-cell-directed trials have been of limited success, is there reason for optimism? *Nature clinical practice. Rheumatology* **2**, 58-59, doi:10.1038/ncprheum0094 (2006).
- 27 Schulze-Koops, H. & Kalden, J. R. The balance of Th1/Th2 cytokines in rheumatoid arthritis. *Best practice & research. Clinical rheumatology* **15**, 677-691, doi:10.1053/berh.2001.0187 (2001).
- 28 Firestein, G. S. & Zvaifler, N. J. Peripheral blood and synovial fluid monocyte activation in inflammatory arthritis. II. Low levels of synovial fluid and synovial tissue interferon suggest that gamma-interferon is not the primary macrophage activating factor. *Arthritis Rheum* **30**, 864-871 (1987).
- 29 Chabaud, M. *et al.* Human interleukin-17: A T cell-derived proinflammatory cytokine produced by the rheumatoid synovium. *Arthritis Rheum* **42**, 963-970, doi:10.1002/1529-0131(199905)42:5<963::aid-anr15>3.0.co;2-e (1999).
- 30 Lubberts, E., Koenders, M. I. & van den Berg, W. B. The role of T-cell interleukin-17 in conducting destructive arthritis: lessons from animal models. *Arthritis Res Ther* **7**, 29-37, doi:10.1186/ar1478 (2005).
- 31 Skapenko, A., Leipe, J., Lipsky, P. E. & Schulze-Koops, H. The role of the T cell in autoimmune inflammation. *Arthritis Res Ther* **7 Suppl 2**, S4-14, doi:10.1186/ar1703 (2005).
- 32 Ehrenstein, M. R. *et al.* Compromised function of regulatory T cells in rheumatoid arthritis and reversal by anti-TNFalpha therapy. *J Exp Med* **200**, 277-285, doi:10.1084/jem.20040165 (2004).
- 33 Behrens, F. *et al.* Imbalance in distribution of functional autologous regulatory T cells in rheumatoid arthritis. *Ann Rheum Dis* **66**, 1151-1156, doi:10.1136/ard.2006.068320 (2007).
- 34 Wagner, U. G., Koetz, K., Weyand, C. M. & Goronzy, J. J. Perturbation of the T cell repertoire in rheumatoid arthritis. *Proceedings of the National Academy of Sciences of the United States of America* **95**, 14447-14452 (1998).
- 35 Cantaert, T. *et al.* Alterations of the synovial T cell repertoire in anti-citrullinated protein antibody-positive rheumatoid arthritis. *Arthritis Rheum* **60**, 1944-1956, doi:10.1002/art.24635 (2009).
- 36 Humby, F. *et al.* Ectopic lymphoid structures support ongoing production of class-switched autoantibodies in rheumatoid synovium. *PLoS medicine* **6**, e1, doi:10.1371/journal.pmed.0060001 (2009).
- 37 Schroder, A. E., Greiner, A., Seyfert, C. & Berek, C. Differentiation of B cells in the nonlymphoid tissue of the synovial membrane of patients with rheumatoid arthritis. *Proceedings of the National Academy of Sciences of the United States of America* **93**, 221-225 (1996).

- 38 Rooney, M., Whelan, A., Feighery, C. & Bresnihan, B. The immunohistologic features of synovitis, disease activity and in vitro IgM rheumatoid factor synthesis by blood mononuclear cells in rheumatoid arthritis. *The Journal of rheumatology* **16**, 459-467 (1989).
- 39 Seyler, T. M. *et al.* BlyS and APRIL in rheumatoid arthritis. *The Journal of clinical investigation* **115**, 3083-3092, doi:10.1172/jci25265 (2005).
- 40 McInnes, I. B., Leung, B. P. & Liew, F. Y. Cell-cell interactions in synovitis. Interactions between T lymphocytes and synovial cells. *Arthritis research* **2**, 374-378, doi:10.1186/ar115 (2000).
- 41 Takemura, S., Klimiuk, P. A., Braun, A., Goronzy, J. J. & Weyand, C. M. T cell activation in rheumatoid synovium is B cell dependent. *J Immunol* **167**, 4710-4718 (2001).
- 42 Edwards, J. C. *et al.* Efficacy of B-cell-targeted therapy with rituximab in patients with rheumatoid arthritis. *N Engl J Med* **350**, 2572-2581, doi:10.1056/NEJMoa032534 (2004).
- 43 Ohata, J. *et al.* Fibroblast-like synoviocytes of mesenchymal origin express functional B cell-activating factor of the TNF family in response to proinflammatory cytokines. *J Immunol* **174**, 864-870 (2005).
- 44 Dorner, T. & Lipsky, P. E. Signalling pathways in B cells: implications for autoimmunity. *Current topics in microbiology and immunology* **305**, 213-240 (2006).
- 45 Harre, U., Kittan, N. A. & Schett, G. Autoantibody-mediated bone loss. *Current osteoporosis reports* **12**, 17-21, doi:10.1007/s11914-013-0185-9 (2014).
- 46 Cao, D., van Vollenhoven, R., Klareskog, L., Trollmo, C. & Malmstrom, V. CD25brightCD4+ regulatory T cells are enriched in inflamed joints of patients with chronic rheumatic disease. *Arthritis Res Ther* **6**, R335-346, doi:10.1186/ar1192 (2004).
- 47 Jiao, Z. *et al.* Accumulation of FoxP3-expressing CD4+CD25+ T cells with distinct chemokine receptors in synovial fluid of patients with active rheumatoid arthritis. *Scandinavian journal of rheumatology* **36**, 428-433, doi:10.1080/03009740701482800 (2007).
- 48 Lawson, C. A. *et al.* Early rheumatoid arthritis is associated with a deficit in the CD4+CD25high regulatory T cell population in peripheral blood. *Rheumatology (Oxford)* **45**, 1210-1217, doi:10.1093/rheumatology/kel089 (2006).
- 49 Sempere-Ortells, J. M. *et al.* Quantification and phenotype of regulatory T cells in rheumatoid arthritis according to disease activity score-28. *Autoimmunity* **42**, 636-645, doi:10.3109/08916930903061491 (2009).
- 50 Han, G. M., O'Neil-Andersen, N. J., Zurier, R. B. & Lawrence, D. A. CD4+CD25high T cell numbers are enriched in the peripheral blood of patients with rheumatoid arthritis. *Cellular immunology* **253**, 92-101, doi:10.1016/j.cellimm.2008.05.007 (2008).
- 51 Kao, J. K., Hsue, Y. T. & Lin, C. Y. Role of new population of peripheral CD11c(+)CD8(+) T cells and CD4(+)CD25(+) regulatory T cells during acute and remission stages in rheumatoid arthritis patients. *Journal of microbiology, immunology, and infection = Wei mian yu gan ran za zhi* **40**, 419-427 (2007).
- 52 van Amelsfort, J. M., Jacobs, K. M., Bijlsma, J. W., Lafeber, F. P. & Taams, L. S. CD4(+)CD25(+) regulatory T cells in rheumatoid arthritis: differences in the presence, phenotype, and function between peripheral blood and synovial fluid. *Arthritis Rheum* **50**, 2775-2785, doi:10.1002/art.20499 (2004).
- 53 Liu, M. F., Wang, C. R., Fung, L. L., Lin, L. H. & Tsai, C. N. The presence of cytokine-suppressive CD4+CD25+ T cells in the peripheral blood and synovial fluid of patients with rheumatoid arthritis. *Scandinavian journal of immunology* **62**, 312-317, doi:10.1111/j.1365-3083.2005.01656.x (2005).
- 54 Mottonen, M. *et al.* CD4+ CD25+ T cells with the phenotypic and functional characteristics of regulatory T cells are enriched in the synovial fluid of patients with rheumatoid arthritis. *Clinical and experimental immunology* **140**, 360-367, doi:10.1111/j.1365-2249.2005.02754.x (2005).

- 55 van Amelsfort, J. M. *et al.* Proinflammatory mediator-induced reversal of CD4<sup>+</sup>,CD25<sup>+</sup> regulatory T cell-mediated suppression in rheumatoid arthritis. *Arthritis Rheum* **56**, 732-742, doi:10.1002/art.22414 (2007).
- 56 van Roon, J. A., Hartgring, S. A., van der Wurff-Jacobs, K. M., Bijlsma, J. W. & Lafeber, F. P. Numbers of CD25<sup>+</sup>Foxp3<sup>+</sup> T cells that lack the IL-7 receptor are increased intra-articularly and have impaired suppressive function in RA patients. *Rheumatology (Oxford)* **49**, 2084-2089, doi:10.1093/rheumatology/keq237 (2010).
- 57 Miyara, M. *et al.* Human FoxP3<sup>+</sup> regulatory T cells in systemic autoimmune diseases. *Autoimmunity reviews* **10**, 744-755, doi:10.1016/j.autrev.2011.05.004 (2011).
- 58 Valencia, X. *et al.* TNF downmodulates the function of human CD4<sup>+</sup>CD25<sup>hi</sup> T-regulatory cells. *Blood* **108**, 253-261, doi:10.1182/blood-2005-11-4567 (2006).
- 59 Pasare, C. & Medzhitov, R. Toll pathway-dependent blockade of CD4<sup>+</sup>CD25<sup>+</sup> T cell-mediated suppression by dendritic cells. *Science (New York, N.Y.)* **299**, 1033-1036, doi:10.1126/science.1078231 (2003).
- 60 Zaiss, M. M. *et al.* Treg cells suppress osteoclast formation: a new link between the immune system and bone. *Arthritis Rheum* **56**, 4104-4112, doi:10.1002/art.23138 (2007).
- 61 Kim, Y. G. *et al.* Human CD4<sup>+</sup>CD25<sup>+</sup> regulatory T cells inhibit the differentiation of osteoclasts from peripheral blood mononuclear cells. *Biochemical and biophysical research communications* **357**, 1046-1052, doi:10.1016/j.bbrc.2007.04.042 (2007).
- 62 Zaiss, M. M. *et al.* Increased bone density and resistance to ovariectomy-induced bone loss in FoxP3-transgenic mice based on impaired osteoclast differentiation. *Arthritis Rheum* **62**, 2328-2338, doi:10.1002/art.27535 (2010).
- 63 Zaiss, M. M. *et al.* Regulatory T cells protect from local and systemic bone destruction in arthritis. *J Immunol* **184**, 7238-7246, doi:10.4049/jimmunol.0903841 (2010).
- 64 Kelchtermans, H. *et al.* Activated CD4<sup>+</sup>CD25<sup>+</sup> regulatory T cells inhibit osteoclastogenesis and collagen-induced arthritis. *Ann Rheum Dis* **68**, 744-750, doi:10.1136/ard.2007.086066 (2009).
- 65 Haringman, J. J. *et al.* Synovial tissue macrophages: a sensitive biomarker for response to treatment in patients with rheumatoid arthritis. *Ann Rheum Dis* **64**, 834-838, doi:10.1136/ard.2004.029751 (2005).
- 66 Seibl, R. *et al.* Expression and regulation of Toll-like receptor 2 in rheumatoid arthritis synovium. *The American journal of pathology* **162**, 1221-1227, doi:10.1016/s0002-9440(10)63918-1 (2003).
- 67 Liew, F. Y. & McInnes, I. B. The role of innate mediators in inflammatory response. *Molecular immunology* **38**, 887-890 (2002).
- 68 Weaver, C. T., Hatton, R. D., Mangan, P. R. & Harrington, L. E. IL-17 family cytokines and the expanding diversity of effector T cell lineages. *Annual review of immunology* **25**, 821-852, doi:10.1146/annurev.immunol.25.022106.141557 (2007).
- 69 Cascao, R., Rosario, H. S., Souto-Carneiro, M. M. & Fonseca, J. E. Neutrophils in rheumatoid arthritis: More than simple final effectors. *Autoimmunity reviews* **9**, 531-535, doi:10.1016/j.autrev.2009.12.013 (2010).
- 70 Nigrovic, P. A. & Lee, D. M. Synovial mast cells: role in acute and chronic arthritis. *Immunological reviews* **217**, 19-37, doi:10.1111/j.1600-065X.2007.00506.x (2007).
- 71 Hueber, A. J. *et al.* Mast cells express IL-17A in rheumatoid arthritis synovium. *J Immunol* **184**, 3336-3340, doi:10.4049/jimmunol.0903566 (2010).
- 72 Schuerwegh, A. J. *et al.* Evidence for a functional role of IgE anticitrullinated protein antibodies in rheumatoid arthritis. *Proceedings of the National Academy of Sciences of the United States of America* **107**, 2586-2591, doi:10.1073/pnas.0913054107 (2010).
- 73 Miossec, P. Interleukin-17 in rheumatoid arthritis: if T cells were to contribute to inflammation and destruction through synergy. *Arthritis Rheum* **48**, 594-601, doi:10.1002/art.10816 (2003).
- 74 Rhee, D. K. *et al.* The secreted glycoprotein lubricin protects cartilage surfaces and inhibits synovial cell overgrowth. *The Journal of clinical investigation* **115**, 622-631, doi:10.1172/jci22263 (2005).

- 75 Sabeh, F., Fox, D. & Weiss, S. J. Membrane-type I matrix metalloproteinase-dependent regulation of rheumatoid arthritis synoviocyte function. *J Immunol* **184**, 6396-6406, doi:10.4049/jimmunol.0904068 (2010).
- 76 van der Heijde, D. M. Joint erosions and patients with early rheumatoid arthritis. *British journal of rheumatology* **34 Suppl 2**, 74-78 (1995).
- 77 Visser, H., le Cessie, S., Vos, K., Breedveld, F. C. & Hazes, J. M. How to diagnose rheumatoid arthritis early: a prediction model for persistent (erosive) arthritis. *Arthritis Rheum* **46**, 357-365 (2002).
- 78 Schett, G. Cells of the synovium in rheumatoid arthritis. Osteoclasts. *Arthritis Res Ther* **9**, 203, doi:10.1186/ar2110 (2007).
- 79 Teitelbaum, S. L. Bone resorption by osteoclasts. *Science (New York, N.Y.)* **289**, 1504-1508 (2000).
- 80 Gravallese, E. M. *et al.* Identification of cell types responsible for bone resorption in rheumatoid arthritis and juvenile rheumatoid arthritis. *The American journal of pathology* **152**, 943-951 (1998).
- 81 Jung, S. M., Kim, K. W., Yang, C. W., Park, S. H. & Ju, J. H. Cytokine-mediated bone destruction in rheumatoid arthritis. *Journal of immunology research* **2014**, 263625, doi:10.1155/2014/263625 (2014).
- 82 Marston, B., Palanichamy, A. & Anolik, J. H. B cells in the pathogenesis and treatment of rheumatoid arthritis. *Current opinion in rheumatology* **22**, 307-315, doi:10.1097/BOR.0b013e3283369cb8 (2010).
- 83 Schett, G. & Teitelbaum, S. L. Osteoclasts and arthritis. *J Bone Miner Res* **24**, 1142-1146, doi:10.1359/jbmr.090533 (2009).
- 84 Schett, G., Stach, C., Zwerina, J., Voll, R. & Manger, B. How antirheumatic drugs protect joints from damage in rheumatoid arthritis. *Arthritis Rheum* **58**, 2936-2948, doi:10.1002/art.23951 (2008).
- 85 Kudo, O. *et al.* Interleukin-6 and interleukin-11 support human osteoclast formation by a RANKL-independent mechanism. *Bone* **32**, 1-7 (2003).
- 86 Jimenez-Boj, E. *et al.* Interaction between synovial inflammatory tissue and bone marrow in rheumatoid arthritis. *J Immunol* **175**, 2579-2588 (2005).
- 87 Bertolini, D. R., Nedwin, G. E., Bringman, T. S., Smith, D. D. & Mundy, G. R. Stimulation of bone resorption and inhibition of bone formation in vitro by human tumour necrosis factors. *Nature* **319**, 516-518, doi:10.1038/319516a0 (1986).
- 88 Diarra, D. *et al.* Dickkopf-1 is a master regulator of joint remodeling. *Nature medicine* **13**, 156-163, doi:10.1038/nm1538 (2007).
- 89 Solomon, D. H. *et al.* Cardiovascular morbidity and mortality in women diagnosed with rheumatoid arthritis. *Circulation* **107**, 1303-1307 (2003).
- 90 Wolfe, F. *et al.* The mortality of rheumatoid arthritis. *Arthritis Rheum* **37**, 481-494 (1994).
- 91 Holmqvist, M. E. *et al.* Rapid increase in myocardial infarction risk following diagnosis of rheumatoid arthritis amongst patients diagnosed between 1995 and 2006. *Journal of internal medicine* **268**, 578-585, doi:10.1111/j.1365-2796.2010.02260.x (2010).
- 92 Kaptoge, S. *et al.* C-reactive protein concentration and risk of coronary heart disease, stroke, and mortality: an individual participant meta-analysis. *Lancet* **375**, 132-140, doi:10.1016/s0140-6736(09)61717-7 (2010).
- 93 Sattar, N., McCarey, D. W., Capell, H. & McInnes, I. B. Explaining how "high-grade" systemic inflammation accelerates vascular risk in rheumatoid arthritis. *Circulation* **108**, 2957-2963, doi:10.1161/01.cir.0000099844.31524.05 (2003).
- 94 Sattar, N. & McInnes, I. B. Vascular comorbidity in rheumatoid arthritis: potential mechanisms and solutions. *Current opinion in rheumatology* **17**, 286-292 (2005).
- 95 Chrousos, G. P. The hypothalamic-pituitary-adrenal axis and immune-mediated inflammation. *N Engl J Med* **332**, 1351-1362, doi:10.1056/nejm199505183322008 (1995).

- 96 De Benedetti, F. *et al.* Impaired skeletal development in interleukin-6-transgenic mice: a model for the impact of chronic inflammation on the growing skeletal system. *Arthritis Rheum* **54**, 3551-3563, doi:10.1002/art.22175 (2006).
- 97 Smitten, A. L., Simon, T. A., Hochberg, M. C. & Suissa, S. A meta-analysis of the incidence of malignancy in adult patients with rheumatoid arthritis. *Arthritis Res Ther* **10**, R45, doi:10.1186/ar2404 (2008).
- 98 Baecklund, E. *et al.* Lymphoma subtypes in patients with rheumatoid arthritis: increased proportion of diffuse large B cell lymphoma. *Arthritis Rheum* **48**, 1543-1550, doi:10.1002/art.11144 (2003).
- 99 Smolen, J. S. & Steiner, G. Therapeutic strategies for rheumatoid arthritis. *Nature reviews. Drug discovery* **2**, 473-488, doi:10.1038/nrd1109 (2003).
- 100 ten Wolde, S. *et al.* Randomised placebo-controlled study of stopping second-line drugs in rheumatoid arthritis. *Lancet* **347**, 347-352 (1996).
- 101 Bathon, J. M. *et al.* A comparison of etanercept and methotrexate in patients with early rheumatoid arthritis. *N Engl J Med* **343**, 1586-1593, doi:10.1056/nejm200011303432201 (2000).
- 102 Elliott, M. J. *et al.* Randomised double-blind comparison of chimeric monoclonal antibody to tumour necrosis factor alpha (cA2) versus placebo in rheumatoid arthritis. *Lancet* **344**, 1105-1110 (1994).
- 103 Lipsky, P. E. *et al.* Infliximab and methotrexate in the treatment of rheumatoid arthritis. Anti-Tumor Necrosis Factor Trial in Rheumatoid Arthritis with Concomitant Therapy Study Group. *N Engl J Med* **343**, 1594-1602, doi:10.1056/nejm200011303432202 (2000).
- 104 Weinblatt, M. E. *et al.* A trial of etanercept, a recombinant tumor necrosis factor receptor:Fc fusion protein, in patients with rheumatoid arthritis receiving methotrexate. *N Engl J Med* **340**, 253-259, doi:10.1056/nejm199901283400401 (1999).
- 105 Weinblatt, M. E. *et al.* Adalimumab, a fully human anti-tumor necrosis factor alpha monoclonal antibody, for the treatment of rheumatoid arthritis in patients taking concomitant methotrexate: the ARMADA trial. *Arthritis Rheum* **48**, 35-45, doi:10.1002/art.10697 (2003).
- 106 Arend, W. P., Malyak, M., Guthridge, C. J. & Gabay, C. Interleukin-1 receptor antagonist: role in biology. *Annual review of immunology* **16**, 27-55, doi:10.1146/annurev.immunol.16.1.27 (1998).
- 107 Dorner, T. & Burmester, G. R. The role of B cells in rheumatoid arthritis: mechanisms and therapeutic targets. *Current opinion in rheumatology* **15**, 246-252 (2003).
- 108 Finckh, A. *et al.* Evolution of radiographic joint damage in rituximab-treated versus TNF-treated rheumatoid arthritis cases with inadequate response to TNF antagonists. *Ann Rheum Dis* **71**, 1680-1685, doi:10.1136/annrheumdis-2011-201016 (2012).
- 109 Chatzidionysiou, K. *et al.* Highest clinical effectiveness of rituximab in autoantibody-positive patients with rheumatoid arthritis and in those for whom no more than one previous TNF antagonist has failed: pooled data from 10 European registries. *Ann Rheum Dis* **70**, 1575-1580, doi:10.1136/ard.2010.148759 (2011).
- 110 Vivar, N. & Van Vollenhoven, R. F. Advances in the treatment of rheumatoid arthritis. *F1000prime reports* **6**, 31, doi:10.12703/p6-31 (2014).
- 111 Kouskoff, V. *et al.* Organ-specific disease provoked by systemic autoimmunity. *Cell* **87**, 811-822 (1996).
- 112 Korganow, A. S. *et al.* From systemic T cell self-reactivity to organ-specific autoimmune disease via immunoglobulins. *Immunity* **10**, 451-461 (1999).
- 113 Matsumoto, I., Staub, A., Benoist, C. & Mathis, D. Arthritis provoked by linked T and B cell recognition of a glycolytic enzyme. *Science (New York, N.Y.)* **286**, 1732-1735 (1999).
- 114 Maccioni, M. *et al.* Arthritogenic monoclonal antibodies from K/BxN mice. *J Exp Med* **195**, 1071-1077 (2002).

- 115 Kamradt, T. & Schubert, D. The role and clinical implications of G6PI in experimental models of rheumatoid arthritis. *Arthritis Res Ther* **7**, 20-28, doi:10.1186/ar1476 (2005).
- 116 Schaller, M., Burton, D. R. & Ditzel, H. J. Autoantibodies to GPI in rheumatoid arthritis: linkage between an animal model and human disease. *Nat Immunol* **2**, 746-753, doi:10.1038/90696 (2001).
- 117 Schubert, D., Schmidt, M., Zaiss, D., Jungblut, P. R. & Kamradt, T. Autoantibodies to GPI and creatine kinase in RA. *Nat Immunol* **3**, 411; author reply 412-413, doi:10.1038/ni0502-411a (2002).
- 118 Ho, P. P. *et al.* Autoimmunity against fibrinogen mediates inflammatory arthritis in mice. *J Immunol* **184**, 379-390, doi:10.4049/jimmunol.0901639 (2010).
- 119 Keffer, J. *et al.* Transgenic mice expressing human tumour necrosis factor: a predictive genetic model of arthritis. *The EMBO journal* **10**, 4025-4031 (1991).
- 120 Niki, Y. *et al.* Macrophage- and neutrophil-dominant arthritis in human IL-1 alpha transgenic mice. *The Journal of clinical investigation* **107**, 1127-1135, doi:10.1172/jci11530 (2001).
- 121 Horai, R. *et al.* Development of chronic inflammatory arthropathy resembling rheumatoid arthritis in interleukin 1 receptor antagonist-deficient mice. *J Exp Med* **191**, 313-320 (2000).
- 122 Matmati, M. *et al.* A20 (TNFAIP3) deficiency in myeloid cells triggers erosive polyarthritis resembling rheumatoid arthritis. *Nature genetics* **43**, 908-912, doi:10.1038/ng.874 (2011).
- 123 Schubert, D., Maier, B., Morawietz, L., Krenn, V. & Kamradt, T. Immunization with glucose-6-phosphate isomerase induces T cell-dependent peripheral polyarthritis in genetically unaltered mice. *J Immunol* **172**, 4503-4509 (2004).
- 124 Iwanami, K. *et al.* Crucial role of the interleukin-6/interleukin-17 cytokine axis in the induction of arthritis by glucose-6-phosphate isomerase. *Arthritis Rheum* **58**, 754-763, doi:10.1002/art.23222 (2008).
- 125 Matsumoto, I. *et al.* Therapeutic effects of antibodies to tumor necrosis factor-alpha, interleukin-6 and cytotoxic T-lymphocyte antigen 4 immunoglobulin in mice with glucose-6-phosphate isomerase induced arthritis. *Arthritis Res Ther* **10**, R66, doi:10.1186/ar2437 (2008).
- 126 Tanaka-Watanabe, Y. *et al.* B cells play a crucial role as antigen-presenting cells and collaborate with inflammatory cytokines in glucose-6-phosphate isomerase-induced arthritis. *Clinical and experimental immunology* **155**, 285-294, doi:10.1111/j.1365-2249.2008.03816.x (2009).
- 127 Wipke, B. T., Wang, Z., Kim, J., McCarthy, T. J. & Allen, P. M. Dynamic visualization of a joint-specific autoimmune response through positron emission tomography. *Nat Immunol* **3**, 366-372, doi:10.1038/ni775 (2002).
- 128 Wipke, B. T., Wang, Z., Nagengast, W., Reichert, D. E. & Allen, P. M. Staging the initiation of autoantibody-induced arthritis: a critical role for immune complexes. *J Immunol* **172**, 7694-7702 (2004).
- 129 Gondolf, K. B., Mihatsch, M., Curschellas, E., Dunn, J. J. & Batsford, S. R. Induction of experimental allergic arthritis with outer surface proteins of *Borrelia burgdorferi*. *Arthritis Rheum* **37**, 1070-1077 (1994).
- 130 van den Berg, W. B., van de Putte, L. B., Zwarts, W. A. & Joosten, L. A. Electrical charge of the antigen determines intraarticular antigen handling and chronicity of arthritis in mice. *The Journal of clinical investigation* **74**, 1850-1859, doi:10.1172/jci111604 (1984).
- 131 Matsumoto, I. *et al.* How antibodies to a ubiquitous cytoplasmic enzyme may provoke joint-specific autoimmune disease. *Nat Immunol* **3**, 360-365, doi:10.1038/ni772 (2002).
- 132 Frey, O., Bruns, L., Morawietz, L., Dunussi-Joannopoulos, K. & Kamradt, T. B cell depletion reduces the number of autoreactive T helper cells and prevents glucose-6-

- phosphate isomerase-induced arthritis. *PloS one* **6**, e24718, doi:10.1371/journal.pone.0024718 (2011).
- 133 Frey, O. *et al.* Regulatory T cells control the transition from acute into chronic inflammation in glucose-6-phosphate isomerase-induced arthritis. *Ann Rheum Dis* **69**, 1511-1518, doi:10.1136/ard.2009.123422 (2010).
- 134 Bartok, B. & Firestein, G. S. Fibroblast-like synoviocytes: key effector cells in rheumatoid arthritis. *Immunological reviews* **233**, 233-255, doi:10.1111/j.0105-2896.2009.00859.x (2010).
- 135 Muller-Ladner, U., Ospelt, C., Gay, S., Distler, O. & Pap, T. Cells of the synovium in rheumatoid arthritis. Synovial fibroblasts. *Arthritis Res Ther* **9**, 223, doi:10.1186/ar2337 (2007).
- 136 Firestein, G. S. Invasive fibroblast-like synoviocytes in rheumatoid arthritis. Passive responders or transformed aggressors? *Arthritis Rheum* **39**, 1781-1790 (1996).
- 137 Noss, E. H. & Brenner, M. B. The role and therapeutic implications of fibroblast-like synoviocytes in inflammation and cartilage erosion in rheumatoid arthritis. *Immunological reviews* **223**, 252-270, doi:10.1111/j.1600-065X.2008.00648.x (2008).
- 138 Lee, D. M. *et al.* Cadherin-11 in synovial lining formation and pathology in arthritis. *Science (New York, N.Y.)* **315**, 1006-1010, doi:10.1126/science.1137306 (2007).
- 139 Valencia, X. *et al.* Cadherin-11 provides specific cellular adhesion between fibroblast-like synoviocytes. *J Exp Med* **200**, 1673-1679, doi:10.1084/jem.20041545 (2004).
- 140 Bottini, N. & Firestein, G. S. Duality of fibroblast-like synoviocytes in RA: passive responders and imprinted aggressors. *Nature reviews. Rheumatology* **9**, 24-33, doi:10.1038/nrrheum.2012.190 (2013).
- 141 Imamura, F. *et al.* Monoclonal expansion of synoviocytes in rheumatoid arthritis. *Arthritis Rheum* **41**, 1979-1986, doi:10.1002/1529-0131(199811)41:11<1979::aid-art13>3.0.co;2-c (1998).
- 142 Firestein, G. S., Yeo, M. & Zvaifler, N. J. Apoptosis in rheumatoid arthritis synovium. *The Journal of clinical investigation* **96**, 1631-1638, doi:10.1172/jci118202 (1995).
- 143 Mor, A., Abramson, S. B. & Pillinger, M. H. The fibroblast-like synovial cell in rheumatoid arthritis: a key player in inflammation and joint destruction. *Clinical immunology (Orlando, Fla.)* **115**, 118-128, doi:10.1016/j.clim.2004.12.009 (2005).
- 144 Garcia-Vicuna, R. *et al.* CC and CXC chemokine receptors mediate migration, proliferation, and matrix metalloproteinase production by fibroblast-like synoviocytes from rheumatoid arthritis patients. *Arthritis Rheum* **50**, 3866-3877, doi:10.1002/art.20615 (2004).
- 145 Matsumoto, S., Muller-Ladner, U., Gay, R. E., Nishioka, K. & Gay, S. Ultrastructural demonstration of apoptosis, Fas and Bcl-2 expression of rheumatoid synovial fibroblasts. *The Journal of rheumatology* **23**, 1345-1352 (1996).
- 146 Meinecke, I. *et al.* Modification of nuclear PML protein by SUMO-1 regulates Fas-induced apoptosis in rheumatoid arthritis synovial fibroblasts. *Proceedings of the National Academy of Sciences of the United States of America* **104**, 5073-5078, doi:10.1073/pnas.0608773104 (2007).
- 147 Baier, A., Meinecke, I., Gay, S. & Pap, T. Apoptosis in rheumatoid arthritis. *Current opinion in rheumatology* **15**, 274-279 (2003).
- 148 Lefevre, S. *et al.* Synovial fibroblasts spread rheumatoid arthritis to unaffected joints. *Nature medicine* **15**, 1414-1420, doi:10.1038/nm.2050 (2009).
- 149 Chabaud, M., Fossiez, F., Taupin, J. L. & Miossec, P. Enhancing effect of IL-17 on IL-1-induced IL-6 and leukemia inhibitory factor production by rheumatoid arthritis synoviocytes and its regulation by Th2 cytokines. *J Immunol* **161**, 409-414 (1998).
- 150 Geiler, T., Kriegsmann, J., Keyszer, G. M., Gay, R. E. & Gay, S. A new model for rheumatoid arthritis generated by engraftment of rheumatoid synovial tissue and normal human cartilage into SCID mice. *Arthritis Rheum* **37**, 1664-1671 (1994).
- 151 Shigeyama, Y. *et al.* Expression of osteoclast differentiation factor in rheumatoid arthritis. *Arthritis Rheum* **43**, 2523-2530, doi:10.1002/1529-0131(200011)43:11<2523::aid-anr20>3.0.co;2-z (2000).

- 152 Lee, H. Y. *et al.* CD40 ligation of rheumatoid synovial fibroblasts regulates RANKL-mediated osteoclastogenesis: evidence of NF-kappaB-dependent, CD40-mediated bone destruction in rheumatoid arthritis. *Arthritis Rheum* **54**, 1747-1758, doi:10.1002/art.21873 (2006).
- 153 Gravallese, E. M. *et al.* Synovial tissue in rheumatoid arthritis is a source of osteoclast differentiation factor. *Arthritis Rheum* **43**, 250-258, doi:10.1002/1529-0131(200002)43:2<250::aid-anr3>3.0.co;2-p (2000).
- 154 Pettit, A. R., Walsh, N. C., Manning, C., Goldring, S. R. & Gravallese, E. M. RANKL protein is expressed at the pannus-bone interface at sites of articular bone erosion in rheumatoid arthritis. *Rheumatology (Oxford)* **45**, 1068-1076, doi:10.1093/rheumatology/kel045 (2006).
- 155 Brennan, F. M. & McInnes, I. B. Evidence that cytokines play a role in rheumatoid arthritis. *The Journal of clinical investigation* **118**, 3537-3545, doi:10.1172/jci36389 (2008).
- 156 Sakuma, M. *et al.* TGF-beta type I receptor kinase inhibitor down-regulates rheumatoid synoviocytes and prevents the arthritis induced by type II collagen antibody. *International immunology* **19**, 117-126, doi:10.1093/intimm/dxl128 (2007).
- 157 Patel, D. D., Zachariah, J. P. & Whichard, L. P. CXCR3 and CCR5 ligands in rheumatoid arthritis synovium. *Clinical immunology (Orlando, Fla.)* **98**, 39-45, doi:10.1006/clim.2000.4957 (2001).
- 158 Tsubaki, T. *et al.* Accumulation of plasma cells expressing CXCR3 in the synovial sublining regions of early rheumatoid arthritis in association with production of Mig/CXCL9 by synovial fibroblasts. *Clinical and experimental immunology* **141**, 363-371, doi:10.1111/j.1365-2249.2005.02850.x (2005).
- 159 Schmutz, C. *et al.* Chemokine receptors in the rheumatoid synovium: upregulation of CXCR5. *Arthritis Res Ther* **7**, R217-229, doi:10.1186/ar1475 (2005).
- 160 Firestein, G. S., Alvaro-Gracia, J. M. & Maki, R. Quantitative analysis of cytokine gene expression in rheumatoid arthritis. *J Immunol* **144**, 3347-3353 (1990).
- 161 Hwang, S. Y. *et al.* IL-17 induces production of IL-6 and IL-8 in rheumatoid arthritis synovial fibroblasts via NF-kappaB- and PI3-kinase/Akt-dependent pathways. *Arthritis Res Ther* **6**, R120-128, doi:10.1186/ar1038 (2004).
- 162 Hirth, A. *et al.* Cytokine mRNA and protein expression in primary-culture and repeated-passage synovial fibroblasts from patients with rheumatoid arthritis. *Arthritis research* **4**, 117-125 (2002).
- 163 Stanton, H. *et al.* Investigating ADAMTS-mediated aggrecanolysis in mouse cartilage. *Nature protocols* **6**, 388-404, doi:10.1038/nprot.2010.179 (2011).
- 164 Wunrau, C. *et al.* Establishment of a matrix-associated transepithelial resistance invasion assay to precisely measure the invasive potential of synovial fibroblasts. *Arthritis Rheum* **60**, 2606-2611, doi:10.1002/art.24782 (2009).
- 165 Lahl, K. & Sparwasser, T. In vivo depletion of FoxP3+ Tregs using the DEREK mouse model. *Methods Mol Biol* **707**, 157-172, doi:10.1007/978-1-61737-979-6\_10 (2011).
- 166 Chattopadhyay, P. K., Yu, J. & Roederer, M. Live-cell assay to detect antigen-specific CD4+ T-cell responses by CD154 expression. *Nature protocols* **1**, 1-6, doi:10.1038/nprot.2006.1 (2006).
- 167 Armaka, M., Gkretsi, V., Kontoyiannis, D. & Kollias, G. A standardized protocol for the isolation and culture of normal and arthritogenic murine synovial fibroblasts. (2009).
- 168 Cho, M. L. *et al.* Toll-like receptor 2 ligand mediates the upregulation of angiogenic factor, vascular endothelial growth factor and interleukin-8/CXCL8 in human rheumatoid synovial fibroblasts. *Immunology letters* **108**, 121-128, doi:10.1016/j.imlet.2006.11.005 (2007).
- 169 Chiu, Y. C. *et al.* Peptidoglycan enhances IL-6 production in human synovial fibroblasts via TLR2 receptor, focal adhesion kinase, Akt, and AP-1- dependent pathway. *J Immunol* **183**, 2785-2792, doi:10.4049/jimmunol.0802826 (2009).

- 170 Brentano, F., Schorr, O., Gay, R. E., Gay, S. & Kyburz, D. RNA released from necrotic  
synovial fluid cells activates rheumatoid arthritis synovial fibroblasts via Toll-like  
receptor 3. *Arthritis Rheum* **52**, 2656-2665, doi:10.1002/art.21273 (2005).
- 171 Harigai, M. *et al.* Interleukin 1 and tumor necrosis factor-alpha synergistically  
increase the production of interleukin 6 in human synovial fibroblast. *Journal of  
clinical & laboratory immunology* **34**, 107-113 (1991).
- 172 Kunisch, E., Chakilam, S., Gandesiri, M. & Kinne, R. W. IL-33 regulates TNF-alpha  
dependent effects in synovial fibroblasts. *International journal of molecular medicine*  
**29**, 530-540, doi:10.3892/ijmm.2012.883 (2012).
- 173 Manabe, N. *et al.* Involvement of fibroblast growth factor-2 in joint destruction of  
rheumatoid arthritis patients. *Rheumatology (Oxford)* **38**, 714-720 (1999).
- 174 Koch, A. E. Chemokines and their receptors in rheumatoid arthritis: future targets?  
*Arthritis Rheum* **52**, 710-721, doi:10.1002/art.20932 (2005).
- 175 Szekanecz, Z., Kim, J. & Koch, A. E. Chemokines and chemokine receptors in  
rheumatoid arthritis. *Seminars in immunology* **15**, 15-21 (2003).
- 176 Szekanecz, Z., Vegvari, A., Szabo, Z. & Koch, A. E. Chemokines and chemokine receptors  
in arthritis. *Frontiers in bioscience (Scholar edition)* **2**, 153-167 (2010).
- 177 Nagase, H., Visse, R. & Murphy, G. Structure and function of matrix metalloproteinases  
and TIMPs. *Cardiovascular research* **69**, 562-573,  
doi:10.1016/j.cardiores.2005.12.002 (2006).
- 178 Tolboom, T. C. *et al.* Invasive properties of fibroblast-like synoviocytes: correlation  
with growth characteristics and expression of MMP-1, MMP-3, and MMP-10. *Ann  
Rheum Dis* **61**, 975-980 (2002).
- 179 Korb-Pap, A. *et al.* Early structural changes in cartilage and bone are required for the  
attachment and invasion of inflamed synovial tissue during destructive inflammatory  
arthritis. *Ann Rheum Dis* **71**, 1004-1011, doi:10.1136/annrheumdis-2011-200386  
(2012).
- 180 Amasheh, S. *et al.* Claudin-2 expression induces cation-selective channels in tight  
junctions of epithelial cells. *Journal of cell science* **115**, 4969-4976 (2002).
- 181 Suzuki, T., Yoshinaga, N. & Tanabe, S. Interleukin-6 (IL-6) regulates claudin-2  
expression and tight junction permeability in intestinal epithelium. *J Biol Chem* **286**,  
31263-31271, doi:10.1074/jbc.M111.238147 (2011).
- 182 Bruewer, M. *et al.* Interferon-gamma induces internalization of epithelial tight  
junction proteins via a macropinocytosis-like process. *FASEB journal : official  
publication of the Federation of American Societies for Experimental Biology* **19**, 923-  
933, doi:10.1096/fj.04-3260com (2005).
- 183 Bockermann, R., Schubert, D., Kamradt, T. & Holmdahl, R. Induction of a B-cell-  
dependent chronic arthritis with glucose-6-phosphate isomerase. *Arthritis Res Ther* **7**,  
R1316-1324, doi:10.1186/ar1829 (2005).
- 184 Lahl, K. *et al.* Selective depletion of Foxp3+ regulatory T cells induces a scurfy-like  
disease. *J Exp Med* **204**, 57-63, doi:10.1084/jem.20061852 (2007).
- 185 Berod, L. *et al.* Rapid rebound of the Treg compartment in DERE mice limits the  
impact of Treg depletion on mycobacterial burden, but prevents autoimmunity. *PloS  
one* **9**, e102804, doi:10.1371/journal.pone.0102804 (2014).
- 186 Kamradt, T. & Mitchison, N. A. Tolerance and autoimmunity. *N Engl J Med* **344**, 655-  
664, doi:10.1056/nejm200103013440907 (2001).
- 187 Wing, J. B. & Sakaguchi, S. Multiple treg suppressive modules and their adaptability.  
*Frontiers in immunology* **3**, 178, doi:10.3389/fimmu.2012.00178 (2012).
- 188 Brunkow, M. E. *et al.* Disruption of a new forkhead/winged-helix protein, scurf, results in the fatal lymphoproliferative disorder of the scurfy mouse. *Nature genetics*  
**27**, 68-73, doi:10.1038/83784 (2001).
- 189 Khattry, R., Cox, T., Yasayko, S. A. & Ramsdell, F. An essential role for Scurfin in  
CD4+CD25+ T regulatory cells. *Nat Immunol* **4**, 337-342, doi:10.1038/ni909 (2003).

- 190 Wildin, R. S. *et al.* X-linked neonatal diabetes mellitus, enteropathy and endocrinopathy syndrome is the human equivalent of mouse scurfy. *Nature genetics* **27**, 18-20, doi:10.1038/83707 (2001).
- 191 Hsieh, C. S. *et al.* Recognition of the peripheral self by naturally arising CD25+ CD4+ T cell receptors. *Immunity* **21**, 267-277, doi:10.1016/j.immuni.2004.07.009 (2004).
- 192 Hsieh, C. S., Zheng, Y., Liang, Y., Fontenot, J. D. & Rudensky, A. Y. An intersection between the self-reactive regulatory and nonregulatory T cell receptor repertoires. *Nat Immunol* **7**, 401-410, doi:10.1038/ni1318 (2006).
- 193 Kim, J. M., Rasmussen, J. P. & Rudensky, A. Y. Regulatory T cells prevent catastrophic autoimmunity throughout the lifespan of mice. *Nat Immunol* **8**, 191-197, doi:10.1038/ni1428 (2007).
- 194 Komatsu, N. *et al.* Pathogenic conversion of Foxp3+ T cells into TH17 cells in autoimmune arthritis. *Nature medicine* **20**, 62-68, doi:10.1038/nm.3432 (2014).
- 195 Treese, C. *et al.* Characterization of fibroblasts responsible for cartilage destruction in arthritis. *Cytometry. Part A : the journal of the International Society for Analytical Cytology* **73**, 351-360, doi:10.1002/cyto.a.20532 (2008).
- 196 Hardy, R. S. *et al.* Characterisation of fibroblast-like synoviocytes from a murine model of joint inflammation. *Arthritis Res Ther* **15**, R24, doi:10.1186/ar4158 (2013).
- 197 Neumann, E. *et al.* Cell culture and passaging alters gene expression pattern and proliferation rate in rheumatoid arthritis synovial fibroblasts. *Arthritis Res Ther* **12**, R83, doi:10.1186/ar3010 (2010).
- 198 Reilkoff, R. A., Bucala, R. & Herzog, E. L. Fibrocytes: emerging effector cells in chronic inflammation. *Nature reviews. Immunology* **11**, 427-435, doi:10.1038/nri2990 (2011).
- 199 Galligan, C. L. & Fish, E. N. Circulating fibrocytes contribute to the pathogenesis of collagen antibody-induced arthritis. *Arthritis Rheum* **64**, 3583-3593, doi:10.1002/art.34589 (2012).
- 200 Strieter, R. M., Keeley, E. C., Hughes, M. A., Burdick, M. D. & Mehrad, B. The role of circulating mesenchymal progenitor cells (fibrocytes) in the pathogenesis of pulmonary fibrosis. *J Leukoc Biol* **86**, 1111-1118, doi:10.1189/jlb.0309132 (2009).
- 201 Bucala, R., Spiegel, L. A., Chesney, J., Hogan, M. & Cerami, A. Circulating fibrocytes define a new leukocyte subpopulation that mediates tissue repair. *Molecular medicine (Cambridge, Mass.)* **1**, 71-81 (1994).
- 202 Yang, L. *et al.* Peripheral blood fibrocytes from burn patients: identification and quantification of fibrocytes in adherent cells cultured from peripheral blood mononuclear cells. *Laboratory investigation; a journal of technical methods and pathology* **82**, 1183-1192 (2002).
- 203 Pilling, D., Fan, T., Huang, D., Kaul, B. & Gomer, R. H. Identification of markers that distinguish monocyte-derived fibrocytes from monocytes, macrophages, and fibroblasts. *PloS one* **4**, e7475, doi:10.1371/journal.pone.0007475 (2009).
- 204 Melnyk, V. O., Shipley, G. D., Sternfeld, M. D., Sherman, L. & Rosenbaum, J. T. Synoviocytes synthesize, bind, and respond to basic fibroblast growth factor. *Arthritis Rheum* **33**, 493-500 (1990).
- 205 Chan, A. *et al.* CD56bright human NK cells differentiate into CD56dim cells: role of contact with peripheral fibroblasts. *J Immunol* **179**, 89-94 (2007).
- 206 Nakano, K., Okada, Y., Saito, K. & Tanaka, Y. Induction of RANKL expression and osteoclast maturation by the binding of fibroblast growth factor 2 to heparan sulfate proteoglycan on rheumatoid synovial fibroblasts. *Arthritis Rheum* **50**, 2450-2458, doi:10.1002/art.20367 (2004).
- 207 Toth, M., Sohail, A. & Fridman, R. Assessment of gelatinases (MMP-2 and MMP-9) by gelatin zymography. *Methods Mol Biol* **878**, 121-135, doi:10.1007/978-1-61779-854-2\_8 (2012).
- 208 Xue, M. *et al.* Endogenous MMP-9 and not MMP-2 promotes rheumatoid synovial fibroblast survival, inflammation and cartilage degradation. *Rheumatology (Oxford)*, doi:10.1093/rheumatology/keu254 (2014).

- 209 Huber, L. C. *et al.* Synovial fibroblasts: key players in rheumatoid arthritis. *Rheumatology (Oxford)* **45**, 669-675, doi:10.1093/rheumatology/kei065 (2006).
- 210 Drube, S. *et al.* The receptor tyrosine kinase c-Kit controls IL-33 receptor signaling in mast cells. *Blood* **115**, 3899-3906, doi:10.1182/blood-2009-10-247411 (2010).
- 211 Bond, M., Fabunmi, R. P., Baker, A. H. & Newby, A. C. Synergistic upregulation of metalloproteinase-9 by growth factors and inflammatory cytokines: an absolute requirement for transcription factor NF-kappa B. *FEBS letters* **435**, 29-34 (1998).
- 212 Unemori, E. N. *et al.* Interleukin-1 and transforming growth factor-alpha: synergistic stimulation of metalloproteinases, PGE2, and proliferation in human fibroblasts. *Experimental cell research* **210**, 166-171, doi:10.1006/excr.1994.1025 (1994).
- 213 Rosengren, S., Corr, M. & Boyle, D. L. Platelet-derived growth factor and transforming growth factor beta synergistically potentiate inflammatory mediator synthesis by fibroblast-like synoviocytes. *Arthritis Res Ther* **12**, R65, doi:10.1186/ar2981 (2010).
- 214 Schwartz, M. A. Integrins, oncogenes, and anchorage independence. *The Journal of cell biology* **139**, 575-578 (1997).
- 215 Muller-Ladner, U. *et al.* Synovial fibroblasts of patients with rheumatoid arthritis attach to and invade normal human cartilage when engrafted into SCID mice. *The American journal of pathology* **149**, 1607-1615 (1996).
- 216 Judex, M. *et al.* "Inverse wrap": an improved implantation technique for virus-transduced synovial fibroblasts in the SCID mouse model for rheumatoid arthritis. *Modern rheumatology / the Japan Rheumatism Association* **11**, 145-150, doi:10.3109/s101650170027 (2001).
- 217 Okada, Y., Nagase, H. & Harris, E. D., Jr. A metalloproteinase from human rheumatoid synovial fibroblasts that digests connective tissue matrix components. Purification and characterization. *J Biol Chem* **261**, 14245-14255 (1986).
- 218 Pap, T. *et al.* Osteoclast-independent bone resorption by fibroblast-like cells. *Arthritis Res Ther* **5**, R163-173 (2003).
- 219 Boyle, W. J., Simonet, W. S. & Lacey, D. L. Osteoclast differentiation and activation. *Nature* **423**, 337-342, doi:10.1038/nature01658 (2003).
- 220 Braun, T. & Zwerina, J. Positive regulators of osteoclastogenesis and bone resorption in rheumatoid arthritis. *Arthritis Res Ther* **13**, 235, doi:10.1186/ar3380 (2011).
- 221 Axmann, R. *et al.* Inhibition of interleukin-6 receptor directly blocks osteoclast formation in vitro and in vivo. *Arthritis Rheum* **60**, 2747-2756, doi:10.1002/art.24781 (2009).
- 222 Kim, J. H. *et al.* The mechanism of osteoclast differentiation induced by IL-1. *J Immunol* **183**, 1862-1870, doi:10.4049/jimmunol.0803007 (2009).
- 223 Hemingway, F., Taylor, R., Knowles, H. J. & Athanasou, N. A. RANKL-independent human osteoclast formation with APRIL, BAFF, NGF, IGF I and IGF II. *Bone* **48**, 938-944, doi:10.1016/j.bone.2010.12.023 (2011).
- 224 Kotake, S. *et al.* IL-17 in synovial fluids from patients with rheumatoid arthritis is a potent stimulator of osteoclastogenesis. *The Journal of clinical investigation* **103**, 1345-1352, doi:10.1172/jci5703 (1999).
- 225 Yago, T. *et al.* IL-17 induces osteoclastogenesis from human monocytes alone in the absence of osteoblasts, which is potently inhibited by anti-TNF-alpha antibody: a novel mechanism of osteoclastogenesis by IL-17. *Journal of cellular biochemistry* **108**, 947-955, doi:10.1002/jcb.22326 (2009).
- 226 Fossiez, F. *et al.* T cell interleukin-17 induces stromal cells to produce proinflammatory and hematopoietic cytokines. *J Exp Med* **183**, 2593-2603 (1996).
- 227 Frey, O. *et al.* Inducible costimulator (ICOS) blockade inhibits accumulation of polyfunctional T helper 1/T helper 17 cells and mitigates autoimmune arthritis. *Ann Rheum Dis* **69**, 1495-1501, doi:10.1136/ard.2009.119164 (2010).
- 228 Wu, L. *et al.* Cardiac fibroblasts mediate IL-17A-driven inflammatory dilated cardiomyopathy. *J Exp Med* **211**, 1449-1464, doi:10.1084/jem.20132126 (2014).

- 
- 229 Baldeviano, G. C. *et al.* Interleukin-17A is dispensable for myocarditis but essential for the progression to dilated cardiomyopathy. *Circulation research* **106**, 1646-1655, doi:10.1161/circresaha.109.213157 (2010).
- 230 O'Brien, R. L., Roark, C. L. & Born, W. K. IL-17-producing gammadelta T cells. *European journal of immunology* **39**, 662-666, doi:10.1002/eji.200839120 (2009).
- 231 Sutton, C. E., Mielke, L. A. & Mills, K. H. IL-17-producing gammadelta T cells and innate lymphoid cells. *European journal of immunology* **42**, 2221-2231, doi:10.1002/eji.201242569 (2012).
- 232 Ito, Y. *et al.* Gamma/delta T cells are the predominant source of interleukin-17 in affected joints in collagen-induced arthritis, but not in rheumatoid arthritis. *Arthritis Rheum* **60**, 2294-2303, doi:10.1002/art.24687 (2009).
- 233 Koenecke, C. *et al.* In vivo application of mAb directed against the gammadelta TCR does not deplete but generates "invisible" gammadelta T cells. *European journal of immunology* **39**, 372-379, doi:10.1002/eji.200838741 (2009).

## DECLARATION OF ACADEMIC INTEGRITY

I hereby declare in lieu of oath that I have researched and written this thesis myself, no passages of text have been taken from third parties without having been identified as such and that all tools, personal notifications, and sources used by the applicant have been indicated in the thesis.

The persons, who have supported the applicant in selecting and analyzing the material, conducting experiments and preparing the manuscript, are declared completely.

The assistance of a professional consultant has not been utilized and no third parties have either directly or indirectly received monetary benefits from the candidate for work related to the contents of the submitted thesis.

The thesis has not yet been submitted as an examination paper for state or other academic examinations.

# CURRICULUM VITAE

## Personal details

---

Name: Martin Böttcher

E-Mail: [Martin.Boettcher@uk-erlangen.de](mailto:Martin.Boettcher@uk-erlangen.de)

Nationality: German

Birthdate: June 16th 1984



## Education

---

January 2014	PostDoc at the Medical Clinic 5 – Hematology and Oncology, University Hospital Erlangen
Sept. 2010 – Dec. 2014	PhD student at the Institute of Immunology, University Hospital Jena, Germany; Prof. Dr. Thomas Kamradt Topic: Osteoimmunological interactions at the switch from acute to chronic arthritis (DFG-SPP 1468 „Immunobone“)
Sept. 2009 - April 2010	Master thesis at the Cancer Centre Karolinska, Karolinska Institute Stockholm, Sweden; Prof. Rolf Kiessling Topic: Thioredoxin in different T cell subsets
Sept. 2004 - Aug. 2010	Friedrich Schiller University Jena, Germany Program: Biochemistry/Molecular Biology

## Practical

---

July – September 2008	Practical at Translational neuro-endokrinology at the Biomedical Centre Lund, Sweden; Dr. Åsa Petersén Topic: Establishment of a new mouse model for Huntington's disease
April – June 2008	Project at the “Department of Molecular Biology”, Umeå University, Sweden; Prof. Thomas Grundström
Nov. 2007 – Jan. 2008	Project at the “Department of medical biosciences – Medical and clinical genetics”, Umeå University, Sweden Prof. Dan Holmberg
Febr. – March 2007	Practical at the Department of Medical Genetics at the University Hospital Tübingen, Germany; Prof. Dr. Olaf Riess Topic: Establishment of a conditional knockout mouse model for spinocerebellar ataxia type 3

## Further qualifications

---

### Methods:

Animal models	handling of mice (injections <i>i.p./i.v./s.c./i.d.</i> , dissections, blood withdrawal, clinical scoring, behavioral studies)
Cell biology	cell culture/sterile work, FACS and flow cytometry, MACS, Immunohistochemistry, Stereology, MATRIN
Molecular biology	genome analysis, isolation of DNA, RNA and plasmids, PCR, qRT-PCR, cloning, ELISA
Protein biochemistry	Protein-Assays (Bradford, Lowry, BCA), protein expression and purification, measuring enzyme activity, Western Blot, zymography

### Teaching:

Mentoring	Practical, Bachelor theses
Organization	Institutional seminars, multidisciplinary seminars
Lectures/Seminars	Flow cytometry, immunology, tumor immunology

## Congress contributions

---

2011 Joint Annual Meeting SIICA/DGfI (Riccione, Italy)	28.09.-01.10.2011
World Immune Regulation Meeting VI (Davos, Switzerland)	18.-21.03.2012
European Congress of Immunology 2012 (Glasgow, UK)	05.-08.09.2012
40 <sup>th</sup> Congress of the German Society of Rheumatology (DGRh) (Bochum, Germany)	19.-22.09.2012
33 <sup>rd</sup> European Workshop for Rheumatology Research (Prague, Czech Republic)	28.02.-02.03.2013
43 <sup>rd</sup> Annual Meeting of German Society for Immunology (DGfI) (Mainz, Germany)	11.-14.09.2013
41 <sup>st</sup> Congress of the German Society of Rheumatology (DGRh) (Mannheim, Germany)	18.-21.09.2013

## Publications

---

Mougiakakos D, Johansson CC, Jitschin R, **Böttcher M**, Kiessling R. *Increased thioredoxin-1 production in human naturally occurring regulatory T cells confers enhanced tolerance to oxidative stress*. Blood. 2011 Jan 20;117(3):857-61. Epub 2010 Oct 28.

Boy J, Schmidt T, Wolburg H, Mack A, Nuber S, **Böttcher M**, Schmitt I, Holzmann C, Zimmermann F, Servadio A, Riess O. *Reversibility of symptoms in a conditional mouse model of spinocerebellar ataxia type 3*. Hum Mol Genet. 2009 Nov 15; 18(22):4282-95